Prefrontal GABAergic Inhibition and Reversal Learning

Jacco Georg Willem Renstrom, BSc. MSc.

Thesis submitted to the University of Nottingham for the degree of Doctor of Philosophy

September 2023

Table of Contents

Abstract

Neural disinhibition, that is reduced GABAergic inhibition, within the prefrontal cortex (PFC) has been suggested to play a key role in the presentation of cognitive impairments in clinical populations, such as schizophrenia. Additionally, several reports have highlighted period of hypofrontality (i.e., reduced activation of the prefrontal cortex or PFC) in patients, particularly during tasks of executive function. Alongside this pathophysiology of schizophrenia, patients have been found to exhibit marked reversal learning deficits, correlating with other symptoms of the condition. Although reversal learning is primarily associated with the orbitofrontal cortex rather than the PFC, earlier evidence suggests that the PFC may still play a role in reversal learning, especially during more demanding reversals. Moreover, we propose that even when the PFC's involvement isn't required, prefrontal neural disinhibition could still hinder reversal performance. This is due to the resulting aberrant firing of prefrontal neurons potentially disrupting processing in projection sites, including the OFC.

To explore a potential relationship between medial prefrontal GABAergic dysfunction and reversal learning, we set out to measure the effect of bi-directional manipulations of prefrontal $GABA_A$ activity in rats on two variations of an operant two-lever reversal task. Of particular interest were early task stages where rats were unfamiliar with task demands, potentially resulting in a reliance on prefrontal activity, and later task stages where extensive training resulted in 'established' reversal performance.

For this, we first validated a within-subject design of the common operant reversal learning protocol, which could subsequently build the foundations of a serial reversal task (chapter 2). At this stage we also applied a novel Bayesian strategy model which estimated rats' probabilities of applying certain response strategies at a trial-by-trial resolution. Findings from this experiment underlined a clear distinction between early and late stages of reversal learning in terms of reversal speed and underlying strategy implementation. Subsequently, we applied both paradigms (early and serial) in a pharmacological investigation of reversal

performance under the influence of GABA$_A$ agonist (muscimol) resulting in prefrontal functional inhibition, or antagonist (picrotoxin) resulting in neural disinhibition (chapter 3). Findings from these experiments indicated a reliance on prefrontal functioning to guide exploration in order to overcome the marked reversal cost during early task stages, but once the task had been established the PFC was no longer required. On the other hand, neural disinhibition disrupted serial, but not early, reversal learning. Further examination revealed a dual impairment in exploration and exploitation underlying this reversal deficit. We hypothesised that the impairment following prefrontal disinhibition to be, at least in part, related to changes in neural firing within the PFC resulting in aberrant neural projection, ultimately disrupting functional processing in prefrontal projection sites more directly implicated in reversal learning.

Finally, we set out to build on findings from chapter 3 by validating a novel chemogenetic approach of prefrontal manipulation, via designer receptors exclusively activated by designer drugs (DREADDs). This approach utilised a transgenic rat line, expressing non-native Cre-recombinase mRNA under the control of the endogenous vesicular GABA transporter (VGAT) promoter. The cell-type specific presence of Cre-recombinase enabled the readout and expression of the inhibitory hM4Di DREADD at GABAergic cells only. Subsequent activation of these receptors via pharmacologically inert actuators, such as clozapine-*N*-oxide (CNO), would result in the silencing of inhibitory GABA-releasing cells pre-synaptically. However, whilst several similar models have already been established in mice, none to date have been validated in rat lines. Therefore, chapter 4 discusses several histological investigations evaluating feasibility of the rat line, as well as penetrance and cell-type specificity of the DREADD expression within the PFC of a transgenic Long Evans rats. Finally, electrophysiological recordings within the PFC of anaesthetised animals supported functionality of the DREADD, with neural burst firing and local field potential patterns resembling those seen following pharmacologically induced prefrontal disinhibition (Pezze et al., 2014).

Acknowledgements

List of tables and figures

List of common abbreviations

PFC	Prefrontal cortex
NHP	Non-human primate
GABA	Gamma-aminobutyric acid
OFC	Orbital frontal cortex
GAD	glutamic acid decarboxylase
VGAT	vesicular GABA transporter
GAT-1	GABA transporter 1
RTC	Responses to criterion
SD	Spatial discrimination
R(1, 2, 3…)	Reversal (1, 2, 3…)
DREADD(s)	Designer receptors exclusively activated by designer drugs
AAV	Adeno-associated virus
CNO	Clozapine-n-oxide
CamKIIα	Camkinase II alpha
FISH	Fluorescence *in situ* hybridisation
LFP	Local field potential
SWD	Spike-wave discharges

Keywords

Medial Prefrontal Cortex (mPFC); Rodent (rat); GABA; Disinhibition; Operant reversal learning; Bayesian strategy analysis; Chemogenetics; DREADD (hM4Di); *In vivo* electrophysiology.

1 General Introduction

Neural disinhibition, that is, reductions in GABAergic inhibition, including in the prefrontal cortex, has been suggested to contribute to cognitive impairment, including in schizophrenia, based on clinical findings and based on experimental studies in animal models (Lewis et al., 2005; Floresco et al., 2009; Bast et al., 2017). However, current understanding of the impact of neural disinhibition on cognition remains limited. Furthermore, little is known about the extent by which disinhibition may affect neural activity in other, interconnected, regions. In order to address this gap in literature, this thesis will further characterise the current model of prefrontal disinhibition in rodents (Pezze et al., 2014), aiming to build on our knowledge of the disruptive role of disinhibition within local prefrontal regions, and extending deeper into the brain. To achieve this, I will examine the effect of prefrontal, specifically medial prefrontal, GABAergic dysfunction on a task not typically associated with this cortical region, namely an operant two-lever reversal learning task (Brady & Floresco, 2015). Reversal learning is an important aspect of cognitive flexibility, which has received a lot of attention in recent years due to its clinical relevance in a range of conditions, including schizophrenia (Leeson et al., 2009; Izquierdo et al., 2017) (more on this in section 1.2), and as such elaborating on current knowledge of cognitive disruption brought about by neural disinhibition may have substantial clinical implications. The second part of this thesis will go beyond current pharmacological methods of prefrontal disinhibition via the validation of a novel chemogenetic approach of selectively silencing inhibitory GABAergic neurons within selected prefrontal areas. This validation will play a crucial role in forthcoming research within the field, with applications to tasks that go beyond the scope of this thesis. With these aims in mind, first it is critical to understand the translatability of both what is meant by a rodent prefrontal cortex in the context of human and primate definitions, as well as to outline our current understanding of reversal learning and models of neural disinhibition. These will be discussed in the following sections.

1.1 What is the rodent prefrontal cortex?

Anatomical classification of a PFC in primates and rodents

It is important to consider what is meant by the term PFC across species, because the comparability of rodent and non-human primate (NHP) prefrontal cortices has long been debated (Uylings et al., 2003; Laubach et al., 2018). Anatomical classifications of the human and NHP PFC were based on early work by Brodmann, basing classifications on the notable granularity of the region, leading to an early synonym of the region to be 'granular frontal cortex' (Garey, 1999). This early classification of the most anterior part of the granular PFC included dorsolateral, as well as medial and orbital subregions. Brodmann further outlined three non-granular regions, now referred to as part of the cingulate and anterior cingulate cortex, situated along the medial wall, dorsal and rostrally to the genu of the corpus callosum (Garey, 1999). Subsequent work by Walker (1940) further defined orbital regions in the macaque, dissociating between lateral and medial orbital surfaces. These accounts were critical for the early classification of the primate PFC. However, a considerable caveat with this cytoarchitectonic classification became apparent when comparing more distantly related species, such as rodents, for which the requirement of a granular cortex did not hold true, with rodent prefrontal regions composed exclusively of agranular regions (Price, 2007). Based on these findings, it was a long-standing assumption that rodents did not possess a PFC (Preuss, 1995; Laubach et al., 2018; Roberts & Clarke, 2019).

However, soon after Walker's (1940) work, an alternative classification was devised based on projection patterns of the mediodorsal nucleus of the thalamus (MD), which was, at the time, assumed to be the only nucleus with prefrontal projections (Rose and Woolsey, 1948; Akert, 1964). Critically, tract-tracing studies also highlighted regions of the frontal cortices in rodents which received substantial projections from the MD, including medial, ventral and lateral parts of the rat OFC (Leonard, 1969; Krettek and Price, 1977), as well as prelimbic and infralimbic cortices within the medial PFC (mPFC). On the other hand, more dorsal regions of the cingulate cortex received substantially fewer MD projections,

and was subsequently omitted from inclusion in the PFC by several groups (Krettek and Price, 1977; Condé et al , 1990; Barbas et al., 1991; Dermon and Barbas, 1994). Interestingly, further fibre-tracing studies in NHPs and rats identified homology between the primate ventromedial PFC and rodent prelimbic and infralimbic regions (Barbas et al., 1991; Roberts et al., 2007). These findings suggested that, whilst rodents may not possess a granular PFC, the prelimbic and infralimbic regions of the rodent mPFC may resemble the primate mPFC, based on comparable MD connectivity (Preuss & Wise, 2022).

However, additional tract-tracing studies challenged this somewhat simplistic classification of a translatable PFC solely based on MD projections (Preuss & Wise, 2022). Rose and Woolsey's (1948) initial assumption was that the PFC, regardless of species, is a primary recipient of MD projections. However, more recent primate and rodent literature has highlighted that MD projections are not limited to dorsal or medial prefrontal regions, including anterior cingulate, prelimbic and infralimbic regions (Barbas et al., 1991; Roberts et al., 2007), but also to premotor areas (Fang et al., 2006), the insular cortex (Mufson & Mesulam, 1984) and temporal and parietal cortices (Groenewegen & Witter, 2004). Additionally, rodent tracing studies showed that the MD also projected to medial precentral regions, also known as M2, which has since been considered an analogue of the NHP frontal eye field (Neafsey et al., 1986; Groenewegen, 1988). These findings contested the original characterisation of the PFC across species by Rose and Woolsey's (1948) based on MD projections. Nevertheless, projection pathways to the other homologous regions (such as the MD) may yet prove to be a promising way to establishing cross-species correlates of the PFC.

For example, rodent anterograde tract-tracing work by Susan Sesack and colleagues examined topographical organisation of efferent mPFC (dorsal anterior cingulate- and prelimbic cortices) projections (Sesack et al., 1989). Results highlighted major targets of prelimbic projections to be orbitofrontal regions, dorsomedial and ventral striatum, basolateral amygdala, as well as the lateral hypothalamus. On the other hand, dorsal anterior cingulate regions primarily projected to motor and somatosensory cortices, which supported the

notion that these dorsal regions are not part of the PFC (Condé, 1990). Comparable tracing studies in monkeys have shown similar projection pathways from the mPFC to the ventral and medial striatum and the amygdala (Krettek and Price, 1977; Berendse et al., 1992; Carmichael and Price 1995; Ongur & Price, 2000). Interestingly, although much less prominent than in rats, a reciprocal connection between orbitofrontal and ventromedial prefrontal regions was also established in NHPs (Carmichael & Price, 1996; Burman et al., 2006; Roberts et al., 2007). Although, in contrast to primates, rodents do not have a granular PFC, tract tracing studies showed that rodent and primate mPFC show comparable anatomical connectivity. This begs the question; what brain regions do rodents recruit to perform tasks that typically require dlPFC functioning in humans and NHPs? One line of thought is that the rodent mPFC supports, at least some of, the type cognitive processes mediated by the primate dlPFC (Brown & Brigman, 2002).

Functional classification of a PFC in primates and rodents

Cross-species studies are generally in agreement that the PFC is crucial for executive function, encompassing a set of neurocognitive processes that facilitate higher-roder cognition (Dalley et al., 2004). In order to assess potential functional correlates of the PFC between species, it is important to compare translatable tasks. For example, a verbal working-memory task in humans (e.g., Barbey et al., 2013) may depend differently on PFC activity to a radial arm maze task of working memory in rodents (e.g., Auger and Floresco, 2014). Human work comprising of neuroimaging studies and clinical behavioural findings has implicated dorsolateral regions of the PFC in the maintenance of working memory (Duncan & Owen, 2000; Curtis & D'Esposito, 2003), attention (Posner & Petersen, 1990; Liston et al., 2009; Petersen & Posner, 2012; Brosnan & Wiegand, 2017), as well as response inhibition (Blasi et al., 2006; Mostofsky & Simmonds, 2008) and attentional set shifting (Weinberger, 1986; Owen et al., 1991; Owen et al., 1993). Similar requirement for dlPFC function was also observed in NHPs (Fuster, 1997; Dias et al., 1996; Dias et al., 1997; Passetti et al., 2002; Rossi et al., 2007; Rossi et al., 2009; Suzuki & Gottlieb, 2013; Katsuki & Constantinidis, 2014). With respect

to the human and NHP mPFC, imaging studies have suggested that the human mPFC is more typically associated with emotional processing and social behaviour (Euston et al., 2012; Giustino & Maren, 2015; Chen et al., 2021). Moreover, the NHP mPFC, particularly ventromedial PFC, has also been implicated in threat and emotional processing (Wallis et al., 2017; Roberts & Clarke, 2019; Roberts, 2020), whilst ventrolateral and orbitofrontal function has been linked to flexible behaviour distinct from those governed by dlPFC function, namely reversal learning (more on this in the next section), in both humans (Nagahama et al., 2001; Remijnse et al., 2005; Hampshire et al., 2012) and NHPs (Clarke et al., 2008; Rygula et al., 2010). In sum, available evidence suggests that, in both humans and NHPs, there is substantial functional differentiation between different subregions of the primate PFC, with the function associated with the different subregions (dlPFC, mPFC and OFC) being similar in primates and NHPs.

As outlined previously, rodents do not possess an anatomical analogue to the primate dlPFC, yet it has been proposed that functionally the rodent mPFC and primate dlPFC are very similar (Birrel & Brown, 2000; Brown & Bowman, 2002). As such, many rodent studies have examined processes typically requiring dlPFC in primates, targeting the mPFC with lesions and functional inhibition resulting in marked deficits in working memory (Goldman-Rakic, 1994; Lee & Park, 2005; Horst & Laubach, 2009; Keefe & Harvey, 2012; Chen et al., 2014; Auger & Floresco, 2014; Tse et al., 2015) and attention (Millan et al., 2012; Pehrson et al., 2013; Pezze et al., 2014). Furthermore, the mPFC has been implicated in similar processes of behavioural inhibition as the dlPFC in primates (Miller and Cohen, 2001; Haddon and Killcross, 2006; Marquis et al., 2007; Alexander and Brown, 2010), as well as in attentional set shifting (Tait et al., 2007; Floresco et al., 2008). Moreover, there is substantial evidence linking the rodent mPFC to emotional processing, likely due to its profuse connections to the amygdala (Baeg et al., 2001; Vertes, 2006; Etkin et al., 2010). Finally with respect to reversal learning, similar reliance on orbitofrontal regions was noted in tasks of reversal learning in rodents, as was in humans and NHPs (Chudasama & Robbins, 2003; Boulougouris et al., 2007).

Functionally, therefore, there is substantial evidence suggesting that the rodent mPFC mediates functions that are distributed across the wider PFC in humans and NHPs. This may reflect higher specialisation in the primate brain with respect to, for example, emotional processing, with larger cortical regions dedicated to such processes (Steele & Lawrie, 2. Nevertheless, these findings indicate that, whilst anatomically-speaking a cross-species classification of the PFC is ambiguous, with the primary candidate for the rodent mPFC being the primate equivalent, functionally the rodent mPFC facilitates functions more typically associated with the dlPFC in humans and primates (Brown & Bowman, 2002). Therefore, the rodent mPFC remains a relevant target for investigations of translatable cognitive function, not only because of its highly connected nature, but also because of its direct involvement in many translatable processes.

1.2 Reversal learning across species

Reversal learning is an important aspect of cognitive flexibility. Cognitive flexibility as a whole describes the ability to adapt behaviour to changes in the environment, typically tested via changing reward contingencies based on stimuli dimensions (Izquierdo et al., 2017). Moreover, cognitive flexibility provides valuable insight into several neuropsychiatric disorders characterised by apparent inflexibility, such as schizophrenia (Remijnse et al., 2006; Murray et al., 2008), Parkinson's disease (Swainson et al., 2000), as well as addiction (Izquierdo & Jentsch, 2012) and age-related cognitive decline (Schoenfeld et al., 2014). In this thesis, we will focus on reversal learning. At its core, reversal learning requires the reversal of a response-reward association, entailing an initial discrimination based on stimulus dimensions (e.g., spatial position), where a particular stimulus feature results in a reward (e.g., only the left lever). Subsequently, a reversal of the response-reward association, such that the previously correct feature is now incorrect whilst he previously incorrect feature is now correct, require subjects to 'reverse' their responses, switching from the old rule (left lever) to the newly correct rule (e.g., right lever). Reversal learning is a popular aspect of cognitive flexibility due to its robust impairment in several neuropsychiatric disorders, such

as schizophrenia where deficits have been found to correlated strongly with other aspects of the illness, such as disorganisation syndrome (Leeson et al., 2009).

Reversal learning paradigms across species

Over the years, there have been many different paradigms of reversal learning where this reversal principle was employed. Of primary focus here are instrumental forms of reversal learning associated with a positive reward for successful responses. However, there are also assays that work via the reversal of aversive outcomes instead (e.g., Morris & Dolan, 2004; Cernotova et al., 2021).

In principle any instrumental learning task can be converted to a reversal learning task as long as one of the response stimuli is unrewarded at the initial discrimination. However, across species there are several common paradigms that are most frequently employed to examine reversal learning, such as aspects of the classical Wisconsin Card Sorting Task (WCST) in humans (Weinberger et al., 1986; Rogers et al., 2000). On this task, participants must respond according to certain visual dimensions on cards (colour, shape, number), with no explicit information about reward contingencies provided at the start, necessitating initial trial and error testing, followed by subsequent changes in response pattern based on trial-by-trial feedback on the accuracy of the response. Nowadays, there are automated testing batteries, such as the Cambridge Neuropsychological Test Automated Battery (CANTAB) (Robbins et al., 1994; Fray et al., 1996). Amongst a host of other tasks, the CANTAB incorporates simple and compound reversal tasks of visual stimuli. For the latter, much like the WCST, participants must reverse their response from one stimulus to another stimulus within the same single dimension, such as colour or shape, whilst compound reversals are more demanding and require reversals between stimuli that are made up of multiple dimensions, such as colour and shape together. Interestingly, much like human paradigms, NHP analogues often use similar, modified, versions of the WCST, where relevant dimensions are aspects of visually presented shapes (Jones and Mishkin, 1972; Dias et al., 1996; Dias et al., 1997; Izquierdo et al., 2004). On the other hand, rodent paradigms of reversal learning can vary quite substantially,

based on the dimension that is reversed. For example, the reversal stages of a widely used bowl digging task reverse olfactory or tactile stimulus dimensions (Birrell & Brown, 2000; Tait & Brown, 2008), whilst spatial reversals can be conducted in mazes (e.g., Bannerman et al., 2003; Ragozzoni & Choi, 2004), or within an operant setting, where lever position (left or right) may be the relevant stimulus dimension that determines whether or not a lever press is rewarded. (e.g., Brady & Floresco, 2015). In such spatial tasks experimenters may include distractor stimuli, such as pseudorandomly illuminating cue lights, in order to increase task difficulty (Boulougouris et al., 2007; Floresco et al., 2008). Alternatively, on touch-screen tasks, which have been developed to mimic procedural demands of CANTAB tasks, rodents must respond via touchscreen based on visual stimuli presented on a screen (e.g., Bussey et al., 1997; Izquierdo et al., 2006).

Reversal paradigms can either be deterministic (i.e., each correct response results in a reward), or probabilistic (i.e., each correct response has a chance to not be rewarded based on a pre-determined probability). Indeed, many human and NHP reversal tasks are probabilistic, in part due to the rate of learning on deterministic tasks being too quick in primates (Izquierdo et al., 2017). On the other hand, deterministic tasks are commonly employed in rodent research (Boulougouris et al., 2007; Kosaki & Watanabe, 2012; Brady & Floresco, 2015; Izquierdo et al., 2017), as rodents show slower acquisition rates due to less optimised use of 'simple' strategies (win-stay/lose-shift) than in humans,. This means deterministic tasks are less likely to be limited by floor effects of performance where the rat becomes too proficient too quickly. One benefit of probabilistic reversal paradigms is that, due to the complexity of the task, one can analyse strategy changes based on feedback sensitivity which may be incorporated in guiding behaviour and 'beliefs. Such examinations often involve computational approaches to analyse or model behaviour, for example using Bayesian inference (Costa et al., 2015) or reinforcement learning models (Rygula et al., 2015; Sutton and Barto, 2018). Whilst such analysis and modelling is possible with deterministic reversals (e.g., Jang et al., 2015; Maggi et al., 2023), it remains

difficult to discern response patterns based on aspects beyond simple strategies (win-stay/lose-shift).

A further consideration, with regards to reversal paradigms, is the duration of reversal testing. Specifically, classical reversal studies can be divided into 'early' and 'serial' reversal paradigms. Early assays focus on reversal learning immediately after the initial discrimination, typically for one or two reversals (Chudasama & Robbins, 2003; Floresco et al., 2008; Enomoto et al., 2011), whilst serial reversal paradigms typically measure reversal performance for upwards of four consecutive reversal stages (Roberts et al., 1994 ; Izquierdo et al., 2004; Rygula et al., 2010;). Importantly, early work by Mackinstosh (1968) was some of the first to show substantial changes in reversal performance across repeated reversals. Specifically, it was shown that within-problem learning increased over serial stages, indicated by faster reversals. However, data was inconclusive as to how these improvements were attained. In addition, rats may begin to form 'expectations' of reversals with serial expose to rule reversals, which, in turn, may aid performance during serial paradigms. More specifically, rats may begin to test the opposite lever in a two-lever paradigm, even if the current lever is still rewarded. This type of behaviour, in conjunction with intact exploitation, may drive rapid reversal learning in these stages. On the other hand, the absence of this expectation during early reversals likely contributes to poor performance as rats do not expect a rule reversal to occur (Izquierdo et al., 2017). More recent work has indicated that there may be a change in regionality between early and serial reversal stages, such as in Boulougouris et al. (2007) who show that, whilst disrupting performance on an initial reversal stage, orbitofrontal lesions improve performance on subsequent stages. Although according to Preuss (1995) this may be a rodent specific trait, arguing that equivalent lesions in primates produce significantly prolonged deficits than they do in rodents (Uylings et al., 2003), these tentative findings of differential cortical involvement based on task stage require more investigation.

One final consideration with reversal learning is the point at which subjects progress to the next stage. Typically, a success criterion is implemented, such as

10-consecutive correct responses (Brady & Floresco, 2015), or at least X% correct responses on one (Bissonette & Powell, 2012) or consecutive sessions (Izquierdo et al., 2010). Ultimately, this aspect is critical for ensuring appropriate task difficulty, with higher criteria resulting in more difficult tasks. Equally, higher criteria may be associated with more salient representations of the correct strategy at the time of stage completion. Interestingly, one may assume the more training a subject receives on the current strategy, the more difficult it will subsequently be to change behaviour (Tighe et al., 1965; Mandler , 1966). However, as demonstrated by studies in the 1950s and 1960s, this is not necessarily the case (Reid , 1953; Mackintosh , 1962; Mackintosh & Little, 1969; Dhawan et al., 2019). Known as 'overtraining', several theories have been proposed to explain this improvement in reversal performance following overtraining (Mackintosh 1969; Dhawan et al., 2019), yet to date understanding of this phenomenon, and what aspects of the task determine its potency, remains limited. Nevertheless, the consideration of a potential overtraining effect needs to be considered in all paradigms of reversal learning where higher success criteria are implemented, or where subjects receive additional reinforcement between stages, such as via retention days (Boulougouris et al., 2007).

Prefrontal cortical and other brain substrates of reversal learning

Evidence for prefrontal cortical involvement in human reversal learning comes from neuroimaging studies, which have highlighted activation within the OFC in participants performing reversal tasks (O'Doherty et al., 2001 ; Remijnse et al., 2005; Remijnse et al., 2006), with additional activity in the anterior cingulate cortex (Nagahama et al., 2001). Interestingly, dlPFC activity was not associated with reversal performance, and instead was implicated in other aspects of cognitive flexibility, namely attentional set shifting (Hampshire et al., 2012). Moreover, clinical patients with lesions of the OFC typically perform more poorly on reversal tasks, than do healthy controls, without exhibiting impairments on the initial rule acquisition (Hornak et al., 2004). Further insight into frontal involvement in reversal learning comes from NHP studies, which further supported the idea that the OFC is a key region in reversal learning. OFC lesions

studies in NHPs revealed marked reversal impairments, typically manifesting as significant perseveration (i.e., propensity to dwell on the previously correct, but now incorrect response) (Iversen & Mishkin, 1970; Jones & Mishking, 1972; Dias et al., 1996; Dias 1997; Izquierdo e al., 2004). Additionally, these studies failed to find impairments on other aspects of cognitive flexibility, namely attentional set shifting, suggesting specialisation of the OFC for reversal learning. Interestingly, other PFC lesions in NHPs resulted in some impairment, yet this was qualitatively different to impairments following OFC lesions. Specifically, whilst OFC lesions were associated with increased perseveration (i.e., impairment in previous rule abandonment), lesions of the dorsal anterior cingulate cortex in NHPs were found to impair the acquisition of the new rule (i.e., maintaining the correct response) (Chudasama et al., 2013). Similarly, lesions of the ventrolateral PFC, typically considered an analogue of the human inferior frontal gyrus unrelated to human reversal learning, was found to disrupt serial reversal performance but only with respect to novel stimuli (as opposed to previously learnt associations) (Rygula et al., 2010). Together, these findings highlight dissociable roles across frontal regions in humans and NHPs with respect to certain aspects of reversal learning, whilst firmly implicating the OFC as a critical component for task performance.

Studies in rodents have implicated corresponding regions of the rodent frontal cortex in reversal learning. Due to the focus of this thesis on reversal learning in rodents, key studies outlining the main findings on an operant spatial reversal task are highlighted for reference in table 1. As with human and NHP findings, lesion and inactivation studies in rodents highlighted a key role of the OFC in reversal learning (McAlonan & Brown, 2003; Chudasama & Robbins, 2003; Boulougouris et al., 2007; Young & Shapiro, 2009; Enomoto et al., 2011; Izquierdo et al., 2013).

More specifically, a common observation following excitotoxic lesions of orbitofrontal lesions include marked reversal learning impairment, manifested via an increase in perseveration, as opposed to non-specific learning errors (or regressive errors) (Chudasama & Robbins, 2003; Boulougouris et al., 2003). On the other hand, similar lesions of the rodent mPFC typically does not result in

reversal impairments. However, findings Chudasama and Robbins did notice marked increases in regressive errors following infralimbic lesions, potentially suggesting a role of infralimbic sites for wider maintenance of goal-directed behaviour, as opposed to explicit reversal learning. Similarly, Floresco et al. (2008) found marked impairments in set shifting following mPFC lesions, but not reversal learning. Interestingly, and in contrast to the above, the study by Kosaki and Watanabe (2012) replicated earlier findings by Bussey et al. (1997) in showing that the rodent mPFC may yet be recruited in reversal learning. In this task, rats had to monitor three-, as opposed to the usual two, levers in the operant chamber. This paradigm inherently increased the attentional demand which, according to the authors, required greater recruitment of the mPFC (Kosaki & Watanabe, 2012). Indeed, lesions of the mPFC resulted in marked perseveration on this task. Finally, the effect of neural disinhibition on reversal learning has received far less attention, and we note Enomoto et al. (2011) as one of only a few studies that have looked into this. However, results indicated that disinhibition via bicuculline did not impair performance. Although this study failed to find a notable effect of mPFC disinhibition, we believe there were several caveats with the design. Firstly, rats were only tested on one reversal stage, as opposed to several consecutive stages in the above studies (e.g., Boulougouris et al., 2007). As such, researchers may have missed a potential effect on the overcoming of the initial reversal cost, or any impairment that became apparent in successive stages. Secondly, animals received testing on set-shifting prior to reversal testing, and as such were not totally task naïve. This extra training may have counteracted any effect of disinhibition in the event that regionality of cortical activation changes with training, whereby prefrontal areas may not be required for familiar tasks, which would be in line with the suggestion by Kosaki and Watanabe (2012).

Table 1. Key operant reversal studies in rodents, focussing on prefrontal manipulations.

Study	Manipulation (Dose)	Cognitive effects	Additional effects
Chudasama & Robbins (2003)	Excitotoxic Infralimbic and orbitofrontal lesions via quinolinic acid (0.09 M in 0.2-0.4 μl).	• No effect of either lesion on spatial discrimination. OFC lesions increased perseveration, whilst infralimbic lesions resulted in 'learning' errors.	• Reduced response latencies and food collection latencies after infralimbic lesions.
Boulougouris et al. (2007)	Excitotoxic lesions of OFC, infralimbic and prelimbic cortex via quinolinic acid (0.06-0.09 M, in 0.2-0.32 μl).	• Lesions of the OFC impaired reversal learning on two-lever spatial discrimination task, IL or PL lesions did not.	• No effect on omissions, food collection latencies or response latencies.
Floresco et al. (2008)	mPFC inactivation via bupivacaine (0.75% in 0.5 μl).	• Impairment on set shifting when induced prior to shift stage, reversal learning left intact.	• No effect on omissions.
Enomoto et al. (2011)	mPFC disinhibition via bicuculine (12.5/25/50 ng in 0.5 μl).	• No impairment in working memory accuracy on radial arm maze task. • Impairment found in set shifting but not rule reversal.	• Increased locomotion only at 50 ng. • Increased response latency at 50 ng.
Kosaki & Watanabe (2012)	Excitotoxic lesions of anterior cingulate cortex and mPFC via ibotenic acid (0.06 M in 0.1-0.15 μl).	• mPFC lesions increased perseveration and impaired reversal learning on three-lever task. • Anterior cingulate lesion disrupted discrimination acquisition, not reversal learning.	• Not measured.

Note: Saline and sham controls are not included in this table. All manipulations were applied bilaterally.

Electrophysiological studies in rodents suggested that the OFC is specifically involved in the representation of expected outcomes critical for reversal learning (Schoenbaum & Eichenbaum, 1995; Schoenbaum et al., 2009). Moreover, several studies highlighted functional differentiation across the rodent OFC, with reports of the lateral OFC being recruited primarily for deterministic reversal learning (Schoenbaum et al., 2003; Bohn et al., 2003; Takahashi et al., 2009; Hervig et al., 2020), whilst some evidence suggests specialisation of medial regions in probabilistic tasks instead (Dalton et al., 2016). Hervig et al., (2020) explained this apparent OFC heterogeneity in terms of differential involvement in guiding exploration and exploitation, both of which are critical for optimal foraging behaviour (Cohen et al., 2007). Under this hypothesis, lateral OFC may be more important for exploration, whilst the medial OFC may be more critical for exploitation (Hervig et al., 2020). Hervig and colleagues (2020) further suggested a competitive relationship between lateral and medial OFC regions, based on their finding that medial OFC lesions tended to improve reversal performance due to improved exploratory lose-shift behaviour (Hervig et al., 2020). These findings also highlight the additional insights that can be gained by complementing classical performance measures with additional strategy analysis.

The rodent mPFC, like the primate dlPFC (see Brown and Bowman, 2002), hast typically not found to be required in reversal tasks (Birrell & Brown, 2000; Chudasama & Robbins, 2003; Boulougouris et al., 2007; Floresco et al., 2008). However, some studies suggested that the mPFC may be required for reversal learning where there is a greater attentional demand, such as when monitoring several stimuli at the same time (Kosaki & Watanabe, 2012), or where 'complex' discriminanda were used (Bussey et al., 1997). These findings suggest that more work is required to further characterise the threshold at which mPFC activity is required.

Beyond frontal regions, several lines of evidence have also implicated striatal regions and the amygdala in reversal learning, although evidence for the latter remains equivocal (Izquierdo et al., 2013). Neuroimaging studies in humans have found task-related activation in the dorsal and ventral striatum (Rogers et al.,

2000; Izquierdo et al., 2017), with reduced activity in these regions associated with poor performance (Remijnse et al., 2006). Similarly, neurotoxin lesions within the dorsomedial striatum of NHPs has been shown to cause perseverative impairments, akin to those observed following OFC lesions, ultimately resulting in reversal learning deficits (Clarke et al., 2008). Rodent work also supports the involvement of the striatum in reversal learning, whilst also highlighting a potential role in the maintenance of the new rule (Ragozzino & Choi, 2004). Taken together, these findings support reversal learning to be primarily an OFC-dependent function, with subregions of the OFC, as well as mPFC and striatal regions being recruited in very specific ways, *ad hoc*.

Neurotransmitter mechanisms implicated in reversal learning

Several neurotransmitter systems have been associated with reversal learning, with substantial research highlighting an important role for the serotonergic, cholinergic and glutamatergic systems (Izquierdo et al., 2017). Studies have reported specific reversal impairments following region selective serotonin depletion, particularly within the OFC and wider PFC in NHPs (Clarke et al., 2005; Rygula et al., 2015), as well as following systemic serotonin antagonism in rodents (Boulougouris & Robbins, 2010). Moreover, chronic stress, which has been reported to result in serotonin dysregulation within the OFC, caused reversal impairment in rats, and this deficit was ameliorated by serotonin reuptake blockers (Lapiz -Bluhm et al., 2009). Given these coherent findings, it remains the question of how serotonin facilitates reversal learning. A study by Bari and colleagues (2010) reported that increasing forebrain serotonin activity improved performance, indexed by the number of probabilistic reversals completed, whereas serotonin blockade resulted in reward insensitivity, characterised by impairments in win-stay and lose-shift behaviour. On the other hand, serotonin depletions within the OFC of NHPs were reported to impair response suppression, whilst depletions of amygdala serotonin increased vulnerability to misleading feedback (Rygula et al., 2014). Together these findings highlight serotonin as critically important for feedback sensitivity, which in turn drives task appropriate strategies.

Acetylcholine has also been suggested to play a critical role in reversal learning. Reductions in prefrontal acetylcholine activity in NHPs, via neurotoxic lesions of the nucleus basalis reducing prefrontal acetyltransferase, resulted in marked reversal impairments, alongside intact retention of the original discrimination (Roberts et al., 1990; Roberts 1992; Robbins & Roberts, 2007), with lesioned monkeys showing a greater tendency to perseverate, whilst levels of new learning were comparable. A rodent study by Ragozzino and Choi (2004) also highlighted an important role of acetylcholine in reversal learning, specifically medial striatal acetylcholine activity, highlighting increased acetylcholine output during reversal tasks. Finally, Cabrera et al., (2006) specifically linked lesions of rodent cholinergic innervation of the PFC to impairments on serial, but not early, reversal learning.

Glutamate's role in synaptic plasticity has warranted research into its involvement in reversal learning. One avenue of research followed N-methyl-D-asparate receptor (NMDAR) function, with systemic administration of NMDAR blockers impairing operant spatial reversal learning whilst leaving initial discrimination intact (Dalton et al., 2011). Moreover, local blockade within the lateral OFC reproduced perseveration-specific impairments, whilst similar antagonism within the striatum produced reversal, as well as discrimination deficits (Brigman et al., 2013). Once caveat with these findings are that NMDAR blockade would be expected to impair a wide range of learning and memory tasks (van der Staay et al., 2011), as well as causing some non-specific behavioural impairment (Ford et al., 1989). Therefore, it is difficult to dissect these reversal impairments further, given that their role in cognition and cortical development is quite non-specific. In sum, reversal learning is a complex behaviour which requires prefrontal cortical and subcortical brain regions and several neurotransmitter systems, including the serotonin, acetylcholine and glutamate system. With this in mind, one system that has not been discussed yet is the inhibitory GABAergic network. Indeed, associations between GABA activity and reversal learning are limited, but as I will outline in the next section, due to the importance of GABAergic control in cognition overall, it may yet play a role in reversal learning too.

1.3 GABA and cognition

An introduction to GABA

GABAergic inhibitory interneurons are a large and diverse population of neurons comprising between 15-25% of cortical neurons in mammals (Bloom & Iversen, 1971; Hendry et al., 1987; Jones, 1993; Conti et al., 2004; Markram et al., 2004). The synthesis of GABA from L-glutamate is controlled by several isoforms of glutamic acid decarboxylase (GAD), most notably those of molecular weight 65 kD and 67 kD (GAD65 and GAD67, respectively) (Erlander et al., 1991). GAD65 and GAD67 can be differentiated through their localisation and the function they serve. GAD65 is predominantly localised at axon terminals, and as such has been implicated in synthesis of synaptic GABA for vesicular release (Fukuda et al., 1998). In contrast, GAD67 has a much wider intraneuronal distribution (Kaufman et al., 1991), and thus a role in the cytoplasmic synthesis of GABA has been suggested (Soghomonian & Martin, 1998). Following synthesis, the release of GABA into the synapse is primarily mediated by the vesicular GABA transporter (VGAT) (Chaudhry et al., 1998).

There are three main types of GABA receptors – GABAA, GABAB and GABAC receptors (Chebib & Johnston, 1999). GABAA receptors are ion-gated Cl- channels and contribute to fast inhibition by hyperpolarization, whereas GABAB receptors are metabotropic receptors involved in slow inhibition (Nicoll et al., 1990). GABAC receptors, whilst structurally very similar to their GABAA counterparts, have been found to be predominantly localised to the retina (Bormann & Feigenspan, 1995), and as such are not relevant to the current investigations of prefrontal activity. Within this thesis, I will specifically focus on GABAA receptor function, because this receptor is the best characterized of the three receptor subtypes (Wassef et al., 2003), and most relevant to the experimental questions posed previously.

Finally, GABAergic cortical interneurons can be separated into several subtypes according to the protein content of the cells, such as calretinin-, somatostatin-, calbindin-, and most commonly parvalbumin-positive (PV+) cells. Further

characterisation of GABAergic interneurons revealed physiological differentiation, based on their involvement in either fast-, or slow-spiking pyramidal cells, with all but PV+ cells involved in slow-spiking electrophysiological activity (Gonzalez -Burgos & Lewis, 2008; Bartos & Elgueta, 2012; Nahar et al., 2021). Moreover, it has been suggested that these fast-spiking PV+ cells mediate synchronisation of pyramidal cell firing, particularly within the gamma (30-120 Hz) range (Gonzales-Burgos & Lewis, 2008; Colgin , 2016), which has been specially implicated in the long-range communication between different brain regions (Gregoriou et al., 2009). This role of inhibitory interneurons in generating cortical gamma oscillations was confirmed *in vivo* (Sohal et al., 2009) and *in vitro* (Cardin et al., 2009), with inhibitory post-synaptic potential recordings of pyramidal cells reflecting gamma oscillations (Penttonen et al., 1998). Together, these studies indicate a critical role of inhibitory cortical GABAergic control, implications of which may reach beyond local GABA receptor function.

Modulation of GABA by other neurotransmitter systems

GABA interacts with several other neurotransmitter systems. I will only briefly mention some main interactions between GABA and other systems that may be of particular relevance within the context of this thesis, without giving an exhaustive review. First, several reports indicate GABA expression, particularly PV expression, within the PFC is critically dependent on NMDA activity (Moghaddam et al., 1997; Homayoun & Moghaddam, 2007). Findings of chronic administration of NMDA receptor antagonists ketamine revealed marked reductions of PV content , as well as GAD67 mRNA, in several prefrontal subregions of rodents (Keilhoff et al., 2004; Behrens et al., 2007). Additionally, Homayoun & Moghaddam (2007) showed that NMDA receptor antagonism reduced GABAergic neuron firing within the rat mPFC. These marked deficits would likely be accompanied by GABAergic hypoactivity, due to reduced GABA synthesis, and could ultimately result in disruptions within gamma-band oscillations outlined above. Second, several studies have suggested connections between the cholinergic system and the GABAergic network within the cerebral cortex (Hasselmo, 2006; Granger et

al., 2016). One line of evidence comes from genetic manipulation studies. Microdeletion of the alpha7 nicotinic-ACh gene in mice was found to impair many aspects of cortical GABA-development, such as levels of PV, GAD65/67 and fewer GABAA receptors (Lin et al., 2014). These reductions in GABAergic markers would likely be associated with inhibitory hypoactivity, reduced control over pyramidal cell firing, and ultimately aberrant oscillatory activity. Third, serotonin has been implicated in the modulation of GABA transmission in many regions, including the PFC (Feng et al., 2001; Ciranna , 2006) and thalamus (Munsch et al., 2003). More specifically, serotonin appears to positively modulate GABA transmission within the frontal cortex, with serotonin typically increasing GABA transmission (Zhou & Hablitz , 1999; Dawson et al., 2001). In sum, GABAergic activity is critically dependent on several other aspects of cortical neurotransmission, and as such may be particularly prone to disruption.

The role of GABA In cognition

As outlined above, GABAergic inhibition is critical for the control of neural firing by pyramidal cells in PFC (Gonzales-Burgos & Lewis, 2008; Colgin, 2016), as well as in the maintenance of oscillatory coherence vital for the long-range communication between PFC and different brain regions (Fries et al., 2001; Saalmann et al., 2007; Lakatos et al., 2008; Gregoriou et al., 2009). Transient reduction in GABAergic activity, resulting in phasic neural disinhibition, has been ascribed an important role in cognition, with suggestions that this disinhibition creates windows of reduced restraint on specific synapses, facilitating the processing of important stimuli, and thus, playing a potentially critical role in forms of learning and memory (Letzkus et al., 2015; Koolschijn et al., 2021). However, problems arise when neural inhibition is not re-established (i.e., when the disinhibition is tonic), or if the disinhibition is not restricted to specific synaptic pathways (Bast et al., 2017). Such dysfunction within the rodent mPFC has been shown to disrupt prefrontal dependent function, such as attentional (Pehrson et al., 2013; Pezze et al., 2014; Bast et al., 2017) and working memory processes (Goldman-Rakic, 1994; Lee & Park, 2005; Horst & Laubach, 2009; Keefe & Harvey, 2012; Chen et al., 2014; Auger & Floresco, 2014; Tse et al., 2015).

Critically, further studies have shown that 'too much' GABAergic control (i.e., increased inhibition) can also be detrimental to prefrontal mediated functions (Young and Shapiro, 2009; Shaw et al., 2013; Hamilton & Brigman, 2015). This suggested that, depending on the brain region and the cognitive function, both too little and too much GABAergic activity may be detrimental to cognitive function (Bast et al., 2017). However, whilst it is intuitively plausible that too much GABAergic activity, resulting in silencing or 'functional inhibition' of the region, causes deficits in processes relying on the targeted region, the extent by which neural disinhibition disrupts performance was less well understood.

One possibility is that reduced GABAergic inhibition within a brain region can disrupt both functions associated with this brain region, by disrupting balanced, well-tuned levels of regional activity, and functions of projection sites, by causing aberrant drive of these projection sites (Bast et al., 2017). Recently, electrophysiological and behavioural work in rats linked disinhibition within the mPFC of rodents with behavioural impairments through intensified burst firing in the mPFC, characterised by greater within-burst firing rate and shorter bursts (Pezze et al., 2014). Briefly, 'bursts' characterize periods of rapid pyramidal cell firing (2-6 action potentials within around 200 Hz; Lisman 1997) separated by periods of relative inactivity. Burst firing has been proposed as a principal pathway of communication between distal cortical regions (Lisman, 1997). Therefore, the aberrant burst firing caused by neural disinhibition may disrupt, not only local processing (such as prefrontal attentional and working memory deficits outlined above), but also processing in prefrontal projection sites, although direct evidence for the latter is currently lacking (Bast et al., 2017).

These quite striking electrophysiological changes following disinhibition were associated with substantial impairment on a sustained attention task (Pezze et al., 2014). With the apparent changes in local neural activity, and presumably oscillatory coherence, perhaps local disinhibition has a role to play in the disruption of interconnected regions. To address this question, we examined the role of mPFC GABAergic inhibition in reversal learning. Our hypotheses were guided by the idea that mPFC disinhibition may disrupt both local processing

withing the mPFC and processing in prefrontal projections sites, including the OFC and striatum (Sesack et al., 1989), which have been implicated in reversal learning (see section 1.2). Moreover, we have aimed to supplement current pharmacological models of rodent disinhibition with a novel chemogenetic model using Designer Receptors Exclusively Activated by Designer Drugs (DREADDs) (Roth, 2016).

1.4 DREADDs, a novel chemogenetic approach

To date, pharmacological studies manipulating prefrontal GABA activity have targeted post-synaptic GABA receptors. In contrast, the post-mortem findings of GABA deficiencies, as reflected by reduced GABA markers, in patients with schizophrenia mainly point to pre-synaptic disinhibition (i.e., impairments in the function of GABAergic neurons). One possible approach to silence GABAergic neurons pre-synaptically is offered by recent innovations of chemogenetic technologies called designer receptor exclusively activated by designer drugs (DREADDs) (Armbruster & Roth, 2005; Sternson & Roth 2014; Roth, 2016). DREADD technologies use site-directed mutagenesis of G-protein-coupled receptors resulting in modifiable receptors. Importantly, these receptors are not activated by endogenous neurotransmitters, but rather via pharmacologically inert 'designer drugs', such as the non-native ligand clozapine-N-oxide (CNO), a metabolite derived from the atypical antipsychotic clozapine (Allen & Roth, 2011; Sternson & Roth, 2014).

DREADDs can be introduced into brain regions of interest by intra-cerebral injection of adeno-associated viral (AAV) vectors containing the DREADD of choice (e.g., Zhu et al., 2014). This method would result in the relatively indiscriminate expression of the DREADD across neurons within the targeted brain region. However, neuron-type specific DREADD expression is also possible. Here, the AAV vector contains single stranded, inverted, DREADD DNA, which cannot be transcribed naturally. Instead, transcription of the DREADD DNA requires the presence of the bacteriophage enzyme Cre-recombinase (Atasoy et al., 2008; Smith et al., 2016). Whilst this enzyme is normally not found in

mammals, innovations in transgenic animal techniques have developed rodent lines selectively expressing Cre-recombinase under the control of desired genes. Nowadays, a wide variety of transgenic rodent lines, especially mouse lines, expressing Cre in specific groups of neurons are available (Roth, 2016; Sciolino et al, 2016). Of particular interest for the study of GABAergic neuron function in rats, is a rat line designed to co-express Cre-recombinase selectively with the VGAT (Slc32a) gene, which is specific to GABAergic neurons (https://www.envigo.com/model/hsdsage-le-vgatem1-ires-Cre-sage). This results in the presence of Cre-recombinase in VGAT+ cells only (i.e., all GABA releasing neurons), allowing for the targeted, Cre-dependent expression of desired DREADDs at GABAergic neurons.

There are number of DREADDs with varying purpose (for overview see Sternson & Roth, 2014; Roth, 2016), including the excitatory hM3Dq (Armbruster et al., 2007; Alexander et al., 2009) and the inhibitory hM4Di DREADD (Urban & Roth, 2015). When stimulated by administration of CNO, the hM3Dq activates the phospholipase-C-pathway, altering intracellular Ca2+, and as a result increasing firing of the stimulated cell (Rogan & Roth, 2011). On the other hand, the hM4Di receptor, when stimulated by CNO administration, decreases cAMP signalling, and increases inward K+ uptake, resulting in membrane hyperpolarization and the temporary suppression of neuronal activity (Rogan & Roth, 2011). This inhibitory DREADD, combined with the commercial availability of a VGAT-Cre rat line (https://www.envigo.com/model/hsdsage-le-vgatem1-ires-Cre-sage), offers a novel opportunity to selectively manipulate GABAergic prefrontal neurons in rats, complementing the pharmacological disinhibition approaches discussed previously.

There is growing interest in the application of DREADDs in the field of translational research, because of the opportunities this approach offers to induce neuron- and pathway-specific manipulations. Additionally, pharmacological methods, manipulating selected brain regions, require the surgical insertion of guide cannula into the target brain region, which later serve as the guide for microinjectors into the region of interest (e.g., Pezze et al., 2014). The indwelling

guide cannulae, held in place by a small pedestal on the skull typically made from dental cement, increase the risk of adverse side effects (e.g., related to poor wound healing or infections or meningitis). In contrast, DREADD injections only require a small incision and small holes drilled into the skull to allow an injector to be inserted into the brain, without the requirement for indwelling cannulae and a head cap, reducing associated potential for health complications.

Moreover, pharmacological models have limited repeatability of microinfusions, typically opting for between 5-6 microinfusions within the same region. This is because each microinfusion damages the surrounding area, resulting in reactive gliosis (Bast & Feldon, 2003; Cunningham et al., 2008), which can reduce the effects of the pharmacological agent on the brain tissue surrounding the injection site (Bast et al., 2001). On the other hand, DREADD technologies are unlikely to be restricted by such drawbacks, as activation of the receptors is carried out via systemic injection. Several studies have shown little to now decay in DREADD activity following repeated activation, as well as no lasting behavioural issues (Mahler et al., 2014; Robinson et al., 2014).

An important consideration with chemogenetics is the specificity and penetrance of the manipulation (Smith et al., 2016; Clark et al., 2022). Specificity refers to how limited expression or manipulation is to the desired cell type, whilst controlling for off-target effects. Penetrance, on the other hand, refers to the scope of this expression or activation on desired cells. Both, the specificity, and penetrance of DREADDs are a product of a robust driver line combined with a well-functioning DREADD construct. DREADD technologies are considered to have a penetrance around 60% of all cells (Gremel & Costa, 2013; Smith et al., 2016), with Cre-mediated expression often resulting in slightly lower penetrance (Nguyen et al., 2014), which may impact subsequent stimulation. In contrast, drug microinfusions would likely stimulate all cells expressing the pharmacological target (e.g., a receptor) within the infused region. This increases the likelihood of an incomplete excitation/inhibition of the target cells, which may be inappropriate for some experimental questions. Nevertheless, for translational studies, it may be considered an advantage, as it may lead to a more naturalistic

modulation of neural activity (Smith et al. 2016), akin to that seen in clinical or neurotypical populations.

Application of DREADD technologies to studies cognitive flexibility has increased in recent years (Parnaudeau et al., 2015; Cope et al., 2019). Yet, to date, only a handful have specifically investigated reversal learning using DREADDs (Bortz et al., 2019; Harris et al., 2021 Bortz et al., 2022), and none examining the effect of prefrontal manipulations on reversal learning. Moreover, these studies have not targeted specific neurochemical system, but instead manipulated entire regions via DREADDs (e.g., excitation via hM3Dq). Nevertheless, these studies have shown that application of DREADDs for behavioural neuroscience are a fruitful avenue, laying the basis for future chemogenetic investigations. These investigations also sparked an interest to further advance the field with several system specific models of chemogenetic manipulation, which is the ground for the second part of this thesis described in chapter 4.

1.5. Project aims

The project aimed to contribute to the further characterisation of the role of GABAergic inhibition in the rat mPFC in cognitive function. Aim 1 was to examine the impact of mPFC disinhibition and functional inhibition by local infusion of a GABA-A receptor agonist (muscimol) or antagonist (picrotoxin) on an operant two-lever reversal task. Aim 2 was to validate a novel chemogenetic approach to selectively silence GABAergic neurons within the mPFC of rats.

To achieve Aim 1, we first validated a within-subject design of the common operant reversal learning protocol (Boulougouris et al., 2007; Brady & Floresco, 2015), which would be suitable to test the impact of pharmacological manipulations of the mPFC on serial late reversal learning within-subjects, in order to control for individual differences in the cohort whilst also reducing the overall number of rats used (chapter 2). For a within-subjects comparison of drug effects on serial reversal learning, it was important to achieve relatively stable between-session performance. Additionally, in this validation study, we

complemented our analysis of classical performance measures (such as trials to criterion, percentage correct or error measures) with a trial-by-trial Bayesian strategy analysis (Maggi et al., 2023). This method takes trial-by-trial information from the first trial of the spatial discrimination up to the current trial to estimate the probability with which individual rats apply a set of response strategies, such as win-stay/lose-shift, on any given trial, making it possible to establish a more nuanced cause-effect relationship between a brain manipulation and behavioural effect than classical performance measures. Next, we examined the impact of prefrontal disinhibition and functional inhibition via local microinfusion of the GABAA receptor antagonist picrotoxin or GABAA receptor agonist muscimol, respectively, on two variations of the two-lever operant task (early and serial reversal) (chapter 3). As outlined earlier, although there is only limited evidence suggesting a contribution of the rodent mPFC to reversal learning, we hypothesised that, first, mPFC inhibition may impair reversal performance in circumstances where the task is particularly demanding, such as during early reversal stages of the assay. Second, prefrontal disinhibition may affect reversal performance, even under conditions when the mPFC is not directly required, because the mPFC projects to regions critical for reversal learning, such as the OFC (Sesack et al., 1989) and the striatum (REFS), and mPFC disinhibition may result in aberrant drive of prefrontal projections and, thereby, disrupt processing in prefrontal projections sites (Bast et al, 2017). Based on previous literature it was also expected that neither manipulation would result in impaired stimulus discrimination or basic operant learning (Enomoto et al., 2011; Pezze et al., 2014).

To address Aim 2, we set out to selectively express an inhibitory hM4Di-DREADD approach in mPFC GABAergic neurons, using Cre-dependent DREADD expression in a VGAG-Cre rat line (chapter 4). We first validated the transgenic VGAT-Cre rat line (https://www.envigo.com/model/hsdsage-le-vgatem1-ires-Cre-sage) via *in situ* hybridisation, measuring co-localisation of VGAT and Cre-recombinase mRNA in mPFC. Furthermore, we compared two volumes (0.5 and 1.0 μl) of the AAV-vector expressing the inhibitory DREADD in order to assess the cell-type specificity, penetrance, and spread within the PFC at each volume. From previous literature, Cre-mediated DREADD penetrance was expected to be around 20-60%

(Nguyen et al., 2014; Smith et al., 2016). These findings guided decisions on which volume would be most appropriate for subsequent cohorts. In a second cohort of VGAT-Cre rats, we extended our histological analysis, using additional immunohistochemical staining, and we assessed the functionality of the DREADD construct within the mPFC using in vivo electrophysiological recordings. For the latter, we designed a within-subject study comparing the effect of intraperitoneal (i.p.) injections of saline and 6 mg/ml/kg CNO2HCl on burst firing patterns and local field potential (LFP) power, qualitatively comparing findings to previous electrophysiological results of pharmacologically induced prefrontal disinhibition (Pezze et al., 2014). We hypothesised that chemogenetic disinhibition of mPFC would result in neural changes similar to those we previously found with pharmacological disinhibition, including intensified burst firing, alongside marked LFP spike-wave discharges and increased overall LFP power.

Finally, chapter 5 summarises the new empirical findings of this thesis, putting main findings into the context of current literature, whilst also discussing general limitations and clinical implications of pharmacological and chemogenetic findings, and highlighting potential avenues for future research.

2 Validating a serial operant reversal learning paradigm suitable for within-subject pharmacological and chemogenetic studies

Declaration: Silvia Maggi ran the Bayesian analysis code and helped in the interpretation of subsequent results.

There are several common reversal learning assays employed in current rodent literature. The critical difference between these paradigms are the stimulus dimension that is being reversed, such as odour in bowl digging paradigms (Birrell & Brown, 2000; Tait & Brown, 2008), spatial position in several forms of maze (e.g., Ragozzoni & Choi, 2004) or arena tasks (Cernotova et al., 2021), or spatial or visual discrimination in operant settings (Floresco et al., 2008; Boulougouris et al., 2007; Enomoto et al., 2011; Kosaki & Watanabe, 2012). On a methodological level, while bowl-digging and potentially also maze tasks have the advantage of greater ecological validity, automated operant procedures provide better environmental control, as they require less experimenter input or handling during the task, and help to limit potential external distractors such as noise or light (Brady & Floresco, 2015). Furthermore, modern operant procedures allow for quicker data collection compared to bowl digging paradigms, although, for example, visual discrimination and reversal tasks using touch screen can require very long training times (Bussey et al., 1997; Brady & Floresco, 2015). Finally, automated operant measures reduce the risk of experimenter bias in data collection. In this chapter I will discuss the application of one such paradigm, namely an operant two-lever-press reversal task, in the examination of serial reversal learning.

The task used is an adaptation of the food-reinforced operant two-lever reversal learning protocol in rats, previously outlined by Brady & Floresco (2015). Briefly, this task involves the pressing of retractable levers to receive a food reward in a deterministic manner, with the inclusion of an unrewarded, pseudorandom, cue light illuminating above one of the two levers on each trial, acting as a distractor. The inclusion of this cue light was to allow fair comparison with similar work in previous literature which also included such a distractor (Boulougouris et al., 2007; Floresco et al.. 2008; Brady and Floresco, 2015). After acquisition of an initial spatial discrimination rule, whereby one of the two levers is rewarded

whilst the other is not, the rule is reversed on the following day so that the opposite lever now results in the reward, whilst the previously correct lever does not. This instance of rule reversal is repeated across several sessions, necessitating the continued acquisition and extinction of spatial rules (i.e., which lever location results in a reward).

Of primary interest for the current experiment was the change in rats' performance across 10 reversal stages, in order to characterise a performance 'curve', with the outlook of establishing a period of several consecutive reversal stages where performance does not significantly fluctuate between session. This performance plateau would enable within-subject examinations of reversal learning in combination with pharmacological and chemogenetics manipulation. Within-subject studies inherently control for inter-subject variability within the dataset, resulting in a lower sample size required to achieve similarly powerful results. Moreover, reductions in sample size is a goal of animal research as a whole, with efforts being made across the field to reduce the use of animals.

Interleaved between reversal stages were so-called 'retention' days, similar to work by Boulougouris et al. (2007). These days which simply reinforced the rule that was acquired on the previous day (i.e., post-reversal rule), without an additional reversal. Whilst the need for retention days in the current experiment was limited, they would be a necessity for any future within-subject pharmacological or chemogenetic work. In such experiments, where manipulations may result in reversal learning impairments, these sessions will be important to ensure rats reach similar baseline performance before the next reversal stage begins. The importance of allowing rats to reach baseline between sessions is to, at its most basic level, ensure any performance change can be fully attributed to learning, and not a residual bias based on previously learnt rules. Whilst the inclusion of a success criterion does result in a certain performance threshold being met on each stage, it does not guarantee a full, and therefore lasting, rule reversal. As such, it is important to ensure that rats reach this criterion on separate sessions to confidently assume the learnt rule has been successfully reversed. Additionally, inclusion of retention days in pharmacological

studies minimises the risk of between-session pharmacological carry-over effects. Finally, I included a fixed number of 20 reminder trials at the start of each reversal stage reinform, as well as 'retention days' interleaved between reversal stages.

Performance metrics examined included classical reversal measures (responses to criterion [RTC], percentage correct, error type, response latencies, omissions), as well as rats' implemented strategies around reversal at a trial-by-trial resolution via Bayesian inferential statistics (Maggi et al., 2023; Jang et al., 2015; Bartolo & Averbeck; 2020). This Bayesian approach considers each rat's response on a trial-by-trial basis, using evidence starting at trial 1 of the first test stage, up until the current trial, to continuously evaluate the behavioural strategies pursued by the rat throughout the sessions. Complementing classical measures with this approach is of great value, as it can account for nuances in behaviour which RTC or percentage-correct may miss. For example, two rats may reach criterion with equal RTC, but where one rat may operate at roughly a 2:1 ratio of correct to incorrect responses before achieving criterion, another may make a continuous series of perseverative errors only to change to a win-stay strategy and achieve criterion within the last 10-15 trials. The RTC data for these two rats would be identical, yet the underlying methods of achieving these criteria would be vastly different. Percentage-correct would be a suitable alternative to RTC given this shortcoming, as it takes into account the average correct vs. incorrect responses. However, it has several drawbacks itself, particularly when testing is stopped after rats reach a performance criterion. In such a scenario, where rats are stopped as soon as they reach a certain degree of performance, percentage-correct is automatically confounded by ceiling effects. In addition, and whilst certainly more sensitive than RTC, percentage-correct is still somewhat impervious to within-session changes in performance brought about by sudden changes in response strategy. Therefore, an approach to analyse trial-by-trial changes in response strategy would be very valuable.

Stable performance in all of these metrics is critical for a within-subject design as this controls for between-stage differences, which would otherwise confound comparisons of drug effects across those days. Typical pharmacological studies

conduct up to six intra-cerebral microinfusions, following which gliosis around the injection site is too great and may interfere with acute drug effects (Bast et al., 2001; Pezze et al., 2014). Therefore, it was important to observe stable performance in at least six consecutive reversal sessions (two repetitions of three infusion conditions). Previous work in-house (Hock, 2020), as well as wider literature, has described two key features of a typical reversal learning 'curve'. The first is an impairment at the first 1-2 reversal stages, due to a marked reversal cost accompanied by increased errors, particularly perseverative errors (Chudasama & Robbins, 2003; Boulougouris et al., 2007; Floresco et al., 2008; Enomoto et al., 2011). This peak is followed by marked improvements in performance over repeated reversals with indications of a plateau after several stages (Mackintosh et al., 1968; Boulougouris et al., 2007; Rygula et al., 2010). From these previous studies we hypothesise that the reversal cost on, at least, the first reversal stage will be significant which would result in poorer performance indexed by many perseverative errors. However, based on serial reversal studies, we also hypothesised that performance on RTC and percentage-correct should stabilise after several sessions, reaching relatively stable, asymptotic performance levels. With regards to strategy implementation, we expected to see improvements in successful strategies across successive reversal stages, indicative of learning, whilst unsuccessful strategies should be reduced with increased training.

2.1 Materials and Methods

2.1.1 Rats

This experiment was conducted on Lister hooded rats (Envigo, UK) (N = 8), all of which were male and weighed 275-300 g, or 8-9 weeks, at the start of the experiment. The sample size was chosen for the purpose of investigating gross behavioural patterns that were evident even in a relatively small sample of rats.

Rats were housed in groups of 4, in individually ventilated, two-level, 'double decker' cages (462 mm X 403 mm X 404 mm; Tecniplast, UK) with temperature and humidity control (21 ±1.5 °C, 50±8%) and an alternating 12 h light dark cycle

(lights on at 0700). All experimental procedures were carried out during light phase. Rats had unlimited access to water throughout the study. Access to food (Teklad Global 18% Protein Rodent Diet 2018C; Envigo) was *ad libitum* until the start food restriction one day prior to the start of pretraining. As part of the food restriction schedule, rats received daily food rations of 15-21 g per rat and were weighed daily to maintain body weights at 85-90% of free-feeding weights, as projected by a pre-established weight growth curve. On pretraining and test days, rats were weighed before the day's operant task session and received their daily food ration after completing the session (in addition to the food reward received during the session). All procedures were conducted in accordance with the United Kingdom (UK) Animals (Scientific Procedures) Act 1986.

2.1.2 Apparatus

All testing was conducted in eight individual operant boxes (30.5 cm x 24.1 cm x 21.0 cm; Med-Associates, USA), placed within wooden sound attenuating cabinets containing an extractor fan. The operant boxes were equipped with a house light (40 lux), two retractable response levers either side of a dish into which sugar reward pellets (5TUL-45 mg, Testdiet, UK) were dispensed, as well as two LED cue lights (40 lux each), one above each lever. The LED cue lights above the levers were illuminated pseudo-randomly throughout all sessions. In the present study, the cue lights were never relevant to the correct lever choice (which was always determined by lever position, left or right), and they were essentially acting as distractors; they were included to allow comparison with other studies where either cue light or lever position determined the correct choice. Each rat was assigned to an operant chamber, where it underwent all operant test sessions. Chambers were cleaned with 20% ethanol between different rats. The stimuli presented, lever operation and data collection were controlled via an interface with the computer and using custom software (MED-PC software).

2.1.3 Operant reversal task

Pretraining

The pretraining and testing protocols were adapted from our previous studies (Maggi et al., 2023; Goncalves et al., 2023) and based on original protocols by Brady and Floresco (2015) . Additionally, retention days were interleaved between reversal sessions to ensure baseline performance prior to each session. Furthermore, 20 reminder trials were included at the start of each stage, prior to rule reversal, reinforcing the same rule as the previous day, to, again, ensure strong salience of the old rule before rule reversal. The testing sequence, including reminder trials and retention days is illustrated in figure 1A. One day before pretraining, rats were habituated to the apparatus by placing them in the operant box for a fixed 15 min, with the doors of the surrounding sound attenuating wooden cabinets open and no levers extended.

Pretraining started with several days of single lever-press training, during which one of the two levers was extended for a fixed 30 min period, with each lever-press rewarded by one sugar pellet. The choice of starting lever (left or right lever) was counterbalanced across rats. The lever was switched once at least 50 responses were made in one session. On the first and second day of lever-press training, if rats did not readily approach the lever, reward pellets were placed in the magazine cup and crushed pellets on the top of the extended lever at the beginning of the session. This stage was completed after the criterion of 50 responses was met for both levers.

Lever-press training was followed by a minimum of 5 days of 90-trial retractable lever training, where rats had to respond to one extended lever within a 10 s response window, after which the lever would be retracted. Both levers were presented in a pseudo-random order, but the same lever would not be extended more than two times in a row. Each lever press was rewarded by one sugar pellet. At the end of this stage rats were expected to make 5 or fewer omissions during a 90-trial session.

On the final day of pretraining, immediately after the last 90-trial session, the side preference of each rat was determined via 7 trials consisting of several sub-trials. At the start of each main trial, both levers were extended into the chamber and the initial press was rewarded, regardless of whether the rat chose the left or right lever. Subsequent sub-trials only rewarded the first response on the opposite lever. Once the opposite lever had been pressed, the next main trial began. Therefore, each of the 7 trials consisted of one rewarded press on each lever. The side preference was determined as the ratio of left and right responses on the first main trial responses.

Spatial discrimination and reversal testing

Testing began with a simple spatial discrimination (SD) task, where rats were rewarded to press the lever opposite to their side preference established on the previous day. Trials began every 20 s, with a 10 s response window. On each trial, both levers were presented, but only the one opposite to the rats' side bias was rewarded. Each correct response was rewarded with one sugar pellet. Sessions were terminated once rats had reached a criterion of 10 consecutive correct responses. If the criterion was not reached within 150 trials, rats were retested the next day.

Following the SD stage, reversal testing was conducted on consecutive days. Each reversal stage started with 20 reminder trials, where the same lever response was rewarded as on the previous day; for example, if during the SD stage the right lever was rewarded, the right lever would also be rewarded during the reminder trials, whilst the left lever response would not be rewarded, and vice versa (see fig. 1B). The reversal occurred after trial 20, where the correct and incorrect lever were flipped, such that the lever opposite to the one rewarded on the previous day and during the reminder trials was now the correct lever and rewarded. Rats were required to reach a criterion of 10 consecutive correct trials for the stage to be completed. If the criterion was not achieved within a maximum of 150 reversal trials, the rats would continue with another reversal session (identical to the first, but without 20 reminder trials at the beginning) on the following day. Within the

present study, all rats completed all reversals within at most two sessions. All rats completed at least 10 reversal stages, with 6 of 8 rats completing 11 reversal stages.

Retention days

Interleaved with the reversal sessions were the aforementioned retention days, when rats underwent sessions where the same lever was rewarded as on the reversal trials of the previous day. Again, the criterion for successful completion was 10 consecutive correct trials. These retention days would also lend themselves as wash out days for any subsequent pharmacological studies, ensuring no carry-over effect of drugs across reversal stages.
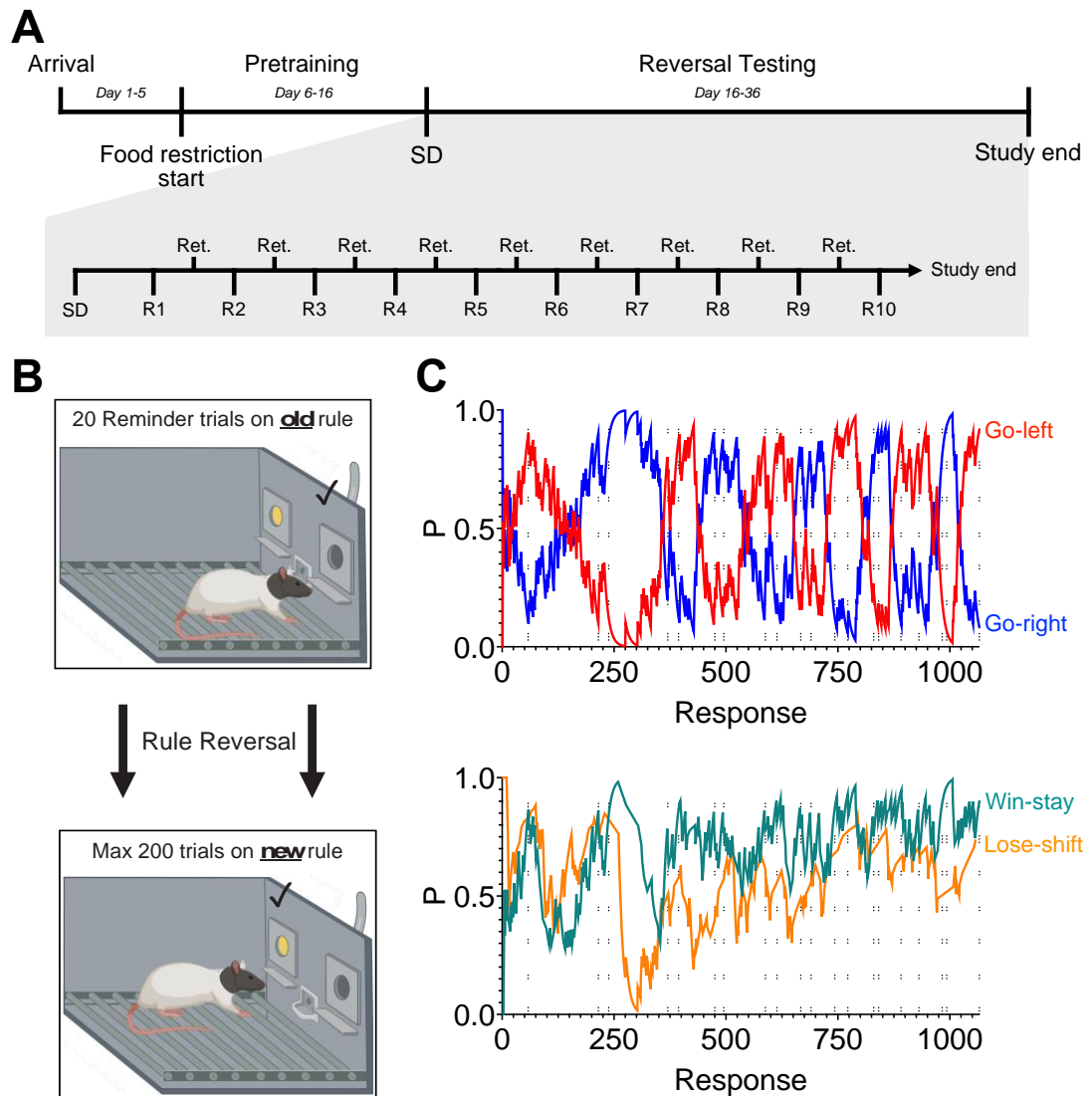
Figure 1. Serial reversal experimental design and example Bayesian strategy pattern example across all responses. A) Timeline and testing sequence for experiment 1. 'Ret.' refers to interleaved retention days between reversal stages B) Within-reversal sequence of reminder trials and rule reversal after 20 trials. C) Response strategies (go-left/right and win-stay(-spatial) and lose-shift(-spatial) plotted across all responses starting at trial 1 of the SD task and finishing at the final response of R10. Vertical dashed lines indicate session separation.

2.1.4 Data Analysis

Classical performance measures

The main measure of operant task performance was RTC (i.e., the number of trials a rat required to achieve the success criterion of 10 consecutive correct responses, excluding omission trials. RTC is not applicable for reminder trials, as there is no success criterion in place on these trials, and instead percentage-correct was used, which calculates the percentage of correct reminder trial responses divided by the total number of reminder trial responses, excluding omissions. Following the procedure outlined in Brady and Floresco (2015), we differentiated errors by type (perseverative/regressive), to examine if rats had difficulties to cease responding to the previous rule or to learn the new rule. Errors were counted as perseverative errors until a threshold of less than 10 errors in a block of 16 responses was reached. After this, all errors were counted as regressive. Average response latencies were split according to correct or incorrect responses and analysed for reminder trials and post-reversal separately, whilst SD latencies were included in the latter group due to the absence of reminder trials at that stage. Whilst omissions were removed from pre- and post-reversal RTC, only post-reversal omissions were analysed. An inclusion criterion of least three responses was in place for reminder trial analysis, as any percentages based on fewer responses would be heavily confounded. For the current experiment, all animals were included in this regard.

Trial-by-trial Bayesian strategy analysis

Complementing the use of the classical performance measures outlined above, data was analysed using a trial-by-trial Bayesian strategy analysis protocol (Maggi et al., 2023). Equation 1 describes the computation which calculated the posterior probability ($P(strategy_i(t)|choices(1:t))$) (i.e., the probability of applying strategy$_i$ at trial t) using Bayes theorem. In this regard, the likelihood ($P(choices(1:t)|strategy_i(t))$) defines the consistency of choices that we are assessing, and the prior ($P(strategy_i(t))$) described the prior probability of

applying the current strategy at a hypothetical trial '0', and thus plays a role in the initial estimation of early probabilities, defined in the range of [0,1] In the current model the prior is set to 0.5. (i.e., chance).

(eq. 1)

$$P(strategy_i(t)|choices(1:t) \propto P(choices(1:t)|strategy_i(t) \times P(strategy_i(t)$$

The protocol estimates a probability of a rat applying a particular strategy on any given trial based on evidence collected up to this trial. This is done by keeping a running total of past success or failures to execute the strategy in question, whereby positive evidence (i.e., evidence for a given strategy, such as win-stay) and negative evidence (i.e., for an opposing strategy, such as win-shift) are related to α and β values, respectively, with positive or negative evidence incrementally increasing its respective value. If no evidence is available probabilities remain the same. Evidence used to update the Bayesian model is weighted based on recency using a decay function (γ). More specifically, γ reduces α and β on every trial, and this decay is exponentially weighted by how far in the past evidence was accumulated. In the current model a γ=0.9 was used. Ultimately, the relationship between the α and β values produces an iteratively changing beta distribution, whereby the peak (i.e., the maximum *a posteriori*) is a product of the relationship between the positive and negative evidence for any given strategy at *t* based on all trials up to *t* (Maggi et al., 2023). If no evidence is present, this vale will decrease with time due to the decay function. Together, this model allows for a continuously updating estimation of strategies employed by the rats at a trial by trial resolution.

With respect to the stimulus and response data, evidence refers to task and response parameters at a trial precision (i.e., lever-press location, location of illuminated lever, accuracy of response immediately prior), relationship between which can be used to define certain rules. For example, lose-shift-spatial is defined as an incorrect response on the previous trial, followed by a response on a different lever on the current trial (*t*). Application of this strategy can be measured by searching for instances of pairs in the dataset where the response on trial *t* is unrewarded, and response on trial *t*+1 is made on the opposite lever. Similarly,

cue-light based strategies incorporate information on cue-light location to assess which strategies have been applied. In the current study, this Bayesian approach was applied to investigate two aspects of strategy employment and response pattern:

1) 'Go-previous' strategy around reversal. This indicates the trial-by-trial probability that the rat applies the strategy that was correct prior to rule change (i.e., go-right or go-left), around reversal. Typically, rats strongly apply this strategy on the reminder trials where this is the correct strategy, whereas the probability of the go-previous strategy decreases after reversal, as the rat begins to switch responses to the newly rewarded lever. Therefore, the go-previous strategy captures perseveration around rule change at a trial-by-trial resolution, as rats struggle to move away from the previously rewarded, but now incorrect response.

2) Learning-specific strategies. These can be divided into task-pertinent strategies and task-inappropriate strategies. The former includes win-stay-spatial and lose-shift-spatial, which describe either 'stay' behaviour on the same spatial rule (i.e., same lever) following a 'win' (rewarded)-trial, and 'shift' behaviour to the opposite spatial rule following a 'lose' (unrewarded)-trial. Task-inappropriate strategies include 'alternate', where a rat is continuously switching between the left and right lever, regardless of reward; 'win-stay-cued', where a rat's response choice depends on the cue light, such that, following a win-trial, the same cued option is selected on the following trial (for example, unlit lever followed by unlit lever, or lit lever followed by lit lever); 'lose-shift-cued', where, in contrast to win-stay-cued, the opposite cue option is selected following a lose-trial (for example, lit lever followed by unlit lever, and vice versa). Importantly, in our task the cue light was not indicative of any reward, meaning both strategies were not appropriate for task success. See figure 1C for example plots of win-stay-spatial and lose-shift-spatial across all measured responses between SD and R10.

Finally, subsequent analyses of Bayesian strategy probabilities focussed on trials that were completed by all rats. Therefore, for experiment 1 analysis was a cut-off

at 25 trials post-reversal, because this was the minimum number trials completed by all rats across all sessions. When interpreting outcomes of the Bayesian strategy analysis it is important to consider that strategies are not mutually exclusive, for example, any win-stay-spatial trial may also alter the probability of other exploratory strategies. As such, changes in the probabilities of strategies that are not dominantly applied (i.e., whose probability is around chance, 0.5) need to be interpreted in context of other, dominant, strategies (>0.5). Additionally, only one of two complementary strategies (e.g., win-stay and win-shift) was examined here, as both equal to P=1 the opposite strategy would always mirror the investigated strategy.

Statistical analysis

Data was analysed by repeated-measures ANOVA, using stage as a within-subjects factor. Where the assumption of sphericity was violated, Greenhouse-Geisser correction was applied to the degrees of freedom. Following a significant main effect of stage, pairwise comparisons between stages were conducted via Fisher's LSD test. As two rats did not reach R11, significantly reducing the power at that stage, analysis was restricted to R1-R10. In addition, SD was excluded from Bayesian strategy analysis, as the main aim was to find a period of relatively stable, asymptotic reversal performance (i.e., no change between reversal stages).

2.2 Results

Classical reversal measures stabilise across stages

As expected, a significant reversal cost, as indicated by increased RTC and reduced percentage-correct, was observed at R1 and R2, compared to the SD stage (fig. 2A and B). Subsequent reversal performance began to improve markedly around R3 and plateaued from around R5. In particular, there was no change between adjacent reversal stages after R5 in terms of perseverative errors, with a fluctuation only observable in the number of regressive errors. This suggests that any observed changes in overall RTC were due to variable regressions in learning,

and less due to between-stage reversal performance differences. In support of these observations a 1-way repeated-measures ANOVA revealed a significant effect of task stage on RTC ($F_{(3.058, 21.405)}$=20.546, $p<0.001$) and percentage-correct ($F_{(2.931, 20.515)}$=7.159, p=0.002). Pairwise comparisons of RTC revealed significant differences between sequential sessions, from SD to R6 (highest p=0.045), excluding the difference between R1 and R2 (p=0.82) and R3 and R4 (p=0.211). With respect to percentage-correct a significant difference was found between all consecutive sessions up to R5 (highest p=0.38), except between R3 and R4 (p=0.90).

Perseveration stabilises from R4, indicating plateauing of reversal performance

In order to understand the changes in performance measures further, error type was analysed across the 10 reversal stages, with perseverative errors indicating difficulties moving away from the previous rule (fig. 2C), whilst regressive errors indicate difficulties engaging in behaviour facilitating learning of the new rule (fig. 2D). Perseverative errors were very high at R1 and R2, contributing substantially to the very high RTCs at these stages. Regressive errors on the other hand were much lower and relatively stable already. There is a rapid decrease in perseverative errors at R3, which begins to level off with no changes between R5-10. Regressive errors decrease slightly at R2 and remain relatively stable with a few fluctuations at R6 and R7, probably mainly reflecting variability. This suggests increased RTC following R5 are not a product of perseveration, but rather individual variability in learning rate. Two 1-way repeated measures ANOVA revealed a significant main effect of reversal stage on perseverative errors ($F_{(9, 63)}$=21.596, $p<0.001$), as well as regressive errors ($F_{(9, 63)}$=4.514, $p<0.001$). Pairwise comparison, however, revealed that the former effect was due to a significantly higher perseveration between R1-R4 compared to all other stages (highest p=0.039). From R5 onwards, no significant difference in terms of perseverative errors was observed between any stages (lowest p=0.456). With regards to the effect of stage on regressive errors, pairwise comparisons revealed significantly higher errors at R1 compared to all other stages (highest p=0.028), except R2 (p=0.120). Between R3 and R10 regression remains relatively stable,

with a few fluctuations due to significantly lower regression at R8 and R9, compared to R1, R4 and R6 (highest p=0.038). These findings indicate that the fluctuations between R5 and R10 are due to variable rates of non-specific learning deficits between rats, instead of explicit differences in reversal learning.

Reminder trial and retention day performance did not fluctuate across all stages indicating strong expression of rule prior to rule change

Reminder trial performance, as reflected by percentage-correct across the 20 reminder trials, indicated very good expression of the previous rule before rule change, which was consistent across subjects and across all 10 reminder trials stages. The average performance was 81.1±1.0% (*SEM*) correct. A 1-way repeated-measures ANOVA confirmed that stage did essentially not affect reminder trial performance (F<1). Performance on retention days, as reflected by RTC, also did not fluctuate across stages, with rats requiring an average of 28.1±1.4 (*SEM*) trials to complete these sessions (1-way repeated-measures ANOVA; F<1). These findings indicate that, after the success criterion is reached, the rule remains salient the following day, and is then expressed strongly during the reminder trials prior to rule change on the next day.
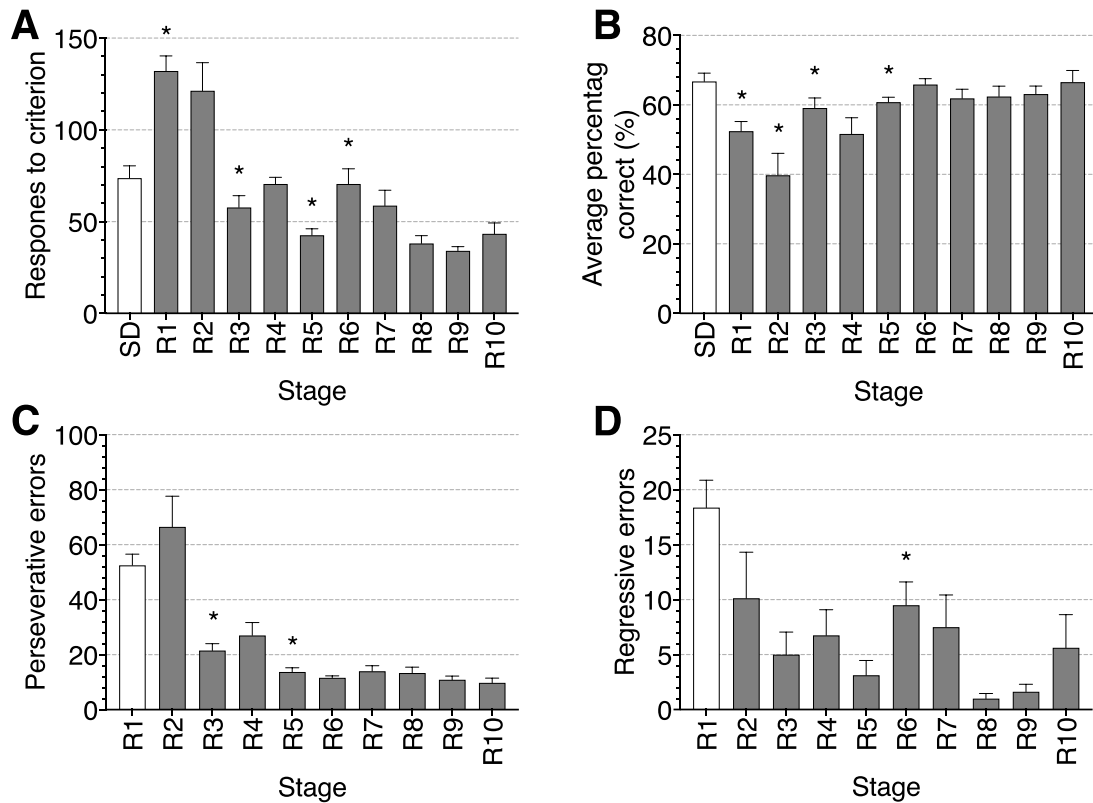
Figure 2. Summary of performance data for experiment 1. Average RTC (A), average percentage-correct for each stage (B), perseverative errors (C), and regressive errors (D). Error bars indicate +*SEM*. Asterisks above bars indicate significant difference to previous stage.

Omissions and reminder trial latencies decrease with stage whilst post-reversal latencies remain stable

Omissions were overall low, but numerically markedly higher during R1 and R2 (average 1.6±0.98 (*SEM*), and 2.0±1.90 (*SEM*), omissions, respectively), Whilst a 1-way repeated-measures ANOVA did not find a significant effect of stage ($F_{(9, 63)}$=1.722, *p*=0.102), this may simply be due to the fact that this study was not powered to observe such subtle effects (observed power=0.729). Reminder trial response latencies were greatest at R1, in particular with respect to incorrect latencies, but then decrease with task stage. A 2-way ANOVA using stage and accuracy as factors revealed a significant main effect of stage ($F_{(9, 36)}$=2.162, *p*=0.049). No main effect of accuracy or stage x accuracy interaction was observed

42

$((F_{(1, 4)}=5.671, p=0.076)$ and $(F_{(9, 36)}=1.985, p=0.070)$, respectively). With regards to post-reversal latencies, no main effect or interaction was found (greatest $F_{(10, 70)}=1.729, p=0.091$). However, as seen in the omissions, observed power was very low (greatest power=0.798), limiting the interpretation of these results.

Rats more readily abandoned the previous rule at later reversal stages, plateauing between R5 and R10

Using the Bayesian strategy analysis, we assessed how strongly rats pursued the strategy that was correct prior to rule change (i.e., go-previous) (fig. 3). A clear dissociation between reversal stages can be seen around the rule change in terms of how strongly rats adhere to the go-previous strategy. During R1 and 2, rats continued to apply the previous rule very strongly even at 25 responses post-reversal, indicating sustained perseveration and corroborating the findings of increased perseverative errors on those stages. Probability of the go-previous strategy was reduced, but remained high, after rule change during R3 and R4. However, from R5 rats more quickly abandoned the go-previous rule during the 25 responses following the rule reversal, indicated by a steeper decline post-reversal. Supporting the finding that rats more quickly abandoned the previous strategy during later reversal stages, a 2-way repeated-measures ANOVA, using reversal stage (R1-10) and trial as factors, revealed a stage x trial interaction ($F_{(315, 2205)}=1.268, p=0.002$). However, when R1-R4 were removed, and analysis was restricted to R5-10, this interaction disappeared ($F<1, p=1$), and there was also no main effect of stage ($F_{(5, 35)}=1.711, p = 0.158$). Only an effect of trial was present ($F_{(35, 245)}=19.818, p<0.001$), reflecting that rats abandoned the go-previous strategy during the 25 responses following rule reversal. The absence of a stage x trial interaction indicates that between reversal stages 5-10, rats reversed similarly well.
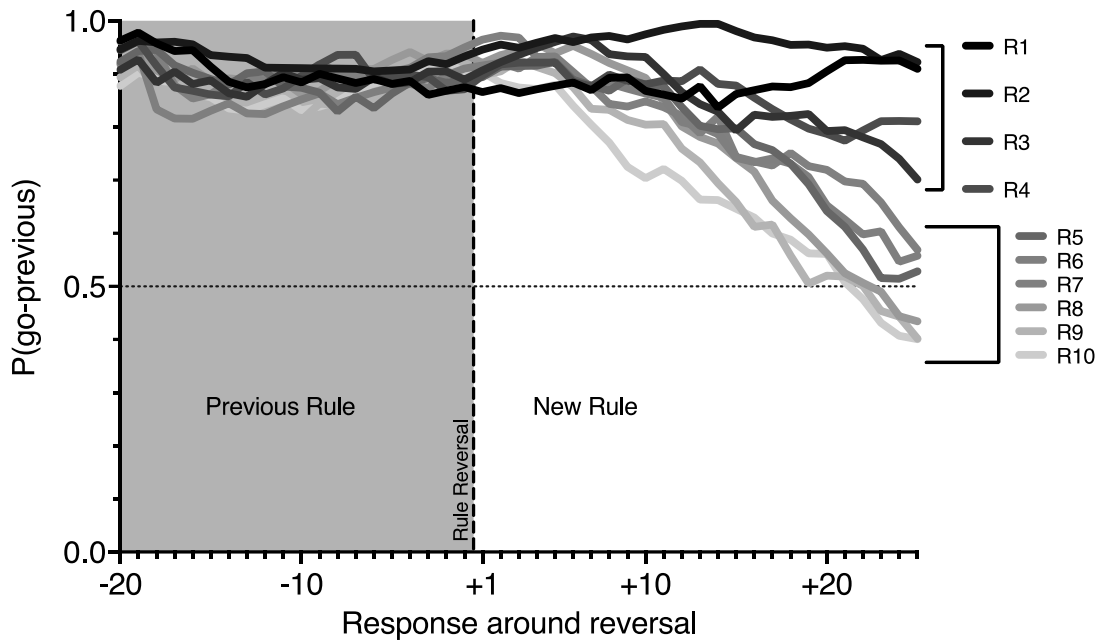
Figure 3. 'Go-previous' strategy implementation around reversal between R1-10. Colour indicates reversal stage (darker=earlier). Grey-shaded region indicates reminder trial performance. Vertical dashed line indicates rule reversal.

Qualitative evaluation of learning-specific strategies across reversal stages

Further to the analysis of go-previous, we intended to also analyse strategy indicating specific behavioural patterns driving learning, as well as strategies that may indicate 'random' task inappropriate behaviour, across R1-10. Specifically, we looked at R1, R5 and R10, as R1 and R10 are the best examples for unfamiliar and established reversal performance, whilst RTC data indicated R5 was a good intermediate point. We expected to see a general change across strategy implementation across these three stages, ending with high probabilities of task-pertinent strategies at R10. When looking at exploratory strategies across these stages (see fig. 4), several patterns become apparent. First, when faced with the rule change in early sessions, rats orientate themselves towards cue-based strategies, at the expense of spatial strategies (i.e., based on lever position, left or right), even though they had previously learnt that cue-based strategies do not support task success (see win-stay-cued and lose-shift-cued at R1 and R5). This

ineffective behavioural strategy choice can be linked to poorer task performance, as reflected by higher RTC, particularly at R1. Second, at R5, there is a general trend in all strategies toward chance, reflecting a reduction in optimal strategy application and an increase in the application of sub-optimal strategies. Third, and contrary to the classical performance measures and the probability of the go-previous strategy, there is still substantial change in the exploratory strategy profiles from R5 to R10.

Figure 4. Learning-specific strategies around reversal at R1, R5 and R10. ±*SEM* indicated by shaded region around data. Grey-shaded region indicates reminder trial performance. Vertical dashed line indicates rule reversal.

2.3 Discussion

This behavioural study set out to adapt a two-lever reversal task for rats (Brady & Floresco, 2015) to a serial reversal learning procedure that is suitable to test the impact of phar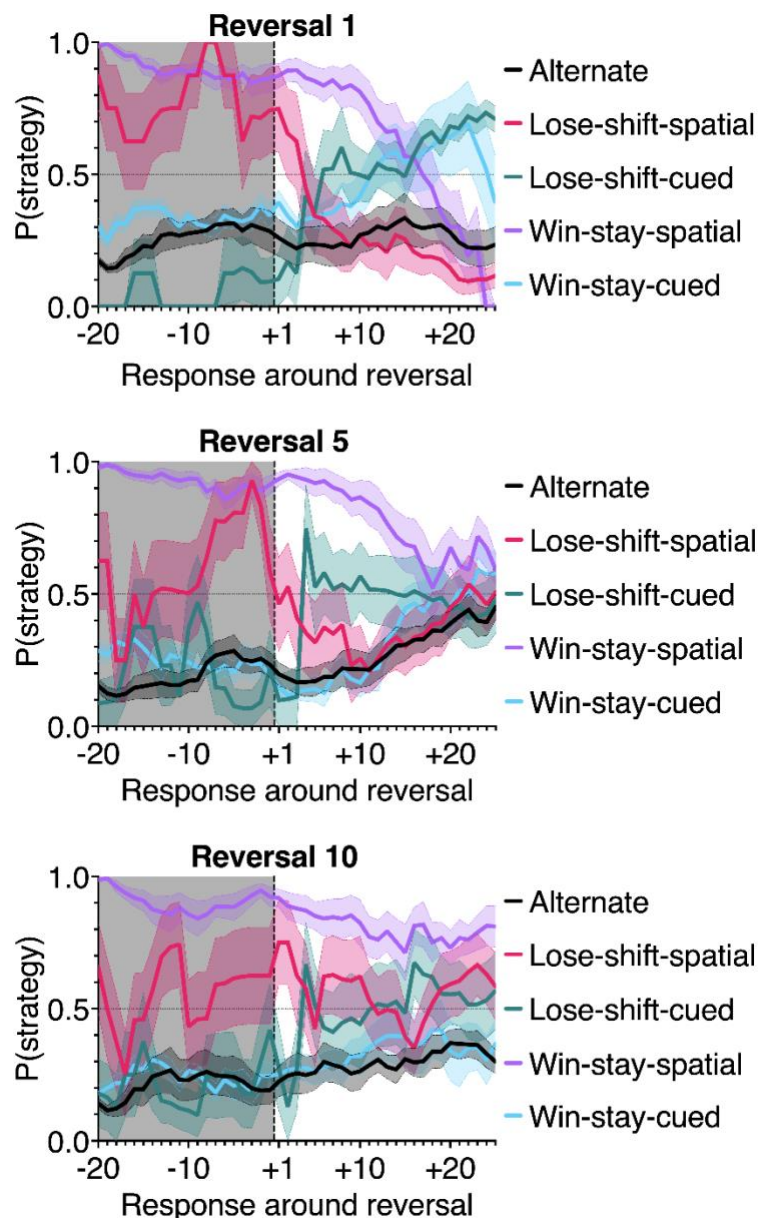macological manipulations in a within-subject design. The main aim was to find a series of sequential reversal stages where performance is stable enough for potential future drug infusions. Additionally, we aimed to apply a new Bayesian approach of trial-by-trial strategy analysis (Maggi et al., 2023) to our reversal learning data. Results showed that, following a large initial reversal cost at R1 and R2 when performance was markedly poorer compared to the initial SD stage, relatively stable reversal performance was reached between R5 and R10. RTC data indicated slight fluctuations at R6 and R7. However, error analysis indicated that these fluctuations were due to individual differences in new learning, whereas no marked changes in perseverative behaviour (as reflected by perseverative errors) were evident beyond R5. This finding was supported by Bayesian trial-by-trial strategy analysis of 'go-previous' which showed similar speeds of previous-rule abandonment across R5-10. This experiment also demonstrated the respective strengths and shortcomings of classical performance measures for the current task. Whilst RTC lends itself well to the overall performance, percentage-correct is more applicable when analysing the reminder trial performance, as its value is restricted by the success criterion. Finally, the inclusions of reminder trials and retention days proved valuable in maintaining baseline performance prior to rule change.

Complementing the classical performance measures, the Bayesian trial-by-trial strategy analysis offered additional information on how rats perseverative behaviour changed across repeated reversals, indicated by a difference in abandonment of the previous rule around rule change, and provided an insight into the changes in exploratory strategy implementation. With regards to the learning-specific strategy implementation, strategy stabilisation is observable between R1-R10 (fig. 4). For example, at R1, task-pertinent strategies such as lose-shift-spatial and win-stay-spatial show marked decreases after reversal to below chance, indicating application of the opposite strategy (i.e., lose-stay and win-

shift), whilst application of lose-shift-cue is increased, indicating an increased focus on the pseudorandom, irrelevant cue lights, which may reflect that rats 'tested out' cue-based strategies. However, at R5 this pattern had already partly recovered. Although win-stay-spatial responding still decreased after the rule reversal, this decrease was less pronounced than during R5 and the probability of this strategy never went below chance. Similarly, lose-shift-spatial, which has been suggested to be particular important for new rule learning (Maggi et al., 2023), showed a dramatic dip prior to reversal, which is recovered very quickly. This may simply reflect variability due to the low sample size used in this experiment. At this point, no cue-based strategies exceed chance, suggesting these are merely side effects of spatially oriented win-stay or lose-shift behaviour. Finally, at R10 task pertinent strategies had stabilised, indicating that rats had learned to respond to the rule change in a more adaptive and effective way by maintaining task-appropriate strategies.

In the present study, we only applied the Bayesian strategy analysis to the first 45 trials at each reversal stage (20 reminder trial, plus 25 reversal trials), as this was the minimum number of trials completed by every rat on every session. Therefore, we cannot rule that marked changes in exploratory strategies may still have occurred for trials that were omitted here (e.g., late trials particularly in early sessions). However, it is these first trials following rule change that provide the biggest indication of how quickly a subject can switch between rules, particularly in shorter sessions, such as here between R5-R10.

Based on the current findings, one can split reversal learning on our two-lever task into two distinct phases. There is an 'early' reversal phase, referring to R1-R4, where the rats encountered the reversal problem for the first time during R1 and then gradually learns to 'reverse' responding more efficiently. Across R1-R4, reversal performance fluctuates greatly. It is plausible that the mPFC may be required for this initial reversal acquisition, due to its involvement in executive control and overcoming prepotent behavioural responses (Bussey et al., 1997; Miller and Cohen, 2001; Haddon and Killcross, 2006; Marquis et al., 2007; Alexander and Brown, 2010). Furthermore, the current findings highlighted a

second phase of reversal learning, when rats have received substantial reversal training, during which they have 'learned to reverse' efficiently, and when they show efficient and relatively stable performance across several repeated/serial reversals. During this late reversal phase, the requirement for contribution of the mPFC may diminish due to diminished requirement of executive control, although prefrontal disinhibition may still cause performance impairments by disrupting processing in projection sites that may be relevant to repeated reversal performance. The following chapter will implement this novel serial reversal paradigm, alongside a classic early reversal design to investigate the impact of mPFC disinhibition and functional inhibition on each type of reversal learning.

3 Dissociable effects of prefrontal functional inhibition and disinhibition on early and established reversal learning

Declaration: Charlotte Taylor and Joanna Loayza assisted during surgeries and transcardial perfusions. Rachel Grasmeder Allen and Luke O'Hara contributed to data collection. Silvia Maggi ran the Bayesian analysis code.

As outlined in chapter 1 and 2, reversal learning has mainly been associated with the OFC, whereas many studies suggest that the dlPFC in primates or the mPFC in rodents, which shares functional-anatomical properties with the dlPFC (Uylings, 2003; Brown & Brigman, 2003; Laubach et al., 2018), is less important for reversal learning (Leeson et al., 2009; Izquierdo et al., 2017). Key evidence for this comes from lesion and pharmacological inactivation studies showing that OFC, but not dlPFC or mPFC was required for reversal learning (Dias et al., 1996; Chudasama & Robbins, 2003; Boulougouris et al., 2007; Floresco et al., 2008; Hervig et al., 2020). In this chapter, I present pharmacological evidence challenging this consensus.

This chapter comprises of two key pharmacological investigations examining the role of mPFC GABA activity on two variations of the operant reversal task. Experiment 2 is an 'early' reversal task, where performance is tested in a between-subjects design, where selected manipulations are administered on consecutive days without retention days (e.g., Enomoto et al., 2011; Floresco et al.., 2008; Rygula et al., 2015), Experiment 3, follows the same testing sequence as in the previous chapter, measuring 'established' reversal performance once rats have reached a performance plateau. Of particular interest was the examination bi-direction manipulation of mPFC GABAergic activity, to discern a potential contribution of coherent inhibitory control within the PFC. As such, we tested the effects of prefrontal functional inhibition and disinhibition via microinfusion of the GABA$_A$ receptor agonist muscimol or antagonist picrotoxin, respectively (Pezze et al., 2014).

The rationale for this investigation is two-fold. As described previously GABA plays a critical role in the shaping of neural activity via its involvement in burst firing, thus being a cornerstone for cortical inter-region communication (Lisman,

1997). Additionally, mPFC disinhibition has recently been shown to induce aberrances in local burst firing and LFP traces (Pezze et al., 2014), which have been shown to disrupt, not only local functioning, but functioning in projection sites as well (Bast et al., 2017). As the rodent mPFC is highly connected, projecting to downstream areas of the cortico-striatal network more directly involved in reversal learning, including the OFC (Sesack et al., 1989), we suggest mPFC disinhibition, resulting in aberrant neural firing may drive aberrant projections and, in turn, disrupt functioning in these projection sites.

Viewing this disinhibition hypothesis from a clinical perspective, evidence from schizophrenia suggests a role of such aberrant projections in driving robustly observed reversal learning impairments. Specifically, patients with first-episode schizophrenia have been shown to exhibit marked impairments on the reversal aspects of the Cambridge Neuropsychology Test Automated Batter (CANTAB) alongside extradimensional attentional set shifting impairment (Murray et al., 2008; Leeson et al., 2009). However, strikingly only simple reversal deficits persisted when retested at all three stages (1-, 3-, and 6-years) after the initial task. Whilst the attentional set-shift impairments are in line with the hypothesis of a dysfunctional dlPFC, with the dlPFC being directly implicated in this type of set shifting (Hampshire & Owen, 2006), the reversal deficits are less well understood. As outlined in chapter 1, human neuroimaging studies, much like animal studies, have linked reversal learning to OFC function (Nagahama et al., 2001; Remijnse et al., 2005; Hampshire et al., 2012), yet schizophrenia is not commonly associated with OFC deficits. Instead, there is compelling and consistent evidence for a substantial deficit in the synthesis and ultimately concentration of dlPFC GABA in schizophrenia, such as reduced GAD_{67} activity (Bennett et al., 1979; Bird, 1985; Hanada 1987; Akbarian et al. 1995; Guidotti et al., 2000; Volk et al., 2001; Lewis et al., 2005), and several protein mRNA markers, including PV, cholecystokinin, somatostatin, and calretinin, within the inhibitory interneurons of patients (Hashimoto et al 2003; Fung et al., 2010). Finally, several imaging studies have highlighted substantial reductions in cortical GABA concentrations in patients compared to controls (for review see Simmonite et al.,

2023). These deficits likely result in a state of neural disinhibition, which may result in the hypothesised aberrances in neural projections.

Further consolidation of the reversal impairments in schizophrenia raises one more interesting point of consideration. Alongside the substantial *post-mortem* evidence for a inhibitory deficit in schizophrenia, several neuroimaging studies have also shown significant hypo-activity within the dlPFC, termed 'hypofrontality' (Ingvar & Franzen, 1974; Carter et al., 1998; Minzenberg et al., 2009, Ortiz-Gil et al., 2011). Whilst findings of hypofrontality remain equivocal across many studies (for an overview see Roberts et al., 1998, chapter 12), evidence for activation hypofrontality in tasks of executive function, such as the Wisconsin Card Sorting Task (Weinberger et al., 1986) or the Tower of London test (Andreasen et al., 1992), are more robustly observed than resting state hypofrontality (Hill et al., 2004). Although animal literature supporting a role of the mPFC in reversal learning is sparse, there seems to be a common trend in the work supporting an involvement. Specifically, mPFC lesions impaired reversal learning when task difficulty was particularly high, which was suggested to reflect a higher demand on mPFC-mediated attentional processes (Bussey et al., 1997; Kosaki & Watanabe, 2012). Therefore, we included a test for functional inhibition, via GABA agonist muscimol, in order to probe for a potential difference in drug effect during unfamiliar task stages of Experiment 2, where demands on attention may be increased, and established performance in Experiment 3, where task proficiency and greater understanding of task demands may result in lower demands on such mPFC-mediated processes.

In the context of the current chapter, comparing the effect of bi-directtional GABA manipulations of early and serial reversal performance, we hypothesised that, although not directly required, mPFC disinhibition may, may disrupt reversal learning, because disinhibition may cause aberrant prefrontal neuron firing and, thereby, disrupt processing in prefrontal projections sites (Bast et al., 2017), including the OFC (Sesack et al., 1989). Furthermore, early reversal learning may differently depend on the mPFC, as early reversal performance may require more mPFC-dependent attention, compared to the serial reversal task. Furthermore, the

mPFC has been implicated in overcoming prepotent behavioural responses (Miller and Cohen, 2001; Haddon and Killcross, 2006; Marquis et al., 2007), which may be particularly relevant at early stages of reversal learning. These considerations would indicate an effect, if any, of mPFC functional inhibition on the early reversal task.

3.1 Methods and materials

3.1.1 Rats

In total, 64 young adult male Lister hooded rats (Envigo, UK) were used, weighing 290-340 g (8-9 weeks old) at surgery, (10-11 weeks at the start of pretraining). In experiment 2, 48 rats were tested in two cohorts of 24 rats, whilst experiment 3 used a single batch of 16 rats. In experiment 2, one rat died unexpectedly following surgery with another rat culled due to complications with the cannula implant prior to testing. In experiment 3, three rats were culled due to complications with the cannula implant resulting in final N of 59 across both studies (experiment 2, N=46; experiment 3, N=13). See section below, experimental design, for further details and sample size justification. Animal housing and feeding schedule were identical to chapter 2. All procedures were conducted in accordance with the United Kingdom (UK) Animals (Scientific Procedures) Act 1986.

3.1.2 Prefrontal cannula implantation

Rats were anesthetized with isoflurane (induction: 3%; maintenance: 1-3%) delivered in medical oxygen (1 L/min). Once induced, rats' scalps were shaved and all rats received subcutaneous (s.c.) injections of analgesia (0.1 ml/100 g Rimadyl; Zoetis, UK, diluted 1:9 with sterile saline, 0.9%) and antibiotics (0.02 ml/100 g Synulox containing 14% Amoxicillin; Zoetis, UK). Rats were transferred to the stereotaxic frame where they were secured in the horizontal skull position with ear bars coated with local anaesthetic cream (EMLA 5%, containing 2.5% lidocaine and 2.5% prilocaine; AstraZeneca, UK). Eye gel (Lubrithal, Dechra, UK) was applied to the eyes to prevent drying out during surgery, and the shaved scalp

was disinfected with alcoholic skin wipes (2% clorhexedine, 70% alcohol; Clinell, UK). Throughout the surgery, body temperature was maintained at 37 °C via a homeothermic heating pad controlled by an external temperature probe placed under the rat.

A small anterior-posterior incision was made into the scalp to expose the skull, and bregma was located. Two small holes were drilled through the skull at the following coordinates: +3 mm anterior and ±0.6 mm lateral from bregma (based on Pezze et al. 2014). Bilateral infusion guide cannulae ("mouse" model C235GS-5-1.2; Plastics One, Bilaney Consultants, UK) were used, consisting of a 5 mm plastic pedestal that held two 26-gauge metal tubes, 1.2 mm apart and projecting 4.5 mm from the pedestal. The guide cannulae were then lowered to -3.5 mm ventral from the skull surface and secured to the skull with dental acrylic (Kemdent, UK) and stainless-steel screws (1.2 mm x 3 mm; MDK Fasteners, UK). Non-protruding double stylets (33 gauge; Plastic One, Bilaney Consultants, UK) were inserted into the cannulae and a dust cap was secured on top. At the end of surgery, rats were injected with 1 ml of saline (s.c.) to minimize the risk of dehydration. Following surgery, rats continued to receive daily antibiotic injections for the duration of the study to reduce the risk of meningitis. Rats were allowed to recover for at least 7 days before the start of food restriction and pretraining.

3.1.3 Prefrontal drug microinfusions

Drug doses and infusion parameters were based on our previous studies, where both prefrontal picrotoxin and muscimol infusions caused marked attentional deficits on the 5-choice serial reaction time task (Pezze et al., 2014). Rats were gently restrained to insert 33-gauge injectors (Plastics One, Bilaney Consultants, UK) into the previously implanted prefrontal guide cannulae. The injectors protruded 0.5 mm below the guides into the mPFC, resulting in the following target coordinates for the infusions: +3 mm anterior and ±0.6 mm lateral from bregma and 4 mm ventral from skull. The injector ends were connected via polyethylene tubing to two 5 μl syringes (SGE, World Precision Instruments, UK)

secured on a micro-infusion pump (sp200IZ, World Precision Instruments, UK). Prior to infusions, the tubing and syringe were backfilled with distilled water and an air bubble was included before any drug solution was pulled up. A volume of 0.5 μl/side of either 0.9% sterile saline (vehicle), GABA$_A$-receptor antagonist picrotoxin (300 ng/0.5 μl/side, $C_{30}H_{34}O_{13}$, Sigma-Aldrich, UK) in sterile saline, or agonist muscimol (62.5 ng/0.5 μl/side, $C_4H_6N_2O_2$, Sigma-Aldrich, UK) in sterile saline was administered over the span of 1 min. Movement of the air bubble within the tubing was monitored to ensure solutions had been successfully injected into the brain. After the initial infusion, injectors were kept in the guides for one additional minute to allow for absorption of the infusion bolus by the surrounding brain tissue. Testing began 10 min after the infusion was complete.

3.1.4 Operant reversal task

The pretraining and serial reversal protocol for experiment 3 were identical to the previous chapter. In contrast, experiment 2 examined the initial SD and subsequent 5 reversal stages. Importantly, this experiment did not involve retention days. Therefore, following a successful rule reversal, rats received successive reversal tasks on the following day. Finally, following findings of experiment 1, the maximum number of post-reversal trials was increased to 200 for experiment 2 and 3 to account for potential drug effects in RTC. All other task parameters (e.g., reminder trials, success criterion etc. were identical between experiments).

3.1.5 Experimental design

Experiment 2 compared the impact of prefrontal disinhibition by picrotoxin, inhibition by muscimol and saline infusion during early stages of the reversal paradigm (SD and R1-5) in a between-subjects design. Our target sample size was calculated as n=16 per group to give a power of >80% for pairwise comparisons (two-tailed independent t-tests, p<0.05), to detect differences between infusion groups that correspond to an effect size of Cohen's d of around 1 (G*Power, Faul et al., 2007). Rats were allocated to one of three infusion groups - saline, picrotoxin

or muscimol - via a randomised block design, with at least one rat in each cage of four being allocated to each infusion group. Furthermore, experiment 2 was run as a sequential design (Neumann et al., 2017), using two cohorts of 24 rats. After the unexpected complications requiring termination of two rats, the final N for experiment 2 was 46 (saline=n: 15; picrotoxin n=15; muscimol n=16), which still satisfied the above power requirements. To test the impact of prefrontal disinhibition and inhibition during early stages of the reversal paradigm, rats received their allocated drug infusions prior to each of their first six sessions, starting with SD training and continuing up to R5. Statistical analysis was restricted to SD and R1-3, as these were the sessions completed by all rats, with only 8 rats in the picrotoxin group successfully completing all 5 reversals.

Experiment 3 compared the impact of prefrontal disinhibition, inhibition and saline infusion on serial, well-established, reversal performance in a within-subjects design. Target sample size was N=12-16 rats. Sample size was determined to achieve the same statistical power as in experiment 2. Appropriate infusion stages were based on findings from experiment 1 (chapter 2), where stable reversal performance was observed starting at R5. Each rat received two series of the three different infusions (saline, picrotoxin, muscimol), with infusion series 1 consisting of infusions before R5-7 and infusion series 2 consisting of infusions before R8-10. Testing order of the three infusion conditions was counterbalanced within each series using a Latin square design. Individual rats were randomly allocated to one of three testing orders, ensuring that at least one rat in each cage of four rats was allocated to each of the three testing orders. The inclusion of retention days between infusion days controlled for any carry-over effects before the next drug infusion was tested. Figure 5 shows the running order of sessions and when infusions were administered in both experiment 2 and 3.
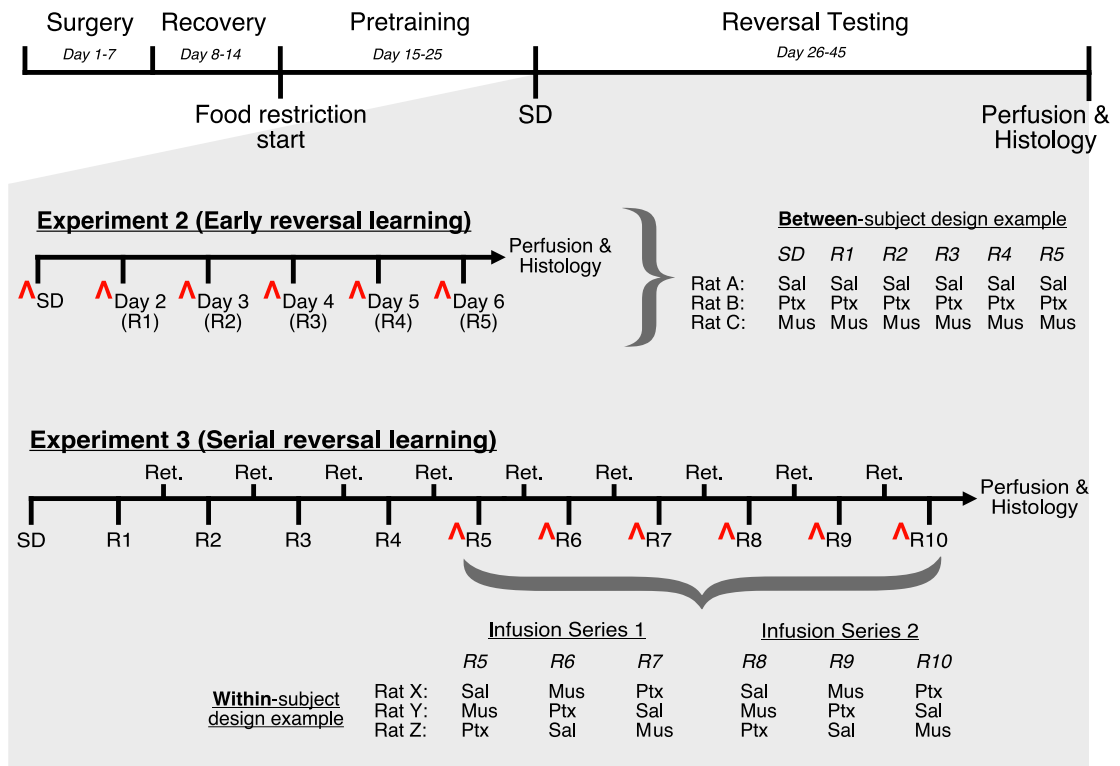
Surgery | Recovery | Pretraining | Reversal Testing

Day 1-7 | Day 8-14 | Day 15-25 | Day 26-45

Food restriction start | SD | Perfusion & Histology

Experiment 2 (Early reversal learning)

Perfusion & Histology

^SD ^Day 2 (R1) ^Day 3 (R2) ^Day 4 (R3) ^Day 5 (R4) ^Day 6 (R5)

Between-subject design example

	SD	R1	R2	R3	R4	R5
Rat A:	Sal	Sal	Sal	Sal	Sal	Sal
Rat B:	Ptx	Ptx	Ptx	Ptx	Ptx	Ptx
Rat C:	Mus	Mus	Mus	Mus	Mus	Mus

Experiment 3 (Serial reversal learning)

Ret. Ret. Ret. Ret. Ret. Ret. Ret. Ret. Ret.

SD R1 R2 R3 R4 ^R5 ^R6 ^R7 ^R8 ^R9 ^R10

Perfusion & Histology

Infusion Series 1 | Infusion Series 2

Within-subject design example

	R5	R6	R7	R8	R9	R10
Rat X:	Sal	Mus	Ptx	Sal	Mus	Ptx
Rat Y:	Mus	Ptx	Sal	Mus	Ptx	Sal
Rat Z:	Ptx	Sal	Mus	Ptx	Sal	Mus

Figure 5. Experimental timeline for pharmacological reversal experiments. Red '^' indicate microinfusions. Experiment 2 (between-subjects, early reversal) combined manipulations with testing in reversal-naïve rats between SD and R5, whilst experiment 3 (within-subjects, serial reversal) introduced manipulations once task parameters had been learnt. Retention days were included between reversal stages for experiment 3. Within-session reversal followed the same principle as outlined in figure 1C. Examples of between- and within-subject infusion schedules for three example subjects are included adjacent to timelines.

3.1.6 Verification of cannula placements

After the completion of the experiments, rats were overdosed with sodium pentobarbitone (1–2 ml Euthatal; sodium pentobarbitone, 200 mg/ml; Genus Express, UK) and transcardially perfused with 0.9% saline followed by 4% paraformaldehyde solution in saline. Following extraction, brains were post-fixed in 4% paraformaldehyde, and cut into 70 μm coronal sections using a vibratome (Leica, UK). Sections were then mounted on slides and analysed under a light microscope, where cannula tip placement was verified and mapped onto coronal

56

sections of a rat brain atlas (Paxinos and Watson, 1998), for example see figure 7A.

3.1.7 Data Analysis

Data analysis followed the same pattern as in the previous chapter, with examination of classical measures first, followed by trial-by-trial analysis of strategy profiles. With respect to strategy patterns examined via the Bayesian model outlined previously, some strategies were examined (e.g., cue-based strategies), but these did not differ from chance level (0.5) and were therefore omitted here. Bayesian analysis focussed on 6 responses prior- and 16 responses post-reversal. Finally, many rats in the picrotoxin group in experiment 2 failed to reach the inclusion criterion of 3/20 reminder trial responses, and as such were excluded from analysis of reminder trials. Due to this low response rate, picrotoxin was excluded from subsequent strategy analysis due to potential group differences in reinforcement of the old rule prior to rule change.

Statistical analysis

Data was analysed by ANOVA. In experiment 2, infusion group (saline, picrotoxin, muscimol) and stage (SD, R1-3) were used as between-subjects, and within-subject factors, respectively. In experiment 3, infusion condition (saline, picrotoxin, muscimol) and infusion series (1 and 2) were also used as within-subject factors. Analysis of strategy profiles also included trial as an additional factor. Where the assumption of sphericity for within-subjects ANOVA was violated, Greenhouse-Geisser correction was applied to the degrees of freedom. Simple main effects were further examined by pairwise comparisons using Fisher's LSD test. To control for differences between sequential experiments in experiment 2, we performed several 2-way ANOVA using infusion group and cohort as factors with no significant differences or interactions in the variables of interest between cohorts (all $F<1$).

3.2 Results

3.2.1 Cannula placements within medial prefrontal cortex

In both experiments, all infusion cannula tips were placed within the mPFC in an area that corresponded approximately to +2.7 to +4.2 mm anterior to bregma in the atlas by Paxinos and Watson (1998) (fig. 6B).
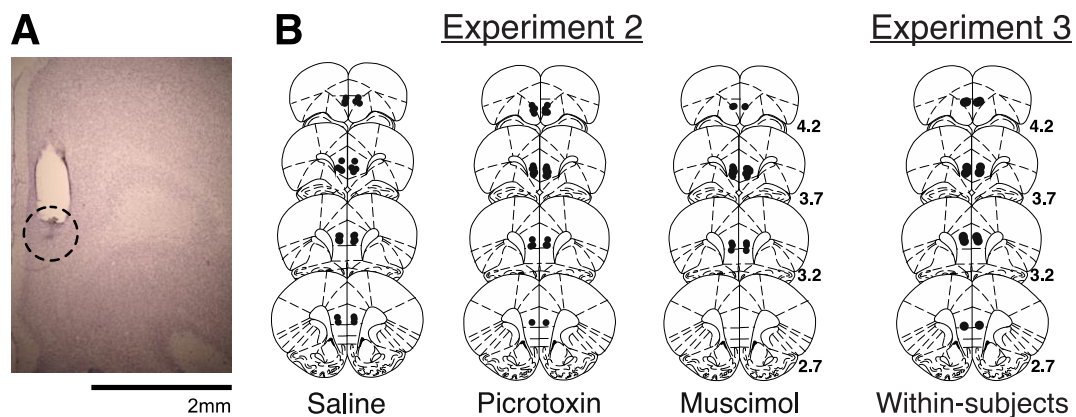
Figure 6. Infusion cannula placement in the medial prefrontal cortex. A) Cresyl-violet-stained coronal brain slice depicting an injector tip placement in the prelimbic cortex. The dashed circle highlights gliosis used to determine tip location. B) Approximate locations of infusion cannula tips (black dots) for experiment 2 (separated by infusion group) and experiment 3 shown on coronal plates adapted from the atlas by Paxinos and Watson (1998). Distance (in mm) from bregma is indicated by numbers on the right.

3.2.2 Experiment 2: Prefrontal inhibition impairs early reversal learning performance, whereas prefrontal disinhibition facilitates early reversal learning

Prefrontal inhibition increased RTCs during reversal 2, whereas disinhibition reduced RTCs during early stages

To measure the effect of our prefrontal manipulations on the operant reversal learning paradigm, first we examined the effect on overall reversal performance

58

indexed via RTC across SD and the following first three reversal stages. In the saline group, there was a clear initial reversal cost, with rats requiring more responses to reach criterion at R1 than at the SD stage, and this cost gradually diminished across reversals, as rats learned to reverse. Inhibition by muscimol slowed down this acquisition of reversal learning, causing a marked reversal deficit at R2 reflected by higher RTCs compared to saline. In contrast, disinhibition by picrotoxin reduced the reversal cost, particularly at R1 (fig. 7A). These findings were supported by a 2-way ANOVA, which found a significant drug x stage interaction ($F_{(6, 171)}$=2.92, p=0.01). Subsequent simple main effect analysis revealed a significant main effect of drug at R1 ($F_{(2, 171)}$=3.57, p=0.03) and R2 ($F_{(2, 171)}$=9.43, p<0.001), but not at SD and R3 (highest $F_{(2, 171)}$=2.169, p=0.118). Pairwise comparisons revealed that, at R1, RTCs were lower in the picrotoxin group than the saline group (p=0.01), with no other significant differences (lowest p=0.7). At R2, RTC increased in the muscimol group compared to both saline (p=0.021) and picrotoxin (p<0.001), with the picrotoxin group, again, requiring significantly fewer RTCs than saline (p=0.49).

Prefrontal inhibition increases perseveration, not regression, at R2

In order to further dissect the RTC observed across R1-3, we dissected errors by error type (perseverative vs. regressive). Following rule reversal, rats tended to perseverate with the previously correct, but now incorrect, response, as seen by a substantial number of perseverative errors in the saline rats at R1. In the saline group, there was a general decrease in perseverative errors across R1 to R3, supporting that rats learn to reverse across these early reversals. Rats in the picrotoxin group showed a similar decrease in perseverative errors across reversal, although they tended to make fewer preservative errors at R2. In contrast, the muscimol rats made markedly more perseverative errors than saline and picrotoxin rats, mainly at R2 (fig. 7B). A 2-way ANOVA on perseverative errors across R1-3 found a significant drug x stage interaction ($F_{(4, 127)}$=3.870, p=0.005). A simple main effects analysis revealed a main effect of drug during R2 ($F_{(2, 127)}$=10.268, p<0.001), but not during R1 (F<1) or R3 ($F_{(2, 127)}$=2.658, p=0.074). Pairwise comparisons showed that, during R2, the muscimol group made more

perseverative errors than the saline (p=0.009) and picrotoxin groups (p<0.001). The saline and picrotoxin group did not differ significantly (p=0.071). Regressive errors were similar across groups or stages, suggesting that prefrontal manipulations did not cause non-specific learning impairments on the early reversal paradigm (fig. 7C). A 2-way ANOVA found no significant main effect of drug ($F_{(2, 127)}$=2.603, p=0.078) or stages (F<1), and no drug x stage interaction (F<1).
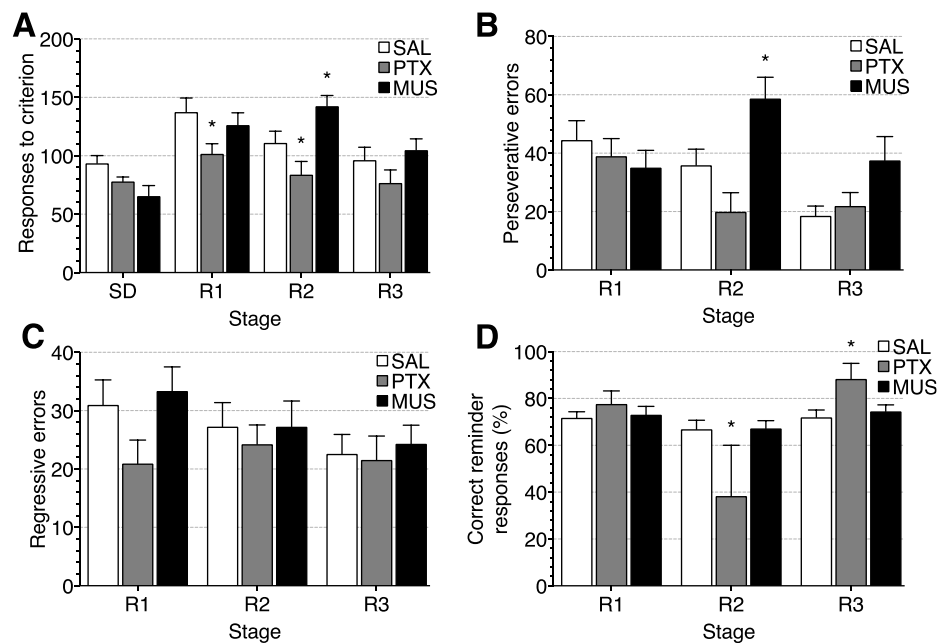
Figure 7. Summary of performance data from experiment 2. Average RTC (A), perseverative errors (B), regressive errors (C) and reminder trial performance indexed via percentage-correct (D) for all drug conditions across each experimental stage. Error bars indicate +*SEM*. Asterisks above bars indicate significant difference compared to saline group within the same stage.

Prefrontal disinhibition increased omissions, limiting reminder trial responses

The findings of the performance improvements in the picrotoxin group motivated analysis of reminder trial accuracy to ensure rats in the picrotoxin group exhibited the previous rule to the same salience as the saline and muscimol groups. Whilst results showed that overall reminder trial performance was only affected at R2 with the picrotoxin group performing worse than the other two groups (fig. 7D),

the inclusion criteria in place significantly restricted the sample size for all stages. This was especially noticeable for stages R2 and R3 (R1, n=10; R2, n=3; R3, n=6), compare to saline (all n=15) and muscimol (all n=16) groups. The reason for this was the significant number of omissions across all task stages in the picrotoxin group (table 2), which resulted in limited reminder trial responding (average responses across R1-R3 out of a maximum of 20: saline=19.78±0.09 (*SEM*); picrotoxin=3.86±0.86 (*SEM*); muscimol=19.66±0.11 (*SEM*), and thus, incomplete reinforcement of the old rule before rule change. A 2-way ANOVA of percentage-correct data during reminder trials, which highlighted a significant drug x stage interaction ($F_{(4, 102)}$=4.54, p=0.002), with the picrotoxin group exhibiting a lower percentage of correct responses compared to saline (p=0.002) and muscimol (p=0.002) rats at R2, whilst at R3, the percentage of correct responses was higher in the picrotoxin group than in saline and muscimol groups (p=0.048 and p=0.009, respectively). Muscimol and saline rats did not differ at either stage (lowest p=0.352). With regards to omissions, the effect of picrotoxin on overall omissions was confirmed via a 2-way ANOVA which found a drug x stage interaction ($F_{(6, 171)}$=2.51, p=0.024). Pairwise comparisons showed that picrotoxin increased omissions at all stages compared to both saline and muscimol (all p<0.001), which did not differ from each other at any stage (lowest p=0.583). Due to the notable reductions in reminder trial responding, the picrotoxin group was excluded from any subsequent strategy analysis of experiment 2.

Prefrontal disinhibition increases reminder and post-reversal response latencies

Finally, to further characterise the physiological effect of the current manipulations, we examined response latencies across all groups. Prefrontal disinhibition markedly increased both correct and incorrect response latencies across both reminder, SD, and post-reversal trials (table 2). Separate 2-way ANOVA revealed significant stage x drug interactions for correct and incorrect reminder trial latencies, as well as for incorrect non-reminder trial latencies (lowest $F_{(6, 169)}$=2.612, p=0.019), but not for correct non-reminder trial latencies (p=0.162). In the latter case, a significant main effect of drug was observed ($F_{(2, 170)}$=88.418, p<0.001), as well as a main effect of stage ($F_{(3, 170)}$=2.839, p=0.040).

61

Simple main effects of the interactions showed a significant effect of drug at all stages (lowest $F_{(6, 169)}$=7.131, p<0.001), except for incorrect reminder trials at R1 (F<1). In all instances, except incorrect latencies at R1, picrotoxin resulted in a significant increase in latencies compared to saline and muscimol (all p<0.001). Saline and muscimol did not differ significantly in any metric (lowest p=0.216).

Prefrontal inhibition impairs early reversal performance by impairing abandonment of the old strategy (go-previous) immediately after rule change

To identify fine behavioural changes around rule reversal, we used the Bayesian strategy analysis model. First, we looked at the probability of 'go-previous' in order to measure speed of rule abandonment immediately after rule change. The saline group exhibits high level of go-previous prior to rule change, indicative of good reminder trial performance, followed by a subtle decrease after rule change representing a gradual shift to the opposite, 'new', lever. In contrast, for muscimol group this pattern is only visible during R1, with R2 and to a lesser extent R3 highlighting a continued implementation of go-previous associated with increased perseveration (fig. 8A). A 3-way ANOVA, using drug, stage and trial as factors, supports these findings with a significant drug x stage interaction ($F_{(2, 1892)}$=10.500, p<0.001). No other main effect or interaction was observed (lowest p=0.124). Simple main effect analysis for the significant interaction confirmed an effect of drug at R2 ($F_{(1, 2018)}$=24.384, p<0.001) and R3 ($F_{(2, 2018)}$=6.491, p=0.011), but not R1 ($F_{(2, 2018)}$=2.352, p=0.125). In, both, R2 and R3 muscimol resulted in significantly greater implementation of go-previous compared to saline (highest p=0.011).

Table 2. Omissions and response latencies for experiment 2 and experiment 3.

	Drug Condition								
	Saline (0.9%)			**Picrotoxin (300ng)**			**Muscimol (62.5ng)**		
	Omissions	Lat_{Cor} (s)	Lat_{Inc} (s)	Omissions	Lat_{Cor} (s)	Lat_{Inc} (s)	Omissions	Lat_{Cor} (s)	Lat_{Inc} (s)
Exp. 2									
SD	9.00±5.66	0.99±0.07	1.31±0.09	109.33±16.58*	2.56±0.16	2.92±0.17	2.38±0.79	1.15±0.09	1.35±0.10
R1	1.13±0.36	(1.07±0.14)	(2.24±0.48)	80.53±19.67*	(4.95±0.52)*	(3.85±0.57)*	3.81±1.01	(1.16±0.11)	(2.12±0.31)
		0.94±0.10	1.10±0.11		2.04±0.23*	2.80±0.18*		1.15±0.08	1.29±0.12
R2	0.53±0.17	(0.99±0.14)	(0.96±0.08)	66.00±10.45*	(3.08±0.78)*	(5.52±0.56)*	2.63±0.65	(1.04±0.16)	(1.07±0.09)
		1.07±0.11	1.06±0.11		2.25±0.43*	2.00±0.22*		1.14±0.10	1.17±0.11
R3	1.07±0.55	(0.93±0.10)	(1.03±0.19)	49.50±11.24*	(5.48±1.16)*	(3.95±0.96)*	1.75±0.87	(0.86±0.12)	(1.54±0.31)
		0.96±0.10	0.99±0.10		1.80±0.25*	2.44±0.35*		1.06±0.11	1.17±0.10
Exp. 3									
Series 1	0.15±0.10	(0.65±0.07)	(0.96±0.17)	34.23±8.33*	(2.65±0.25)*	(2.45±0.14)*	0.46±0.27	(0.68±0.09)	(0.83±0.14)
		0.59±0.04	0.59±0.05		2.37±0.34*	2.99±0.38*		0.66±0.09	0.88±0.14
Series 2	0.38±0.21	(0.66±0.08)	(0.69±0.17)	23.54±7.64*	(2.75±0.32)*	(2.38±0.38)*	0.31±0.13	(0.62±0.08)	(1.07±0.24)
		0.50±0.04	0.66±0.09		1.44±0.18*	1.95±0.21*		0.69±0.06*	0.63±0.08

Note: Values are shown are mean±*SEM*. Reminder trial response latencies are enclosed in brackets. Accuracy of response latencies is indicated by 'cor' (correct) or 'inc' (incorrect). Asterisks indicate significant difference to saline condition at the same stage.

Prefrontal inhibition disrupts maintenance of exploratory behaviour in response to false lever presses (lose-shift), while leaving exploitative behaviour in response to correct lever presses (win-stay) intact.

Next, we wanted to examine the implementation of task pertinent strategies in lose-shift-spatial and win-stay-spatial in order to further characterize the reversal impairment around rule change. Regarding the former, one can see high, stable, implementation of this strategy prior to rule change in the saline group, indicating that, where necessary, responses are shifted readily to search out the rewarding lever. Immediately after the rule reversal, however, there is a steep decline, indicating evidence for the opposing, lose-stay, strategy which coincides with normal perseveration following a sudden change in reward contingency. This decrease tends to recover at around 8 to 10 responses after reversal. Whilst the pre-reversal implementation of lose-shift-spatial is comparable between the saline and muscimol groups across all three reversal stages, the subsequent decrease after rule reversal is not rescued at around 8 responses after reversal and instead continues to decrease, particularly at R2, indicating a stronger tendency to perseverate and reduced exploration in the face of an unrewarding stimulus in the muscimol group (fig. 8B). This effect was supported by a 3-way ANOVA. A significant drug x stage interaction was observed ($F_{(2, 1892)}$=8.592, $p<0.001$) alongside a main effect of trial ($F_{(21, 1892)}$=74.024, $p<0.001$). No drug x trial ($F_{(2, 1892)}$=1.003, p=0.456), stage x trial ($F<1$, p=1) or drug x stage x trial ($F<1$, p=0.995) interaction was found. Simple main effect analysis of the drug x stage interaction revealed a significant effect of drug at all stages (lowest $F_{(1, 2018)}$=7.850, p=0.005), with a significantly lower implementation of the lose-shift-spatial strategy in the muscimol group, compared to saline (highest p=0.005).

With regards to implementation of the win-stay-spatial strategy, one can see equally strong win-stay behaviour prior to reversal followed by a gradual decline post-reversal, in both groups. This decline is evidence for the opposite strategy (i.e., win-shift), which indicates a reluctancy to exploit a newly rewarding response. Notably, muscimol does not impair this form of exploitative behaviour

compared to saline, and in fact there is some evidence for improved win-stay behaviour following prefrontal inhibition, particularly at R1 (fig. 8C). A 3-way ANOVA revealed a main effect of drug ($F_{(1, 1892)}$=34.628, $p<0.001$), stage ($F_{(2, 1892)}$=9.712, $p<0.001$) and trial ($F_{(21, 1892)}$=13.900, $p<0.001$). No significant interaction was observed between factors (highest F=1.970, p=0.140). Pairwise comparison analysis revealed a significantly higher implementation of win-stay-spatial in the muscimol group compared to saline between R1-3 ($p<0.001$).
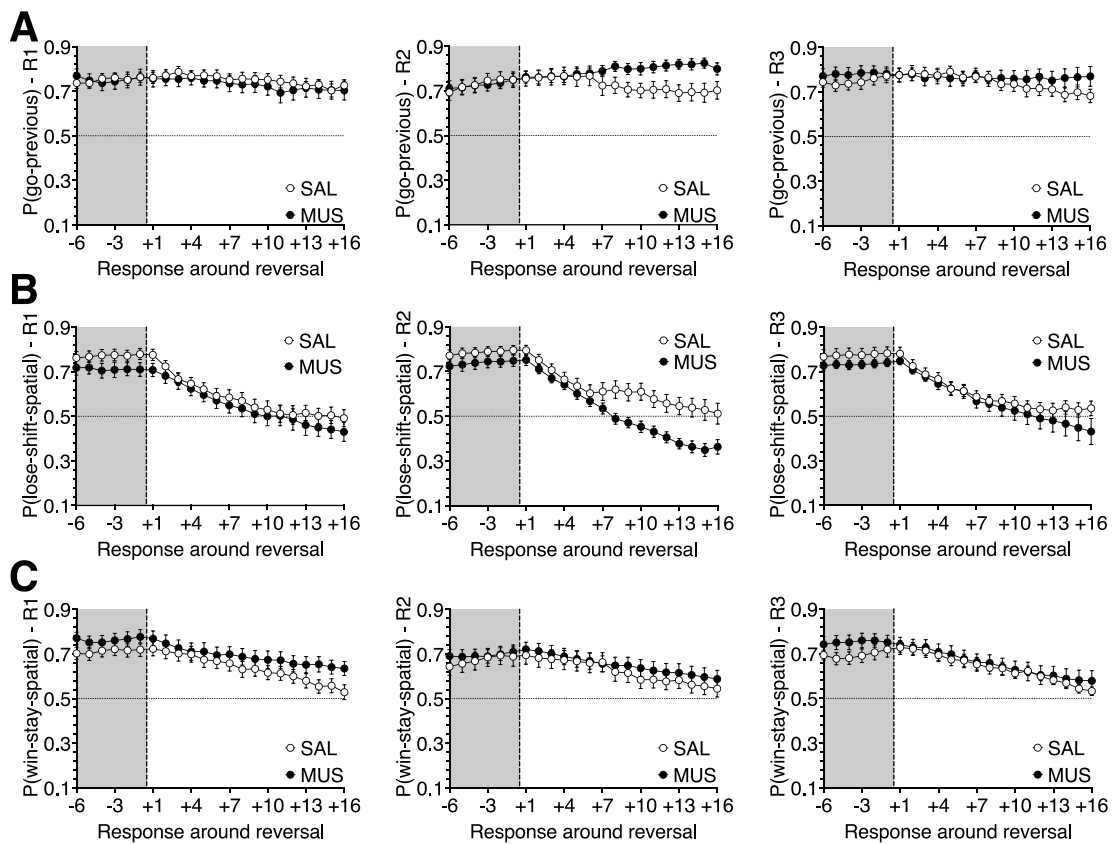

Figure 8. Bayesian trial-by-trial strategy profiles (±*SEM*) for experiment 2. Analysed strategies are go-previous (A), lose-shift-spatial (B), and win-stay-spatial (C). Grey-shaded region indicates reminder trial performance. Vertical dashed line indicates rule reversal.

3.2.3 Experiment 3: Prefrontal disinhibition, but not inhibition, impairs established reversal learning performance

Prefrontal disinhibition resulted in increased RTC once the task had been established

During R5-10, rats infused with saline readily switched their responses from one lever to the other after reward contingencies had been reversed, requiring on average less than 100 RTC (fig. 9A). Importantly, there was no 'reversal cost' at this stage compared to the initial SD supporting that rats had 'learnt to reverse'. Prefrontal picrotoxin, but not muscimol, markedly impaired established reversal learning performance, reflected by higher RTC across R5-10. A 2-way repeated-measures ANOVA revealed a significant main effect of drug ($F_{(2, 24)}$=8.612, p=0.002), but not infusion series ($F_{(1, 12)}$=4.255, p=0.061). No drug x infusion series interaction was observed (F<1). Pairwise comparisons revealed that picrotoxin increased RTC compared to the saline (p=0.015) and muscimol (p=0.002) conditions, which did not differ themselves (p=0.274).

Prefrontal disinhibition increased both perseverative and regressive errors

Again, error type was dissected to investigate whether the impaired performance following picrotoxin was due to increased perseveration or due to non-specific impairments in learning. Results showed that picrotoxin increased both perseverative and regressive errors compared to prefrontal saline or muscimol infusions (fig. 9B & 9C). 2-way repeated-measures ANOVAs revealed a main effect of drug on both perseverative ($F_{(1.269, 15.231)}$=4.592, p=0.041) and regressive errors ($F_{(2, 24)}$=5.427, p=0.011). A main effect of infusion series was also observed in regressive errors ($F_{(1, 12)}$=7.416, p=0.018), but not perseverative errors (F<1) Neither error type revealed a significant drug x infusion series interaction (lowest p=0.140). Pairwise comparisons of the drug effect revealed that perseverative errors were higher in the picrotoxin group compared to the saline group (p=0.043) and the muscimol group (p=0.046), whilst no significant difference was observed between muscimol and saline (p=0.602). Regressive errors were

increased by picrotoxin compared to muscimol ($p=0.018$), but not saline ($p=0.051$). Muscimol and saline did not differ significantly $(p=0.175)$.
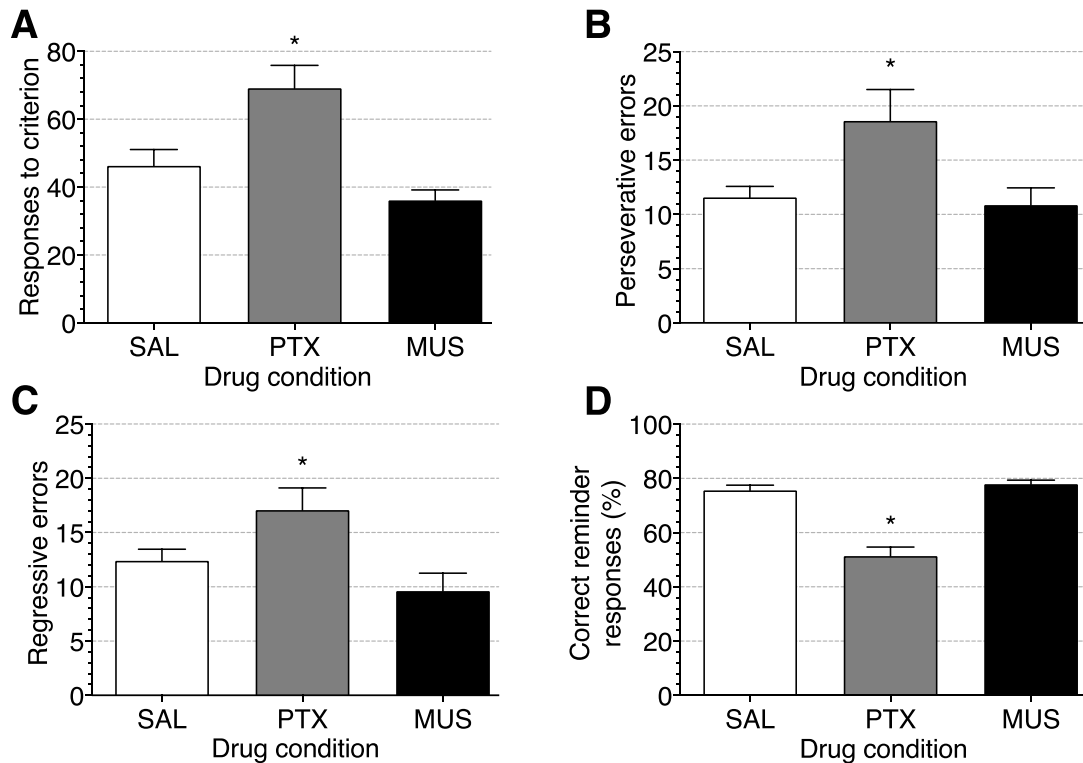

Figure 9. Summary of performance data from experiment 3. Average RTC (A), perseverative errors (B), regressive errors (C) and reminder trial performance indexed via percentage-correct (D) and errors split into perseverative and regressive type (C) for experiment 3. Data for all drug conditions was averaged across infusion series. Error bars indicate +*SEM*. Asterisks above bars indicate significant difference compared to saline group.

Prefrontal disinhibition impaired expression of the previous rule during reminder trials

Next, we looked whether reminder trial performance impacted overall reversal performance, by examining reminder trial accuracy. Prefrontal picrotoxin reduced the percentage of correct responses during the 20 reminder trials compared to muscimol and saline conditions (fig. 9D). A 2-way repeated-

measures ANOVA revealed a main effect of drug ($F_{(2, 24)}$=35.000, p<0.001), without a main effect or interaction involving infusion series (main effect of infusion series, F<1; drug x infusion series interaction, $F_{(2, 24)}$=1.766, p=0.128). Pairwise comparisons showed that reminder trial performance was significantly reduced in the picrotoxin group compared to the saline and muscimol groups (both p<0.001), which did not differ from each other (p=0.378).

Prefrontal disinhibition increased omission rates and response latencies

Similar to experiment 2, we checked omissions across all drug conditions to characterize whether high levels of distractibility accompanied poor reminder and reversal performance. Again, prefrontal disinhibition markedly increased omission rates and correct and incorrect latencies across both reminder and reversal trials, whilst inhibition did not affect these measures (table 2). However, in contrast to experiment 2 omissions were not as detrimental to reminder trial responding, meaning all rats were included in the analysis. A 2-way repeated-measures ANOVA of omissions revealed a main effect of drug ($F_{(1.001, 12.017)}$=24.16, p<0.001), with no main effect or interaction involving infusion series interaction (both F<1). Pairwise comparisons showed that picrotoxin infusion increased omission rate compared to saline and muscimol infusions (both p<0.001), which did not differ (p=0.534). Two 3-way repeated-measures ANOVA were conducted for reminder and reversal trial latencies using drug, series, and response accuracy as factors. With regards to reminder trial latencies, a significant drug x accuracy interaction was observed ($F_{(2, 22)}$=4.317, p=0.026). Simple main effects analysis highlighted a significant effect of drug for both correct and incorrect latencies (lowest $F_{(2, 24)}$=30.394, p<0.001). Pairwise comparisons revealed significantly greater correct and incorrect response latencies for the picrotoxin condition compared to both saline and muscimol (all p<0.001), which did not differ (lowest p=0.459). No other interaction or main effect was observed (all F<1). With regards to reversal trials, the 3-way repeated-measures ANOVA revealed a significant drug x accuracy interaction ($F_{(2, 24)}$=3.902, p=0.034), as well as a significant drug x series interaction ($F_{(1.078, 12.940)}$=4.747, p=0.46). Subsequent simple main effect analysis revealed a significant effect of drug across both series and accuracy (lowest $F_{(1.100,}$

$_{13.201)}$=15.869, *p*=0.001). Pairwise comparisons highlighted that significantly greater response latencies following picrotoxin, compared to saline and muscimol, independent of series and accuracy (highest *p*=0.005). Additionally, muscimol exhibited greater correct response latencies than saline in series 2 (*p*=0.009), but not for incorrect latencies or across series 1 (lowest *p*=0.101). No drug x accuracy x series or accuracy x series interaction was observed (all *F*<1).

Prefrontal disinhibition reduced probability of following the previous rule around rule reversal

Following prefrontal infusions of saline and muscimol, rats showed high probabilities of following the previous rule during the 6 last responses before the rule change, with probabilities remaining high until about the 7th response after rule change before beginning to decrease, indicating that rats abandoned the previous rule and switch to the opposite lever. This pattern following saline and muscimol infusions was evident in both infusion series. Following prefrontal disinhibition, however, the pattern differed between infusion series 1 and 2. In series 1, the probability of following the previous rule was reduced compared to saline and muscimol infusions during the reminder trials, at or below P=0.65, but, in contrast to saline and muscimol infusions, hardly declined following rule reversal, such that towards the end of the first 16 responses after reversal the probability of following the previous rule was similar in all three infusion conditions. In infusion series 2, this effect of picrotoxin had completely disappeared, with all three infusion conditions showing similar probabilities to follow the previous rule both before and after reversal (fig. 10A). A 3-way repeated-measures ANOVA of the probability of rats following the previous rule revealed a drug x trial x infusion series interaction ($F_{(42, 504)}$=1.598, *p*=0.012). Therefore, separate 2-way repeated-measures ANOVA were run for series 1 and 2, using drug and trial as factors. There was a significant drug x trial interaction in infusion series 1 ($F_{(42, 504)}$=2.970, *p*<0.001), whereas, for series 2, there was only a main effect of trial ($F_{(21, 504)}$=8.762, *p*<0.001), without any main effect or interaction involving drug (both *F*<1). Simple main effects analysis of the drug x

trial interaction in infusion series 1 revealed a significant main effect of drug between 3 responses prior- and 9 responses post-reversal (lowest $F_{(2, 24)}=4.192$, $p=0.027$). Pairwise comparisons revealed that picrotoxin infusion reduced the probability of following the previous rule, compared to saline, 2 responses before, and 2, 3, 5, 7 and 8 responses after reversal (highest $p=0.049$). Muscimol slightly increased the probability of following the previous rule, compared to saline, during the first response after reversal ($p=0.022$), with no differences on any other trials (lowest $p=0.081$).
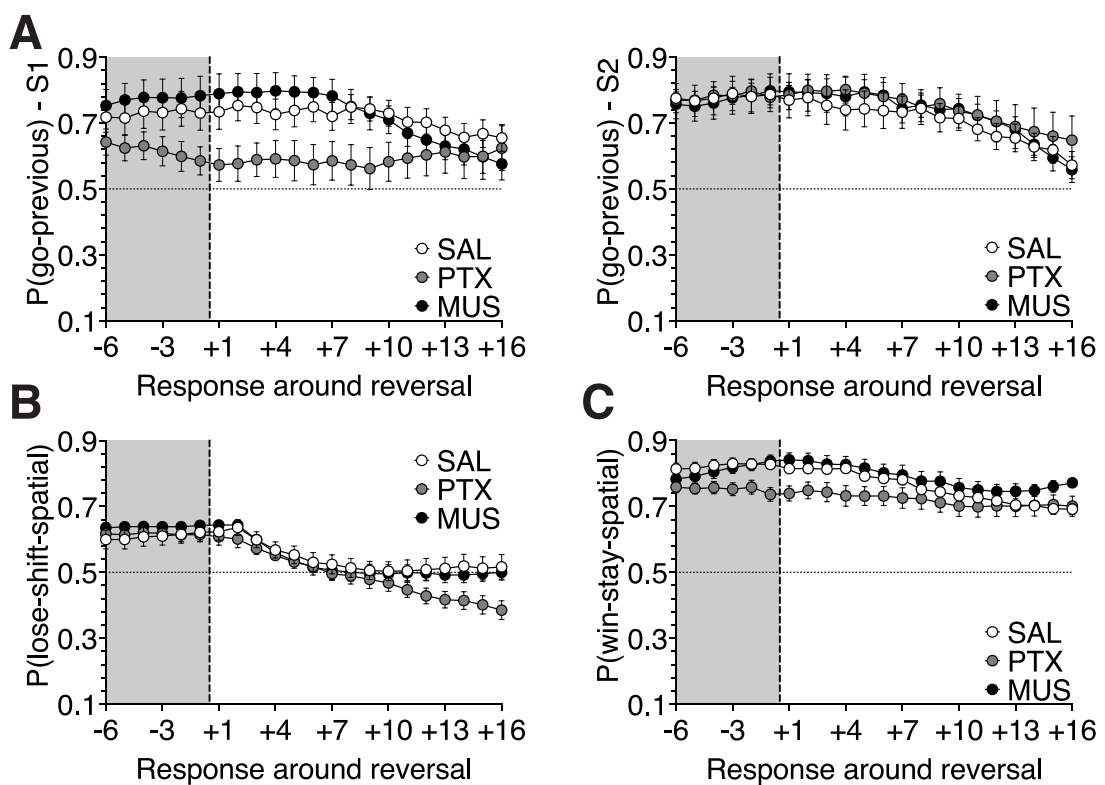
Figure 10. Bayesian trial-by-trial strategy profiles (±*SEM*) for experiment 3. The following rules are illustrated: go-previous (A; series 1 – left, series 2 - right); lose-shift-spatial (B), and win-stay-spatial (C). Grey-shaded region indicates reminder trial performance. Vertical dashed line indicates rule reversal.

The strategy pattern of go-previous encompasses both the impaired reminder trial and reversal performance following prefrontal picrotoxin microinfusions, with reduced adherence to the old rule prior to rule change compared, compared

to saline, indicating poor reminder trial performance, in combination with no abandonment of the previous rule immediately after rule change. Interestingly, the data suggests that disinhibition results in more pronounced deficit around reversal in infusion series 1, than infusion series 2. However, a significant reversal deficit, indicated by continued adherence to the old rule, is still observed in the latter, albeit smaller. It is important to consider that the Bayesian analysis was only shown for the first 16 responses after reversal, as this was the lowest number of responses that all rats completed before reaching criterion.

Prefrontal disinhibition disrupts both exploratory and exploitative behaviour indexed via win-stay and lose-shift implementation

Prior to rule reversal, implementation of lose-shift-spatial was high across all groups, and after rule reversal, there was a steep decline in this strategy indicating a tendency to stick with the previous, but now incorrect, response for several trials. This decline plateaued at around 5 responses after reversal for saline and muscimol, which implies the beginning of shift behaviour in rats. However, following prefrontal disinhibition via picrotoxin, this rescuing of lose-shift-spatial was not present, and the application of this strategy continued to decline for all measured trials after reversal, coinciding with increased perseveration following picrotoxin (fig. 10B). A 3-way repeated-measures ANOVA revealed a significant drug x trial interaction ($F_{(42, 504)}$=2.179, $p<0.001$). No further effects or interactions were observed (smallest p=0.115). Simple main effect analysis revealed significant effect of drug at 15 and 16 responses after reversal only (lowest $F_{(2, 24)}$=4.185, p=0.0.28). Pairwise comparison further showed that, in both cases, picrotoxin performed a lose-shift-spatial at a significantly lower probability that both saline (highest p=0.043) and muscimol (highest p=0.029). Muscimol and saline did not differ significantly (lowest p=0.647).

On the other hand, application of win-stay-spatial was reduced following picrotoxin, compared to saline and muscimol, even prior to rule reversal. This impairment remained for several trials after rule reversal compared to saline and muscimol (fig. 10C). A 3-way repeated-measures ANOVA revealed a significant

drug x trial interaction ($F_{(42, 504)}$=2.904, p<0.001). No further effects or interactions were observed (smallest p=0.254). Simple main effect analysis revealed significant effect of drug from 4 responses pre- to 4 responses post-reversal (lowest $F_{(2, 24)}$=3.900, p=0.034). Pairwise comparisons showed that, in all cases, the main effect of drug was driven by a significantly lower implementation of a win-stay-spatial strategy between picrotoxin and both saline and muscimol (highest p=0.049), whilst muscimol and saline did not vary significantly (lowest p=0.116).

3.3 Discussion

Prefrontal functional inhibition by muscimol impaired early reversal performance in conjunction with increased perseveration, impaired lose-shift behaviour, and a tendency to dwell on the previously rewarded, but now incorrect, rule. In contrast, prefrontal functional inhibition did not affect serial reversal performance. Prefrontal disinhibition by picrotoxin, however, was less disruptive on early reversal performance, whilst markedly impairing established reversal performance, resulting in increased RTC and perseveration, increased regressive errors, as well as impaired reminder trial performance and more sub-optimal strategy implementation. Neither prefrontal inhibition, nor disinhibition, impaired performance on the simple spatial discrimination task. Across both experiments a pattern of increased omissions and response latencies was observed following prefrontal picrotoxin, with the rate of omissions decreasing gradually as more reversal iterations are completed.

3.3.1 Prefrontal inhibition disrupts exploration resulting in impaired reversal acquisition during early reversal learning

The PFC is known for its involvement in integrating information about reward outcome and error correction (Rushworth et al., 2011; Shenhav et al., 2013), as well as guiding exploratory behaviour (Daw et al., 2006; Caracheo et al., 2013), and there is evidence that prelimbic inhibition and lesions impair lose-shift behaviour and increase perseveration (Yang et al., 2014; Laskowski et al., 2016).

Moreover, Maggi et al. (2023) have highlighted the importance of exploratory behaviour, in particular lose-shift behaviour, in driving the initial acquisition of the new rule, whilst exploitative alternatives (e.g., win-stay) are more important for the maintenance of learnt behaviour. Findings from experiment 2 support this notion, with a clear disruption in lose-shift behaviour, centred around R2, in combination with marked reversal learning deficits at that stage following prefrontal muscimol. The lack of impairment at R1 indicates that prefrontal inhibition does not additionally impair performance beyond the typically observed reversal cost (Floresco et al., 2008), but, rather, prefrontal functional inhibition impairs processes necessary to overcome this reversal cost.

This line of reasoning suggests that the pattern of reversal performance across early task stages as a direct product of the implementation of lose-shift behaviour. Specifically, early poor performance is driven by sub-optimal implementation of lose-shift, evident in the large reversal cost at R1. This is corrected between subsequent stages, resulting in a gradual reduction in overall RTC. Indeed, human research has shown that in situations with increased cognitive demand participants tend to decrease lose-shift behaviour (Ivan et al., 2018). It may, then, be this increased cognitive demand during early reversal stages (i.e., the initial encounter with a rule change alongside uncertainty of cue-light relevance) requires mPFC engagement. In turn, this engagement drives subsequent corrections in exploration, whilst inhibition of the mPFC impedes this strategy correction. This notion would be in line with similar rodent studies conducted previously (Bussey et al., 1997; Chudasama & Robbins, 2003; Kosaki & Watanabe, 2012).

Interestingly, the lack of effect of prefrontal functional inhibition on serial reversal performance in experiment 3 indicates that, once rats have adapted their behavioural strategies, the mPFC is no longer required for reversal performance. Furthermore, functional inhibition does not impair exploitative behaviour in either of the two experiments reported here. Therefore, the impairment following prefrontal inhibition may be a task-independent exploratory impairment, that

results in impaired reversal performance due to restricted strategy correction in the face of high cognitive load during early reversal stages.

3.3.2 Prefrontal disinhibition impairs exploration <u>and</u> exploitation on established, but not early reversal performance

Prefrontal disinhibition by picrotoxin caused marked impairments on the established reversal paradigm, manifested through increased RTC, more perseveration and increased regressive errors, as well as impaired expression of the old rule on reminder trials. Furthermore, disinhibition also impaired task-relevant exploration and exploitation, as reflected by reduced lose-shift and win-stay behaviour, respectively. These findings are in stark contrast with experiment 2 and previous work by Enomoto et al. (2011), which did not reveal any such impairment during early reversal stages. On the one hand, this suggests that the early lose-shift strategy correction, which is disrupted by mPFC dysfunction, is not sensitive to mPFC hyperactivity. This further supports the idea that different processes are involved in early and serial reversal performance respectively.

If mPFC involvement is restricted to early stages of the reversal paradigm, where task demands are greatest, and once learning has occurred the mPFC is no longer required, the impaired exploration and exploitation caused by disinhibition must be a product of disruption of brain areas outside the mPFC. $GABA_A$ receptor mediated control of neuronal burst firing is crucial for functional coupling between inter-connected areas (Lisman, 1997; Tremblay et al., 2016). As such, it has been proposed that regional neural disinhibition may cause aberrant drive of a brain region's projections to other brain regions and, thereby, disrupt processing in these projection sites (Bast et al., 2017).

3.3.3 Prefrontal disinhibition increases omissions and response latencies

The current experiments found a marked increase in omissions following infusions of picrotoxin, indicating a significant behavioural impairment that was

not detrimental to reversal performance.. The number of omissions decreased both within each experiment and across experiments, whereby the highest number of omissions were made early in experiment 2, and omissions decreased gradually between R1 and R3. A further decrease is noted across both infusion series of experiment 3. These findings suggest that, whilst prefrontal disinhibition increases distractibility (Auger et al., 2017), increasing task proficiency reduces requirement of GABA transmission to keep rats 'on task'. Likewise, prefrontal disinhibition increases response latencies. Much like omissions, this increase is negatively correlated with task proficiency, which, again, may reflect a reduced dependence on prefrontal GABAergic inhibition with increased training.

These findings highlight the potential for prefrontal GABAergic dysfunction to disrupt reversal learning performance. Whilst these findings are encouraging with respect to uncovering the underlying mechanisms contributing to the clinically observable reversal learning impairment (e.g., Leeson et al., 2009), this translation suffers from one caveat that needs to be addressed first. Specifically, the clinical GABAergic dysfunction outlined previously is predominantly pre-synaptic in nature (e.g., Volk et al., 2001). However, pharmacological models, like the one outlined in the current chapter, act post-synaptically. Therefore, it would be beneficial to examine the effect of pre-synaptic manipulations of GABAergic neurons on reversal learning. Whilst this is not traditionally possible via available pharmacological methods, novel chemogenetic (DREADD; Roth, 2016) alternatives offer an interesting approach to this problem. The next chapter discusses several validation experiments seeking to establish a chemogenetic model of prefrontal disinhibition, with the aim to complement findings from the current chapter.

4 Selective presynaptic inhibition of GABAergic interneurons in the mPFC of rats using DREADDs – histological and electrophysiological validation

Declaration: Rachel Grasmeder Allen assisted with the viral injection surgery. Mathias Heil supervised histological staining and scanning. Joanna Loayza supervised electrophysiological procedures.

As discussed in chapter 1, chemogenetic rodent models offer a range of advantages compared to pharmacological models. However, to date, no chemogenetic model of prefrontal disinhibition has been established, and there is, overall, a limited number of validated Cre-recombinase knock-in rat lines for neuron-type specific chemogenetic manipulations. The current chapter reports a series of histological and electrophysiological validation experiments, with the aims of validating an appropriate Cre-recombinase knock-in rat line, as well as showing functionality of the inhibitory hM4Di DREADD expression within the mPFC of these animals.

To briefly recap, via targeted insertion of a Cre-recombinase transgene into an animal's genome, specifically into genes expressing cells of interest (such as the Slc32a gene encoding for VGAT), one can achieve cell-type specific expression of Cre. We used a commercially available VGAT-Cre knock-in Long Evans rats (HsdSage:LE-VGAT^em1(IRES-Cre)Sage), expressing Cre-recombinase under the control of the endogenous VGAT (Scl32a1) promoter. As VGAT is solely found in GABAergic neurons, Cre-recombinase expression should be restricted to GABAergic neurons. Combining this rat line with an AAV-vector of serotype 8 (i.e., preferential to neuronal transfection; Watakabe et al., 2015) containing a single stranded, inverted, open reading frame DNA expressing a mutant human muscarine receptor (hM4Di), one can selectively express this DREADD in the VGAT-positive neurons. This is because the inverted DNA can only be transcribed via Cre-recombinase (Nagy, 2000). Here, we aimed to validate both the rat line, ensuring that Cre-recombinase is only expressed in cells of interest, and also evaluate the viral construct in terms of cell-type specificity (type of cells

expressing the DREADDs) and penetrance (coverage of targeted cells by DREADDs). Following completion of histological validation steps, we measured the functionality of the DREADD via *in vivo* electrophysiological recordings within the mPFC of anaesthetised rats.

Aim 1: Validation of the transgenic VGAT-Cre knock-in rat line

To validate the rat line, we primarily used fluorescence *in situ* hybridisation (FISH, for review see Levsky & Singer, 2003) to fluorescently label mRNA of VGAT and Cre-recombinase and examine their co-expression. FISH was the only suitable methodology for validation, as at the writing of this, there are no viable commercially available antibodies for Cre-recombinase. To target the DREADD to GABAergic (i.e., VGAT-expressing) neurons, very high levels of VGAT-Cre co-localisation were required, with limited off-target expression. Nevertheless, off-target Cre-expression is not uncommon, with previous literature reporting up to 6-10% of off-target Cre expression in mice (Heffner et al., 2012; Hu et al., 2013).

Aim 2: Validation of Cre-mediated DREADD expression within the mPFC of the rat line

Key aspects of the prefrontal hM4Di expression, with an outlook towards application in models of prefrontal disinhibition, include the spread of expression across the PFC, the specificity to GABAergic neurons with virtually no expression by any other cell type (such as excitatory neurons), and the penetrance of the DREADD (i.e., the total percentage of GABAergic cells expressing the DREADD). To assess specificity and penetrance, several immunohistochemical investigations were carried out across two cohorts of VGAT-Cre rats. The first cohort of rats was the same as used for the abovementioned FISH investigations under aim 1. We qualitative analysed DREADD spread across the PFC (+4.2 to +2.7 mm from bregma) at two AAV-solution volumes (0.5 and 1.0 μl) of the same titre. Additionally, cell-type specificity, assessed via co-localisation of DREADD with GAD_{67} (used as a proxy for VGAT), and DREADD penetrance were compared between the two injection volumes. Although these assessments of specificity and

penetrance of DREADD expression in the brains of the first cohort of rats were limited by small sample size and partially poor tissue condition (as brains were initially fresh frozen, as required for *in situ* hybridisation analysis), they helped guiding subsequent DREADD injection protocols. Based on the findings in the first cohort, we chose an injection volume of 1 µl for further studies.

In a second cohort of rats, we then characterized DREADD spread further at the selected volume of 1.0 µl across the mPFC, supplementing prior findings of cell-type specificity and penetrance. Brain tissue in this cohort was perfusion-fixed to improve conditions for immunohistochemical stains. The DREADD spread was visualised across a wider range of coronal sections, corresponding to sections ranging from +5.5 to +2.0 mm from bregma in the rat brain atlas of Paxinos and Watson (1998). In addition to assessing DREADD co-localisation with GAD_{67}, we also examined co-expression with Camkinase-II-alpha (CamKIIα). CamKIIα has been reported to be exclusively expressed in excitatory glutamatergic neurons (Zhang et al., 1999), and, therefore, we expected virtually no DREADDs expression in CamKIIα+ cells. Moreover, expression of the DREADD in cholinergic neurons was also quantified co-staining for choline acetyltransferase (ChAT), the primary enzyme responsible for the synthesis of acetylcholine (Eckenstein & Thoenen, 1983).

Previous studies have found functional effects even at varying degrees of Cre-mediated DREADD penetrance, ranging from 20-60% penetrance (Smith et al., 2016; Nguyen et al., 2014; Fujita et al., 2017; Kakava-Georgiadou et al., 2019). Therefore, we aimed for penetrance within that range, with lower penetrance potentially limiting any functional effects. Similarly, cell-type specificity has been found to vary to a large degree, with some studies finding as low as 20% specificity and as high as 95% (Ngyuen et al., 2014; Fujita et al., 2017). The primary goal of investigations of specificity was to express DREADDs at GABA neurons only, with some expression at cholinergic neurons likely, given that a substantial proportion of prefrontal GABAergic neurons show co-release of acetylcholine and GABA (Granger et al., 2020). However, it was critical that no DREADD expression was

78

localised at excitatory cells, as this would directly interfere with the purpose of this model of prefrontal disinhibition.

Aim 3: Assessing DREADD functionality via in vivo electrophysiological recordings

We assessed DREADD functionality using *in vivo* electrophysiological recordings within the PFC of rats from cohort 2. In this experiment, we compared neural firing patterns within the mPFC following systemic injections of the DREADD actuator, CNO2HCl (6 mg/ml/kg), and sterile saline (0.9%). This experiment was run in a within-subjects design. Results were qualitatively compared to previous electrophysiological findings following pharmacologically induced prefrontal disinhibition (Pezze et al., 2014). Of particular interest were burst firing patterns and LFP power, as these parameters were markedly altered following prefrontal picrotoxin (300 ng/0.5 µl). Specifically, Pezze and colleagues (2014) found an enhancement in local burst firing in combination with an increase in the percentage of spikes fired in bursts and a reduction in average burst duration. In addition, prefrontal pharmacological disinhibition also altered the LFP pattern and power, causing marked spike-wave discharges (SWD), consisting of a sharp negative LFP deflection followed by a positive LFP wave alongside an increase in LFP power. Together, these findings indicate a distinct change in neural activity following GABAergic disinhibition, and for the current DREADD construct to be considered functional, similar changes in burst firing and LFP patterns were expected. Furthermore, Pezze and colleagues found a peak in most neural parameters at around 15 min post-injection, which declined back to baseline within around 1 h. In the current electrophysiological investigation, we measured activity for 2 h post-injection in order to characterize the time course of any potential chemogenetic effect.

4.1 Materials and methods

4.1.1 Rats

A total of 12 male homozygous transgenic LE-VGAT^{em1(IRES-Cre)Sage} rats and 3 male heterozygous wildtype (WT) Lister hooded rats (Envigo US; Envigo UK) were used across two cohorts (n=7 in cohort 1, n=8 in cohort 2). Cohort sizes were determined such that broad histological comparisons would be possible, whilst no formal analysis was planned. Cohort 1 consisted of 4 VGAT-Cre and 3 WT rats, which were used to validate the transgenic rat line, as well as for a preliminary assessment of spread, specificity and penetrance of the DREADD transfection following unilateral injections of two different volumes, 0.5 or 1 µl, containing the viral vector. Cohort 2 consisted of an additional 7 VGAT-Cre rats, which were used to further characterise spread, specificity and penetrance following bilateral injections of 1 µl/side. Cohort 2 was also used for the electrophysiological experiments. All rats weighed between 300-412 g, and were 9-12 weeks of age, at time of surgery. Rats were housed as described in chapter 2. All procedures were conducted in accordance with the United Kingdom (UK) Animals (Scientific Procedures) Act 1986. It should be noted here that in cohort 2 seizure-like behaviour was observed (convulsive seizures, loss of postural control, hyperactivity). Repeated seizures required the early termination of one rat (final n=7).

4.1.2 Viral vector

We used a double-floxed Gi-coupled hM4Di DREADD fused with mCherry reporter under the control of human synapsin promoter and packed in an AAV vector (pssAAV-8-hSyn1-dlox-hM4D(Gi)_mCherry(rev)-dlox-WPRE-hGHp(A), https://www.addgene.org/44362/). For injections, we used an undiluted solution of the DREADD-containing viral vector, serotype 8, with a physical titre of 6.3×10^{12} vg/ml (v84-8, Viral Vector Facility, University of Zürich, Switzerland). The

solution was aliquoted into 12.5 µl vials and stored in low protein binding PCR tubes at -80 °C until use.

4.1.3 Stereotaxic injection of viral vector

Prior to surgery, all rats were prepared as outlined in chapter 3. After incision, exposing the skull, bregma was located. Two small holes were drilled through the skull at the following coordinates: +3.0 mm anterior and ±0.6 mm lateral from bregma. Coordinates were based on previous coordinates used in our group for drug microinfusion studies targeting the mPFC in Lister hooded rats (Pezze et al., 2014; Prior et al., 2021), which closely corresponded to previous work in Long Evans rats targeting the mPFC (Auger & Floresco, 2014, 2017; Auger et al., 2017). Bilateral double injectors (C235I-SPC, Plastics One, Bilaney Consultants, UK) were glued into bilateral infusion guide cannulae ("mouse" model C235GS-5-1.2; Plastics One, Bilaney Consultants, UK), so as to protrude with 4.0 mm projection. They were then and attached to the stereotaxic frame via a stainless-steel cannula holder. The end of the injectors were attached to two 5 µl syringes (SGE, Australia) via PE50 tubing (Plastics One, Bilaney Consultants, UK), and syringes were secured on a micro-infusion pump (SP200IZ syringe pump, World Precision Instruments, UK). Prior to infusions, the tubing and syringe were backfilled with distilled water and an air bubble was formed before any viral solution was pulled up.

Injector tips were slowly lowered to -0.5 mm below-, and then pulled back to-, the target dorsoventral coordinate of -4.0 mm from skull, to create a small 'pocket' for the injection bolus from where the viral vector could then diffuse into the surrounding brain tissue. In cohort 1, rats were injected with 0.5 µl of viral solution on one side, and 1.0 µl on the other, at a rate of 0.1 µl/min, with the sides counterbalanced across rats. These volumes and injection rate were based on previous literature performing similar injections (Yau & McNally, 2015; Smith et al., 2016). In the second cohort, all rats received 1.0 µl bilaterally, infused at 0.1 µl/min. Following injections, the injectors were left in place for 5 min for the 0.5

µl injection volume and 10 min for 1.0 µl, to allow for absorption of the injection bolus. After completion of the injection, the incision was sutured up and rats were placed in recovery cages under red light overnight, before being moved to their home cage, where they were held for at least 28 days before any further procedures to allow for strong viral expression (Smith et al., 2016).

4.1.4 Cohort 1: FISH and preliminary immunohistochemistry

Brain extraction and preparation

Rats in cohort 1 were humanely killed using CO_2 asphyxiation (1 L/min). Brains were extracted and immediately placed on a metal plate on dry ice, rapidly freezing the tissue, and placed in a -80 °C freezer. Once frozen, brains were stored in 50 ml Falcon Tubes (Thermo Fisher Scientific, UK) and shipped on dry ice to facilities at Boehringer Ingelheim, Germany, where all further processing was carried out.

Frozen brains were placed in a polythene cup (22 mm x 16 mm; Agar Scientific, UK) which was placed on a metal block on dry ice. Tissue Tek O.C.T Compound (Sakura Finetek, USA) was added around the brain ensuring no air bubbles were introduced. Due to the low temperatures of the block, the liquid compound froze around the brain, creating a cylindrical block.

Coronal brain sections were cut on a Cryostat ("Cryostar NX70"; Thermo Fisher Scientific, Germany) with the block cooled to –10 °C and the blade to –7 °C. Prior to slicing, embedded brains were taken out of the –80 °C and placed in a –20 °C freezer overnight. On the day of sectioning, brains were placed inside the cryostat (at –10 °C) to allow the tissue temperature to equilibrate.

From each brain, several 10 µm coronal sections were taken around +4.2, +3.7, +3.2 and +2.7 mm from bregma, based on landmarks from a rat atlas (Paxinos & Watson, 1998). Filled slides were immediately placed inside a slide holder on dry

ice. Once all sections were collected, the holder was placed back in a −80 °C freezer until subsequent steps.

Fluorescent in-situ hybridisation

All FISH steps were carried out using the RNAscope Multiplex Fluorescent Assay (ACDBio, USA), as per the relevant protocol from ACDBio. Slices used for FISH were removed from the -80 °C freezer and immediately submerged in +4 °C 4% PFA for 15 min. Following this, slices were dehydrated by submerging in increasing concentrations of ethanol (50, 70, 100%) at room temperature. Hydrophobic barriers were drawn around each brain slice with the ImmEdge Pen (Thermo Fisher Scientific, Germany) and all slides were fixed into the EZ-Batch Slide holder (ACDBio). The following steps all took place in the HybEZ Humidity Control Tray (ACDBio), and humidity was ensured by the inclusion of wet humidifying paper in the tray. Next, tissue was hybridized at room temperature by hydrogen peroxide for 15 min, followed by protease IV (ACDBio) for 30 min. Target probes (Rn-Slc32a1 and Cre; ACDBio) were applied to the tissue and incubated at +40 °C in the HybEZ II (ACDBio) oven for 2 h. Afterwards, fluorophores (Opal 520, Opal 690; Akoya Biosciences, USA) were applied to designated probes and the signals were amplified. Following counterstaining with a nuclear DAPI stain (ACDBio), slices were mounted via ProLong Diamond Antifade Mountant (Thermo Fisher Scientific, Germany), cover-slipped, and stored at +4 °C in the dark, until scanning.

Immunohistochemistry

As all slices were fresh frozen and on slides, all immunohistochemistry steps for cohort 1 were carried out using the FISH equipment (EZ-batch holder, HybEZ Humidity control tray and wash tray; ACDBio), where solutions were directly applied to the slices, and held in place by a hydrophobic barrier. Again, required slices were taken out of the −80 °C freezer and immediately submerged in +4 °C PFA for 15 min. However, unlike FISH, no dehydration of the slices was carried

out. All incubation steps were carried out on a plate shaker (Duomax 1030, Heidolph Instruments, Germany).

Blocking solution (1% Bovine serum albumin (BSA), 0.3% Triton-X 100, 10% Normal goat serum (NGS), diluted in PBS) was applied to the slices and incubated at room temperature for 2 h. Then, primary antibodies (red fluorescence protein 'RFP' antibody (mouse monoclonal purified IgG); GAD_{67} antibody (rabbit polyclonal purified antibody); Synaptic Systems, USA), diluted in an antibody solution (1% BSA, 0.3% Triton-X 100, 1% NGS) were applied and incubated at +4 °C overnight. Following washing (45 min), via a washing solution (PBS, 0.1% Triton -X 100), of the slides using a plate shaker, secondary antibodies conjugated to Alexa 568 and Alexa 488 (Thermo Fisher Scientific, Germany), respectively, were applied and slides were incubated at room temperature for 3 h in the dark. Following another wash (60 min), 1-2 drops of ProLong Diamond Antifade Mountant containing DAPI (Invitrogen, USA) were put on each slide and slides were cover slipped.

Tissue scanning

Following both FISH and immunohistochemistry, slides were scanned on a florescence microscope using a 20x objective, with a pixel resolution of 0.22 μm/px and controlled by ZEN software (Zeiss AxioScan Z1 scanner; Carl Zeiss, Jena, Germany). The scanner was equipped with a Zeiss Colibri 7 LED light source (Carl Zeiss, Jena, Germany). Following image capture, scans were exported into HALO (IndicaLabs, USA) running the Multiplex FISH module for cell classification and quantification.

Cell classification and quantification

Parameters for automated cell classification were determined by examination of unambiguously VGAT+ and Cre+ cells for FISH analysis, and of GAD_{67} and mCherry positive cells for immunohistochemistry. Subsequently, each slice was examined

for potential false positive cases of cell classification, and the inclusion threshold was adjusted to best account for unambiguously positive cells, whilst minimizing the inclusion of false positive cases. Finally, each slice was examined once more to confirm parameters were suitable before automated cell counting was started.

During scanning, we noticed problems with tissue quality (such as damage or sub-optimal nuclei staining via DAPI in the VGAT-Cre rats), which resulted in the automated classification and quantification method not recognising cells correctly due to low intensity of DAPI signal, or other light artefacts, particularly with respect to the FISH signal. Therefore, FISH scans were re-quantified manually to complement the automated method.

Because analysis of all slices and each full slice via manual quantification would have been too time consuming, manual sampling was limited to slices corresponding to +3.7 mm from bregma. Additionally, areas were randomly sampled within each slice whereby a grid was placed over each scan with each box within the grid measuring 400 μm x 300 μm. The grid was then divided into rows and columns and for each brain ten boxes were selected by randomizing the row and column number. In case the box was either outside of the brain, or containing only part of the brain scan, new numbers were generated. Screenshots were taken of the sampled boxes and exported for later quantification. In total, 10 random samples were collected from each brain.

Cell-type classification parameters were determined prior to sampling. First, for cells to be counted as positive for a FISH marker, marker signal had to be located within, or immediately around, the nuclear DAPI stain. Second, cells were only counted as either VGAT- or Cre-positive if at least three fluorescent mRNA signals were observable. In some cells, multiple adjacent marker signals had merged into one large cluster. These cells were considered positive for the marker when it was evident from the size of the cluster that this was composed of at least three marker signals.

All visualisation steps of DREADD spread were carried out using Affinity Designer (Version 1.10.4, Serif). For visualisation of the DREADD spread in cohort 1, scans showing mCherry signal were superimposed onto a digital template of the Paxinos and Watson (1998) rat atlas. Scans were flipped if necessary, such that, between rats, all sides that received 1.0 µl were on the right hemisphere. Subsequently, scans were matched with coronal sections of the rat atlas based on apparent morphological landmarks. Due to variability in brain shape and size, scans were manipulated to best fit the template at the approximate distance from bregma. mCherry signal was traced by hand, and opacity of the regions reduced to 25% such that overlapping regions appeared darker.

4.1.5 Cohort 2 – Acute *in vivo* electrophysiology to characterise DREADD functionality and further immunohistochemical characterisation of DREADD expression

Implantation of recording array

Rats were anesthetized with isoflurane (induction: 3%; maintenance: 1-3%) delivered in medical oxygen (1 L/min). Once induced, rats' scalps were shaved, rats were transferred to the stereotaxic frame where they were secured in the horizontal skull position with ear bars coated with local anaesthetic cream (EMLA 5%, containing 2.5% lidocaine and 2.5% prilocaine; AstraZeneca, UK). Eye gel (Lubrithal, Dechra, UK) was applied to the eyes to prevent drying out during surgery, and the shaved scalp was disinfected with alcoholic skin wipes (2% clorhexedine, 70% alcohol; Clinell, UK). Throughout the surgery, body temperature was maintained at 37 °C via a homeothermic heating pad controlled by an external temperature probe placed under the rat. Following a scalp incision, bregma was located and aligned with the centre of the electrode array. The skull was removed over the target area above the right mPFC (AP: +3.0 mm, ML: +0.6 mm). The exposed dura was incised and removed via forceps. Throughout the duration of the recording session the cortex was kept moist with 0.9% saline.

A four-channel microwire array (four 50 μm stainless steel Teflon-coated electrodes, 0.25 mm wire spacing, with a stainless-steel ground wire; MicroProbes for Life Science, USA; see fig. 11A) was then implanted into the right mPFC. The array was connected via a head stage to the recording system (see below, *Multi-unit and LFP recordings*). The assembly was slowly lowered to the target coordinates (DV from skull -4.0 mm) such that the electrodes were running parallel to the midline. Positioning of the electrodes at the target coordinates was followed by a stabilisation period of at least 30 min, during which anaesthesia was adjusted to a stable level (50±10 breaths per minute, around 1.5–2% isoflurane).

Drug preparation and systemic injection of saline or CNO2HCl

One of the most frequently used actuators of DREADDs remains CNO. Previous studies have typically used 5-10 mg/ml/kg of freebase CNO to activate relevant DREADDs (Smith et al., 2016). For the DREADD activation in the current experiment, CNO2HCl was used, provided by our collaborative partner Boehringer Ingelheim, Germany (synthesised in-house). The addition of the 2HCl group improves solubility compared to the freebase alternative. Due to the increased molecular weight of CNO2HCl compared to CNO (factor of 1.2x; 415 g/mol compared to 342 g/mol), the dose of the former was adjusted to reflect this difference (i.e., 6 mg/ml/kg).

Multi-unit and LFP recordings

The setup of the recording system was as in Pezze et al. (2014). In short, the electrode array was connected via a unity-gain multichannel head stage to a multichannel preamplifier (Plexon, USA). The analogue signal was amplified (1000x) and filtered, via a band-pass filter, into multi-unit spikes (250 to 8 kHz) and LFP signals (0.7 to 170 Hz). All recordings were made against ground, with the ground wire attached to the ear bar of the stereotaxic frame. The analogue signal was further amplified via a multichannel acquisition processor system (Plexon) (final gain up to 32,000). This system also provided additional filtering

of multi-unit data (500 to 5 kHz), digitalisation of spikes at 40 kHz, and LFP data at 1 kHz. Both, multi-unit and LFP data were viewed online with Real-Time Acquisition System Programs for Unit Timing in Neuroscience (RASPUTIN) software (Plexon). Using RASPUTIN, neural activity was recorded for 30 min for both baseline and post-saline injection, and 2 h post-CNO2HCl injection. Multi-unit spikes were recorded when a pre-defined threshold of -240 µV was exceeded, and LFP data was recorded continuously.

Following the initial period of 30 min recording baseline activity without any drug manipulation, each rat received an i.p. injection of sterile saline (0.9%; 1 ml/kg), by gently raising the rat's right hindlimb and injecting into the lower abdomen. Once injected, the rat's hindlimb was gently lowered again, and the start and end times of the injection were noted to later accurately identify the pre- and post-injection times. After a further 30 min recording post-saline, rats received an injection of CNO2HCl (6 mg/ml/kg) in the same manner and location as the saline injection. All rats received saline first, followed by CNO2HCl. Visual inspection of LFP traces and multi-unit data indicated some changes following movement of the hindlimb and injection of either drug, primarily manifested by increased spiking immediately following injection, as well as rapid fluctuations in LFP traces. These effects subsided within 20 min post-injection.

Verification of electrode placement

Following the 2 h post-CNO2HCl period, a current (1 mA, 10 s) was passed through the first and fourth microwire to create an electrolytic lesion at the tip of the electrode and mark its position (see fig. 11B for an example). Following this marking, the electrode assembly was removed from the brain. As these brains were subsequently used for immunohistochemical procedures, tissue slicing and scanning protocols are as outlined below. Locations of marked electrode tips were mapped onto coronal sections of the rat brain atlas (Paxinos & Watson, 1998) (see fig. 11C).
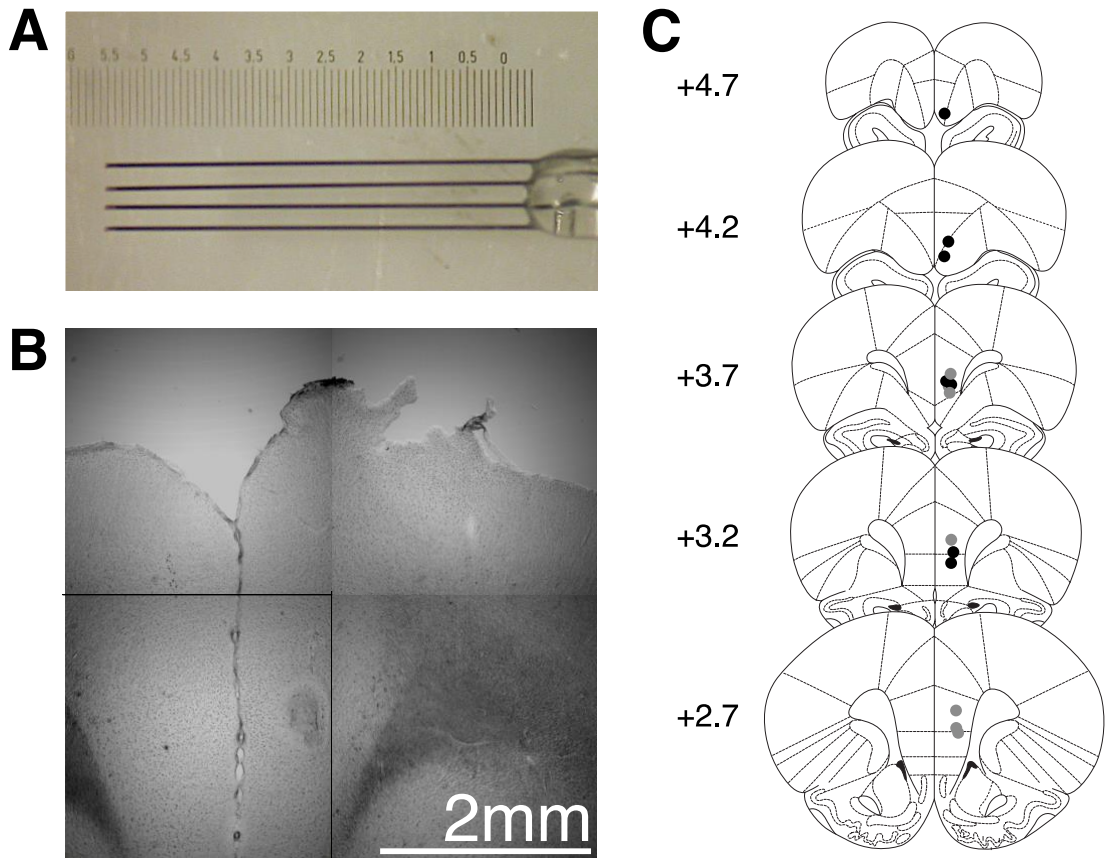
Figure 11. In vivo electrophysiology electrode placement. A) Photograph showing four-microwire-electrode array used in electrophysiological recordings. Depicted scale is in 0.01 mm. B) Image of electrolytic markings in the mPFC of one coronal slice used to verify electrode placement. C) Approximate locations of electrode tip markings for anterior (black) and posterior (grey) electrodes. Locations are plotted on coronal plates from Paxinos and Watson (1998), with numbers indicating distance from bregma (in mm).

Brain extraction and preparation

Immediately after the electrophysiological recording session was finished, rats were overdosed with sodium pentobarbitone (1-2 ml Euthatal; sodium pentobarbitone, 200 mg/ml; Genus Express, UK) and transcardially perfused with approximately 160 ml of cold PBS followed by approximately 160 ml of cold paraformaldehyde solution (4%). Following extraction, brains were post-fixed in 4% paraformaldehyde overnight at +4 °C, and then transferred into sucrose solution (30%) and stored at +4 °C until slicing. Brains were shipped to facilities

at Boehringer Ingelheim, Germany, where all further processing was carried out by the lead investigator.

Brains were cut into coronal sections on a sliding microtome (Microm HM450, Thermo Fisher Scientific, Germany) with integrated freezer platform (BFS-3MP, Physitemp, Germany). Prior to slicing, the platform was cooled to -30 °C. After removal of the cerebellum, the brain was placed onto the platform and frozen. 50 μm coronal section were taken from between +6.5 and +1.0 mm from bregma, and placed immediately into wells (24-well, Nuclon Delta Surface; Thermo Fisher Scientific, Germany), filled with 2 ml PBS and 0.01% thimerosal. Brain sections were stored at +4 °C until further processing.

Slice selection

Slices used for immunohistochemistry within the second cohort were selected based on proximity to the injection site (i.e., between +3.7 to +3.0 mm from bregma). The reason for this selection was to ensure maximal DREADD expression on each slice, as more distal regions would have received less viral solution, and thus would have resulted in less DREADD expression, irrespective of viral potency.

Slices used to visualize the spread of hM4Di expression across the PFC (by using the endogenous fluorescent mCherry reporter) were selected according to morphological landmarks, from between +5.5 and +2.0 mm from bregma, including the majority of the mPFC, centered at the approximate injection site.

Immunohistochemistry to visualize co-expression of DREADD with neuronal markers

Unlike immunohistochemistry in the first cohort, all steps for this cohort were carried out in wells. First, tissue was incubated in a blocking solution (1% BSA, 0.3% Triton, 10% NGS, diluted in PBS) at room temperature for 2 h. Subsequently,

primary antibodies (GAD$_{67}$ antibody (mouse monoclonal purified antibody, Millipore, Germany); CamKIIα antibody (mouse monoclonal purified antibody, Millipore, Germany); ChAT antibody (rabbit polyclonal purified antibody, Synaptic Systems, Germany)) were applied and incubated overnight in +4 °C. The following day, slices were washed for 45 min, and secondary antibodies conjugated to Alexa Fluro 488 (Thermo Fisher Scientific, Germany) were applied and incubated at room temperature for 3 h. After a final wash (60 min), slices were transferred into a glass bottom 24-well plate (Sensoplate, Greiner Bio-One, Austria), mounted via DAPI-containing Fluoroshield (Sigma Aldrich, Germany), and stored in the dark at +4 °C until scanning.

Visualisation of DREADD spread

Slices for DREADD spread analysis using the fluorescent mCherry reporter did not require additional staining. Therefore, they were placed in a glass bottom 24-well plate, and then mounted via DAPI-containing Fluoroshield. Spread was visualised as in cohort 1.

Tissue scanning

Slices were scanned on the Opera Phenix high-content confocal microscope (PerkinElmer, USA) running Harmony high-content imaging software (PerkinElmer). Slices used for the visualisation of DREADD spread were imaged using a 5x objective (2.39 µm/px), whilst slices used for co-localisation analysis were imaged using a 63x water immersion objective (0.19 µm/px). At this stage, verification of electrode placement was conducted on a fluorescent light microscope (Olympus CK40; Olympus Life Science, USA) with adjustable magnification, ensuring endogenous mCherry signal was substantial around the electrode tips.

4.1.6 Quantification of penetrance and specificity

All analysis across both cohorts was carried out in Prism (Version 9.4.1, GraphPad). DREADD spread was qualitatively quantified, using a rat brain atlas (Paxinos and Watson, 1998). One animal was excluded from the second cohort, due to a large ventral prefrontal lesion in the left hemisphere, limiting analysis potential.

Penetrance and specificity of Cre-recombinase

FISH data from cohort 1 was only analysed at +3.7 mm from bregma. This was based on the fact that the driver responsible for Cre-expression was the Slc32a gene (expressing VGAT). Therefore, we expected Cre-expression to be proportional to VGAT localisation, regardless of localisation. Cell-type specificity was calculated as a proportion of Cre+ cells that also expressed VGAT as well as identifying those that do not (i.e., off-target expression), whilst penetrance was calculated as the total number of VGAT+ cells that also expressed Cre.

Penetrance and specificity to DREADD expression

Immunohistological data for the first cohort was exported from HALO into Prism. Quantification was limited to the prelimbic cortex at +3.2 mm from bregma only, as it was of interest to quantify DREADD expression, when injection parameters were optimal (i.e., close to injection site). For this analysis, slices were matched via anatomical landmarks to sections corresponding to +3.2 mm in the Paxinos and Watson (1998) rat atlas. Subsequently, relative prelimbic cortex location was determined via its proximity to the forceps minor, accounting for dorsal and ventral regions of the anterior cingulate, and infralimbic cortex, respectively. One rat from cohort 1 was excluded from this analysis due to indications that the DREADD injections did not work, with below 5% DREADD expression at 1 µl at +3.2 mm from bregma. Analysis for cohort 2 used four slices per rat, between +4.7 to +3.0 mm from bregma, encapsulating the majority of the PFC. Analysis was also

limited to prefrontal areas only. Collected images from cohort 2 were exported into Acapella Studio (Version 5.2.0.125910; PerkinElmer) running a custom script used to select fields to be analyzed. Here, cell-type specificity was calculated as the percentage of mCherry+ cells that also expressed GAD_{67}, as well as CamKIIα and ChAT. Good specificity would be related to high levels of GAD-mCherry co-localisation, whilst CamKIIα and ChAT would be minimal. Overall penetrance was calculated as the total number of GAD_{67}+ cells that also expressed the DREADD.

4.1.7 Analysis of electrophysiological data

Unsorted multi-unit data was imported and analysed in Neuroexplorer (Version 3.2.2.6 Nex Technologies). As in Pezze et al. (2014), parameters of multi-unit activity (overall firing rate, number of bursts, percentage of spikes fired in bursts, mean within-burst firing rate, mean burst duration, inter-burst interval) and LFP power data, as reflected by the area under the curve (AUC) of power spectral density (PSD) were calculated in 5-min blocks across the whole recording session, including baseline, post-saline and post-CNO2HCl periods. Prefrontal burst firing was defined as spike trains with relatively high firing rate (three or more spikes with an inter-spike interval of less than 6 ms), which are surprising (i.e., improbable) in relation to the rest of the analysis window. LFP AUC of PSD was calculated by applying a fast Fourier transform analysis to the LFP signal from 0.7-170 Hz (Pezze et al., 2014). All data was normalised to baseline by dividing values from each channel by the average value obtained from the same channel during the six 5-min baseline recording blocks. Normalised values were averaged across all four channels to obtain one single value of each parameter per 5-min block for each rat, resulting in 36 5-min blocks per rat (6 baseline, 6 post-saline and 24 post-CNO2HCl). With respect to sample size justifications of this examination, as we did not intend on carrying out formal analysis of the electrophysiological data collected, and instead focussed on large scale changes in burst firing pattern and LFP power observable via qualitative inspection, the low sample size was deemed sufficient for this purpose. Finally, two out of seven rats were excluded from the

electrophysiological analysis due too minimal DREADD expression around the electrodes.

4.2 Results

4.2.1 Seizure related behaviour in VGAT-Cre rats

As outlined above, several behaviours that may be seizure 'precursors', including marked hyperactivity and forelimb twitching, as well as convulsive seizures were noted in the VGAT-Cre rats, in particular in cohort 2 which also received behavioural testing accompanied by food restriction (85-90% if free feeding weight). Seizures typically manifested in the form of hyperactive running, followed by convulsions and loss of postural control, in total lasting approximately 20-30 s. In total precursor behaviour was noted in one rat in cohort 1, and three rats in cohort 2, with one rat of the latter requiring termination due to the occurrence of multiple convulsive seizures within the same week.

4.2.2 Cohort 1

Validation of the transgenic VGAT-Cre rat line: high co-expression of VGAT and Cre and limited off-target expression of Cre

Whole-slice automated analysis at +3.7 mm from bregma, investigating fluorescent signal of VGAT and Cre mRNA via FISH revealed, on average, 88.49±3.32% (*SEM*) of VGAT+ cells were also Cre+ across all 4 VGAT-Cre rats. As expected, Cre was not expressed in the WT rats (*n*=3), with minimal signal attributable to light artefacts whilst scanning. Interestingly, in the VGAT-Cre rats, an average 9.17±4.36% (*SEM*) of total Cre expression was not co-localised with VGAT, indicating quite substantial off-target expression. However, similar to the WT data, these findings were confounded by damaged tissue, which the automated quantification counted as positive cells. Manual sampling supported high penetrance of the Cre-expression VGAT-Cre rats, with an average of

98.49±0.004% (*SEM*) of all counted VGAT+ cells containing Cre. Furthermore, off-target Cre expression was found to be lower than in the automated method, yet still substantial at an average 4.40±0.31% (*SEM*). Example FISH images for VGAT-Cre and WT rats can be seen in figure 12A.
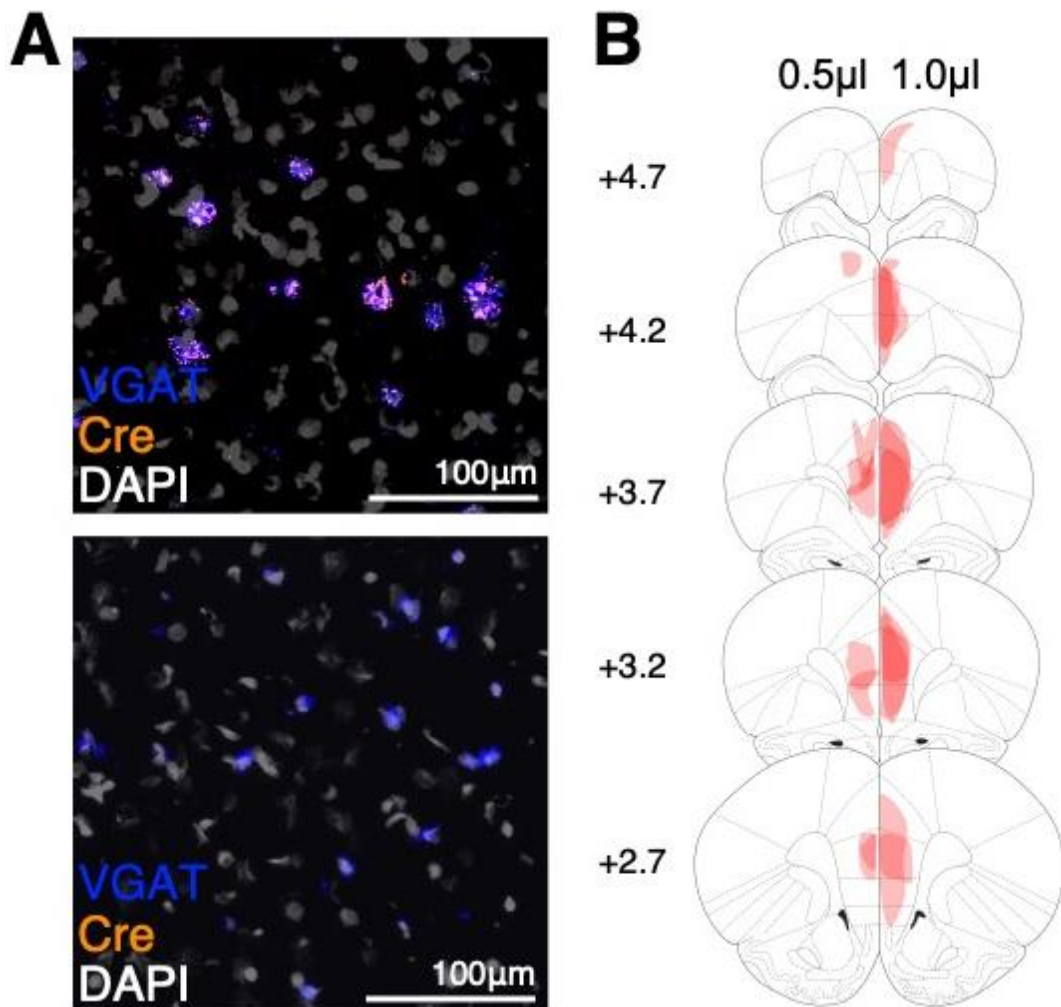

Figure 12. Example FISH scans and DREADD spread quantification of cohort 1. A) VGAT and Cre-recombinase expression in VGAT-Cre (top) and WT rat (bottom) with nuclear DAPI counterstain. In both examples, VGAT is stained blue and Cre is stained orange, with purple signal indicating overlap of the two stains. B) Spread of DREADD expression measured via immunohistochemistry across prefrontal cortex at 0.5 μl (left) and 1.0 μl (right). Each rat's expression is uniformly shaded, meaning darker regions indicate overlap between rats. Distance from bregma (in mm) indicated on the left.

Preliminary evidence for DREADD penetrance in and specificity to GABAergic neurons of mPFC with viral vector injection volumes of 0.5 and 1 μl

Co-localisation of GAD_{67} and hM4Di receptors, labelled via endogenous mCherry signal at +3.2 mm from bregma was significantly greater with an injection volume of 1.0 than 0.5 μl. Penetrance of the DREADD was 66.66±6.80% (*SEM*) of all GAD_{67}+ cells for the hemisphere that was injected with 1.0 μl of the viral vector and 13.95±4.48% (*SEM*) for the hemisphere injected with 0.5 μl (*n*=3, one-tailed paired t-test, $t(2)=3.843$, $p=0.031$). Cell-type specificity of the DREADD expression was also very good, with an average off-target expression of 0±0% (*SEM*) at 0.5 μl, and 7.23±1.16% (*SEM*) at 1.0 μl (one-tailed paired *t*-test, $t(2)=5.079$, $p=0.018$).

Greater DREADD expression spread at 1.0 μl, compared to 0.5 μl of the AAV vector

As expected, greater volume of viral solution (1.0 μl) resulted in better DREADD expression around the injection site, and greater spread to more distal regions to, compared to 0.5 μl (fig. 12B). The difference in expression is particularly noticeable in prelimbic, infralimbic, and anterior cingulate regions at +3.2 and +2.7 mm from bregma. Strong DREADD expression can be seen even at +4.2 mm from bregma following 1.0 μl, but not 0.5 μl. Based on these findings, we decided to use a volume of 1.0 μl of viral vector solution for cohort 2 (and subsequent DREADD studies).

4.2.3 Cohort 2 – histological findings

Cell-type specificity and penetrance of DREADD expression

Expression of the inhibitory DREADD was predominantly limited to GAD_{67}+ cells (fig. 13A & B). Nearest to the injection site (i.e., around +3.2 mm from bregma) an average of 60.8±1.81% (*SEM*) of all DREADD expression was localised to GAD_{67}+ cells (consistent with our finding of about 67% in cohort 1), whereas co-localisation of mCherry and CamKIIα was minimal at 2.35±0.52% (*SEM*). This

apparent co-localisation probably reflects, at least partly, close proximity of glutamatergic (CamKIIα+ cells) to mCherry positive GABAergic (GAD$_{67}$+) cells. Finally, there was some co-expression of mCherry in ChAT+ cells with an average co-localisation of 5.33±0.89% (*SEM*), which, upon closer inspection, was truly reflective of mCherry expression in ChAT+ cells. Average penetrance of the DREADD construct was 29.58±1.23% (*SEM*) of all GAD$_{67}$+ cells within area around the injection site, compared to 0.67±0.19% (*SEM*) of all CamKIIα cells. Of all cells labelled by DAPI, 6.77±0.33% (*SEM*) also exhibited GAD$_{67}$ signal, indicating that at least about 7% of all cells in the mPFC were GABAergic.

Spread of DREADD expression within the prefrontal cortex

The DREADD injection was targeted at the prelimbic cortex, similar to our picrotoxin infusions in our behavioural pharmacological studies, and we aimed for DREADD expression to extend throughout the mPFC, including prelimbic, infralimbic and anterior cingulate cortex. As shown in figure 13C, DREADD expression was very strong across the entire PFC. All rats appeared to express the DREADD in central portions of the prelimbic cortex around our target coordinates (corresponding to coronal sections between +3.2 and +2.7 mm from bregma), but expression is less consistent at the most anterior and posterior parts of the prelimbic cortex. The anterior cingulate cortex also showed very high expression in all rats, likely due to viral solution moving up the injector tract after injection, resulting in high levels of expression in more dorsal areas of mPFC. Ventral areas of the mPFC, such as the infralimbic cortex, show comparatively less expression, with only some of the rats (2 out of 7) showing notable DREADD expression between +3.7 and +2.2 mm from bregma.

Some DREADD expression was also evident in several areas adjacent to the mPFC, including areas of the OFC and secondary motor cortex. With regards to the OFC, expression was primarily limited to the medial OFC, corresponding to coronal sections between +5.2 +3.2 mm from bregma. Additionally, large portions of the medial secondary motor cortex show DREADD expression (+5.2 to +2.2 mm from bregma). Most notable is this expression in the most anterior regions (between

+5.2 to +3.2 mm from bregma), with expression in more posterior slices limited to only two rats. As for the anterior cingulate cortex, this expression may be attributed to spread of the viral solution from the injector tract after injection.
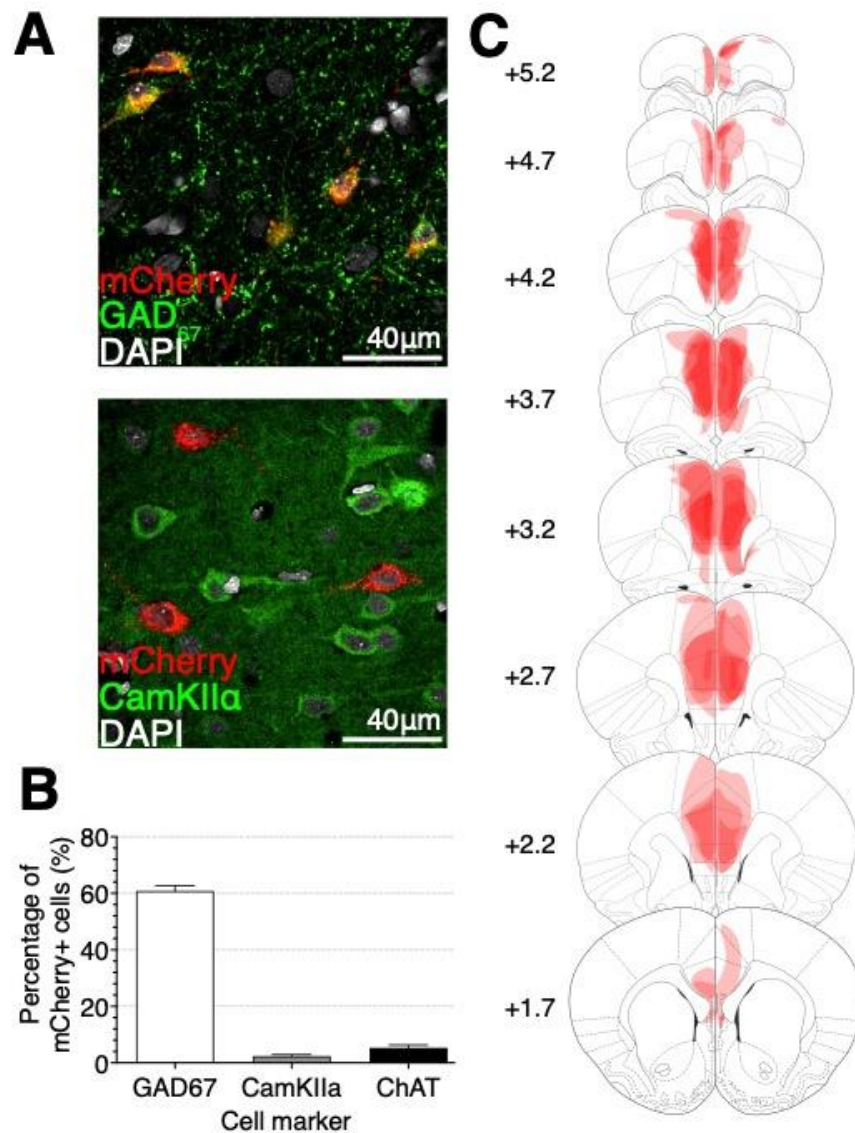

Figure 13. Summary of ex vivo findings from cohort 2. A) Example histological staining for mCherry and GAD_{67} (top), CamKIIα (bottom) with DAPI counterstain. B) Cell-type specificity as percentage of total DREADD expression. Error bars indicate +*SEM*. C) Findings of DREADD spread across PFC. Each rat's expression was uniformly shaded, meaning darker regions indicate overlap between rats. Distance from bregma (in mm) indicated on the left.

A further region that shows DREADD expression is the dorsal peduncular cortex, located below the infralimbic cortex starting at +3.2 mm from bregma. However, in comparison to the above, expression in this ventral area was not common, with only two rats showing minor spread into this region, particularly at very posterior slices (+1.7 mm from bregma). These two rats also showed very minor expression in the indusium griseum and encroaching into the lateral septum (+1.7 mm from bregma).

4.2.4 Cohort 2 - *In vivo* electrophysiological findings

Electrode placement

Two out of seven rats did not have sufficient DREADD expression surrounding the marked electrode site and were therefore excluded from analysis. Within the remaining 5 rats, all electrodes were placed within the mPFC corresponding to between +4.2 to +2.7 mm from bregma (see fig. 11C).

Comparison of mean baseline values with Pezze et al. (2014)

We first examined baseline values of the current electrophysiological measures with the baseline values of the saline condition reported in Pezze et al. (2014). Overall- and within-burst firing rates were very comparable between the current investigation (in spikes/s: 17.6±4.2 and 237.6±8.6, respectively) and previous work (in spikes/s: 17.5±5.9 and 223.3±33.3, respectively). On the other hand, average number of bursts within a 5-min block, percentage of spikes fired in bursts, and mean burst duration were substantially different in the current investigation (190.0±42.6, 85.9±3.2%, and 0.15±0.01 s, respectively) compared to previous work (132.4±57.7, 69.3±4.1%, and 0.23±0.3 s, respectively). Finally, with regards to AUC of LFP PSD, current baseline power was an average of 0.007±0.0007 μV^2, compared to 0.015±0.004 μV^2 from previous work. These comparisons indicate several similarities in baseline activity between current and previous work. Some differences are noted, but it is unclear whether these reflect strain differences, or simply methodological differences from previous work.

Regardless, as all values were normalised to pre-saline baseline within each animal, the effect of these strain-dependent difference should be limited.

Qualitative observations, CNO2HCl injection caused marked LFP SWD within the mPFC.

Chemogenetic disinhibition resulted in notable changes in LFP pattern, with an increased frequency of SWD in the mPFC of rats following systemic injection of CNO2HCl compared to saline (fig. 14). Notably, and in contrast to saline, following CNO2HCl burst were predominantly localised to the marked negative inflection of the LFP signal, which is followed by a long positive 'wave'. In comparison, LFP traces following saline injection fluctuated greatly and at a much-reduced magnitude. Previous work has highlighted these LFP SWD as a key characteristic of prefrontal disinhibition, and visual comparison between current and previous work suggests similar levels of effect (Pezze et al., 2014).
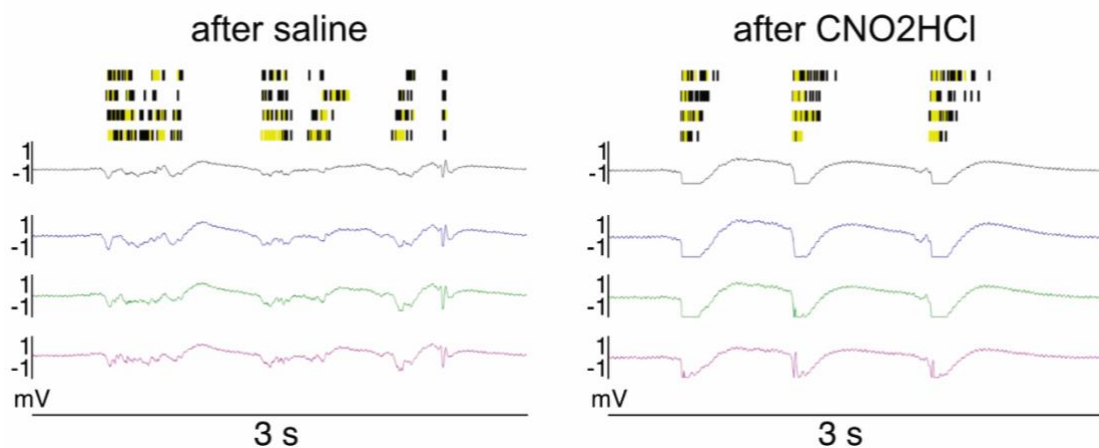

Figure 14. Multiunit activity and accompanying LFP traces 15 min post-saline and CNO2HCl. Black vertical lines indicate individual spikes, with yellow shaded regions automatically classified as bursts. Coloured lines indicate LFP traces

Chemogenetic prefrontal disinhibition intensifies burst-firing and increases LFP power, similar to picrotoxin

Within-burst firing rate markedly and robustly increased following prefrontal disinhibition compared to baseline and the saline condition (fig. 15A). Furthermore, inter-subject variability was very low for this parameter, indicating a stereotypical effect on within-burst firing. Again, the effect of CNO2HCl was long lasting, with a stable effect for up to 2 h post-injection, and the peak within-burst firing rate of approximately 1.5x of baseline within-burst firing was very similar to values observed in previous work (peak at 1.5-1.6x; Pezze et al., 2014).
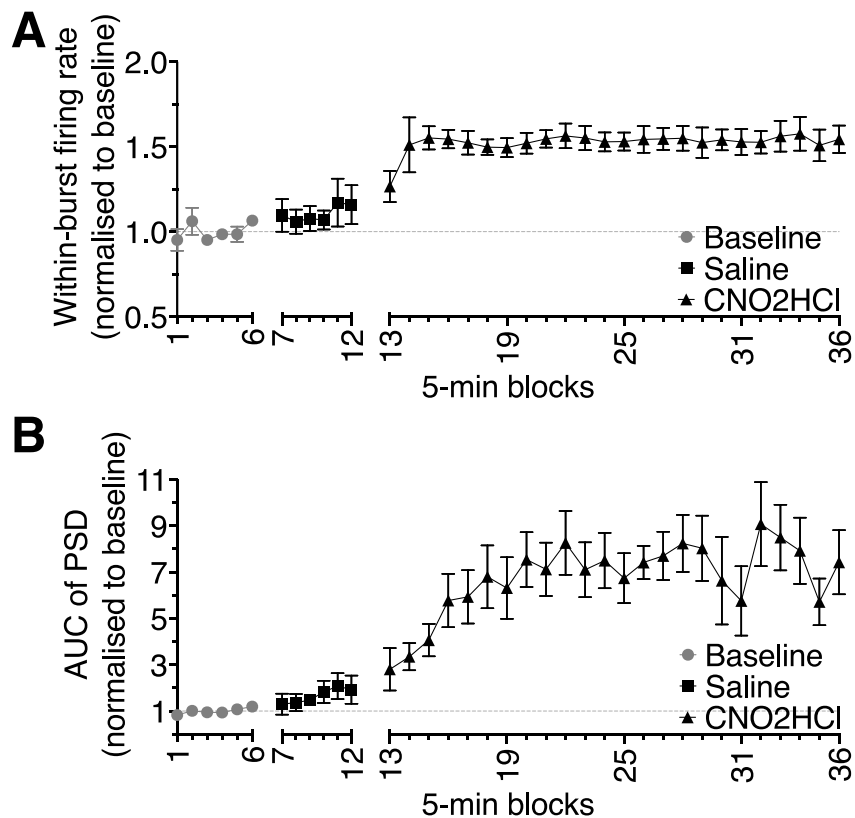

Figure 15. Key electrophysiological pattern observed following chemogenetic prefrontal disinhibition. A) within-burst firing rate, B) LFP power (AUC of PSD). Error bars indicate ±*SEM*.

With respect to overall LFP power, as measured by AUC of PSD, baseline and post-saline values were very stable with a slight upwards drift noted during the saline recording. However, following CNO2HCl, LFP power increased substantially, albeit at a slower rate than in some of the burst firing parameters (an increase of around 50% of baseline power per 5-min block), peaking at around 7x baseline power 30 min post-CNO2HCl injection. Furthermore, LFP power remained above at least 5x baseline power until the end of the recording, with some substantial fluctuations during later stages of the session, likely due to inter-subject variability of the DREADD expression or drug absorption (fig. 15B). In previous work, higher doses of picrotoxin resulted in a sharper, more rapid increase in LFP power, peaking at 7x baseline power 15 min post-injection, whilst lower doses peaked at around 5x baseline power 25 min post-injection. In both cases, power decreases rapidly after each peak returning to baseline around 90 min post-injection. In the current examination, the magnitude of the peak post-injection was most analogous to the higher dose of picrotoxin, whilst the onset of the peak was much more akin to the lower alternative. Furthermore, the duration of the effect is substantially longer, which may reflect the difference in drug administration (microinfusions of 0.5 µl versus systemic injection).

Main electrophysiological differences to previous work

Overall firing rate was very variable between animals, much like previous pharmacological work (Pezze et al., 2014) (fig. 16A). In contrast, however, systemic injection of saline resulted in a rapid peak in activity 15 min post-injection, which returned to pre-saline levels at around 25 min post-injection. Similarly, injection of CNO2HCl also resulted in such an early spike in activity followed by a rapid decrease shortly thereafter. In both cases, this sharp and transient peak may reflect residual activity of the central nervous system in response to somatosensory stimulation of the rear limb movement required for injection, or the injection itself. It has previously been noted that similar stimulation can affect firing properties of prefrontal neurons of rats (Cenci et al., 1992; Lupinsky et al., 2010; Nogueira & Lavin, 2010), and the observed pattern in

current work may, thus, be of similar nature. This difference in pattern would therefore reflect a key methodological difference between systemic injections and previously used intra-cerebral microinfusion.

Previously, pharmacologically induced prefrontal disinhibition was shown to result in marked increases in the average number of bursts in each 5-min block at low doses (150 ng), but not high doses (300 ng; Pezze et al., 2014). Results of the current examinations revealed similar findings to the high doses in this regard. Interestingly, this effect followed a comparable trajectory to the pattern of overall firing rate post-CNO2HCl injection, consisting of an immediate spike following injection of CNO2HCl which returned to baseline soon thereafter, which was followed by a gradual, but minimal increase across the subsequent 2 h (fig. 16B). This sudden increase immediately after injection likely reflects similar non-specific activity following somatosensory stimulation, with the marked increase in overall firing rate inevitably resulting in an increase in the number of bursts.
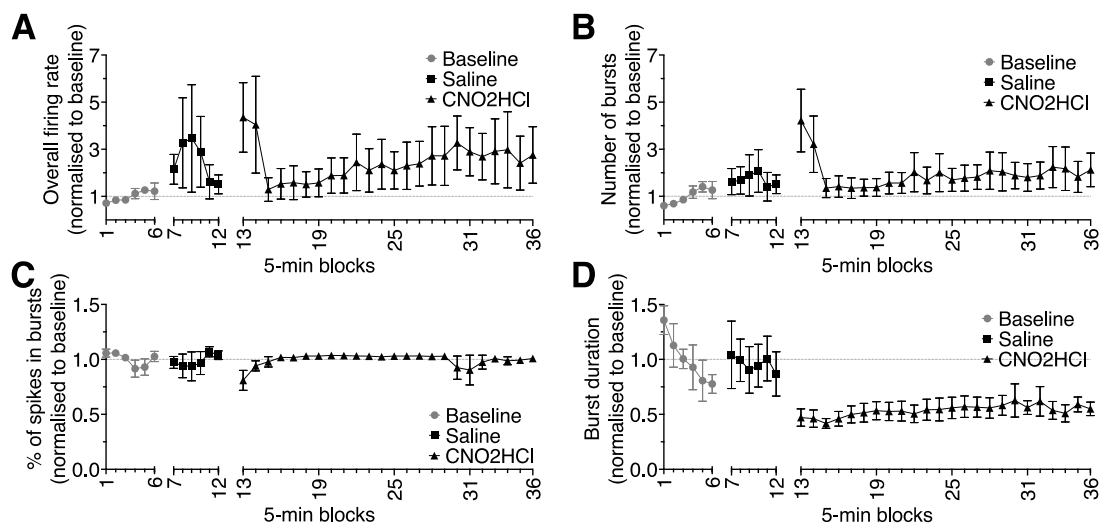

Figure 16. Additional findings of multi-unit recording. A) overall firing rate, B) number of bursts, C) percentage of spikes fired in burst, D) average burst duration. Error bars indicate ±*SEM*.

Chemogenetic prefrontal disinhibition did not increase the percentage of spikes fired in bursts post-CNO2HCl (fig. 16C). In fact, immediately after injection of CNO2HCl, a sharp decrease was noted, which may, again, be concurrent with the somatosensory-specific increase in overall firing rate. Percentage of spikes fired in bursts quickly returned to baseline levels and remained stable for the 2 h post-injection. The absence of a notable effect in this parameter may reflect strain-dependent differences, with the current cohort having an average of 85.9±3.2% (*SEM*) spikes fired in burst, limiting potential for any further increase. Interestingly, previous work has found that percentage of spikes fired in burst only increased at high doses of picrotoxin, whilst 150 ng did not increase this parameter. As such, it remains unclear if the absence of an effect is due to ceiling effects due to inherently high baseline activity, or whether it merely aligns with effects following lower doses of pharmacologically induced disinhibition.

Finally, the temporal pattern of burst firing notably decreased injection of CNO2HCl, to around 50% of baseline burst duration, starting as soon as 5-min post-injection and lasting for the entire 2 h post-injection period (fig. 16D). This effect is consistent with the effects of low doses of picrotoxin from previous work, whereas higher doses showed a biphasic effect with an initial increase in burst duration followed by a subsequent decrease.

4.3 Discussion

The VGAT-Cre Long Evans rats in conjunction with the inhibitory hM4Di DREADD offer a novel approach to inhibiting prefrontal GABA neurons. The histological studies in this chapter suggest greater spread across the PFC and expression is achieved following injections of 1.0 compared to 0.5 μl into the prelimbic cortex. Furthermore, the DREADD is primarily expressed by GABAergic cells, as opposed to cholinergic or glutamatergic cells. Observed penetrance of the DREADD across the total population of $GAD_{67}+$ cells in the PFC is substantial, at around 30% of all $GAD_{67}+$ cells expressing DREADDs. Subsequent *in vivo* electrophysiology highlighted functionality of the DREADD construct, with several key electrophysiological characteristics of prefrontal disinhibition being evident

following hM4Di activation via 6 mg/ml/kg of CNO2HCl. Chemogenetic prefrontal disinhibition resulted in a marked, long lasting change in LFP pattern, characterized by marked SWD and an overall increase in LFP power. Additionally, several burst firing parameters were markedly altered, with an increase in within-burst firing rate, as well as a decrease in burst duration.

4.3.1 Penetrance, specificity and spread of the DREADD

Strong DREADD penetrance was observed at GABAergic neurons, with an average of around 30% of all GABA neurons near the injection site expressing the hM4Di construct. Furthermore, specificity of DREADD expression was approximately 60%, with near-zero expression at excitatory cells, which was laid out as a requirement for the validation of the hM4Di construct. Whilst histological findings indicated some DREADD expression in cholinergic neurons, this co-localisation may simply represent a sub-population of GABA-acetylcholine co-releasing neurons (Saunders et al., 2015; Granger et al. , 2016), which has been suggested to be as large as 30% of all GABA releasing neurons (Granger et al., 2020). Our findings of DREADD expression at around 5% of ChAT+ neurons, therefore, falls into an acceptable range when considering the total penetrance of all GAD_{67}+ cells.

In the present study, we found that 30% of the DREADD expression cannot be attributed to inhibitory, excitatory, or cholinergic markers. One plausible explanation for this unexplained expression might be related to the limitations of the GAD_{67} antibody. Previous research has estimated that approximately 20-30% of neurons in the rodent cortex are GABAergic (Markram et al., 2004). Additionally, in the rat mPFC, it has been reported that around 16% of neurons are GABAergic (Gabbott et al., 1997), with a neuron-to-glial cell ratio of roughly 2:1, meaning that two-thirds of all cells in the mPFC are neurons (Markham et al., 2007). In our current work, we observed that approximately 7% of all cells tested positive for GAD_{67}. Assuming the same neuron-to-glial cell ratio and considering that GAD_{67} is exclusively expressed in neurons, our findings suggest that the proportion of neurons expressing GAD67 is approximately 10.5% (calculated as

(3/2)*7%, or 21/2). This estimation is notably lower, by about one-third, compared to previous research (e.g., Gabbott et al., 1997), indicating that a significant portion of the GAD_{67} signal may have been missed during our current immunohistological staining. As such, we believe the true penetrance and specificity of the DREADD may be even higher than what our current examinations revealed.

4.3.2 Electrophysiological results

Previous work by Pezze et al. (2014) combined behavioural and electrophysiological findings following pharmacologically induced prefrontal disinhibition via two doses of picrotoxin. That study highlighted substantial changes in prefrontal multi-unit firing pattern and LFP traces and power, correlating with subsequent behavioural impairments. Specifically, within-burst firing rates increased across both doses, with an additional increase in the total number of bursts and percentage of spikes fired in bursts at high doses, whilst the low dose notably decreased burst duration. The current electrophysiological findings following prefrontal disinhibition by CNO2HCl injection in rats expressing an inhibitory DREADD in the mPFC replicate many of these patterns. Most notably, the occurrence of SWD accompanied by increased LFP power and within-burst firing rate all replicate patterns overserved following pharmacologically induced disinhibition at both doses of picrotoxin. In contrast, the absence of an effect on the percentage of spikes fired in bursts, average number of bursts, and burst duration is more akin to findings of low doses of picrotoxin used previously. Moreover, the percentage of spikes fired in bursts are similarly unaffected in the current investigation as following low doses of picrotoxin (Pezze et al., 2014). Finally, the largest differences between pharmacological and chemogenetic models of prefrontal disinhibition lies in the duration of the effect, with pharmacologically induced effects largely dissipating within one-hour post-infusion, whilst the current findings highlight stable changes for up to two hours post-injection. This may reflect differences in the nature of the manipulation (acute microinfusions versus systemic injections), and

aligns with previous DREADD work showing equally long-lasting behavioural changes following DREADD manipulation (Urban & Roth, 2015).

4.3.3 Considerations for future *in vivo* behavioural investigations

To summarise, the current chapter aimed to validate an inhibitory cell-type specific DREADD construct via histological and electrophysiological methods. Here we showed applicable hM4Di expression, as well as comparable electrophysiological changes following DREADD activation to pharmacological alternatives. As such, these findings support the subsequent use of this construct in *in vivo* behavioural testing. There are several important considerations with regards to the use of this rat line and associated DREADD construct for behavioural testing. Firstly, there may be baseline differences between task proficiency or rate of learning between Lister hooded and the current transgenic Long Evans rats. Therefore, it would be recommended to measure baseline performance on relevant tasks with the new strain, before comparing these to previous findings in Lister hooded rats (similar to chapter 2).

Based on the electrophysiological pattern of chemogenetic disinhibition, the duration of the manipulation is significantly longer lasting than the effects of pharmacological prefrontal disinhibition in previous work (Pezze et al., 2014). This aspect is largely beneficial for behavioural *in vivo* work, with long testing session often limiting the effectiveness of pharmacological agents near the end of the session. Combining this finding with the notion that DREADDs can be activated repeatedly with little-to-no receptor desensitisation (Smith et al., 2016), the current model enables the investigation of novel tasks, such as chronic manipulation of GABAergic activity.

5 General discussion

5.1 Project aims and outcomes

As outlined in chapter 1, the work discussed in this thesis sought to address two aims. Firstly, we aimed to examine the impact of mPFC neural disinhibition in rats on a two-lever operant reversal learning paradigm. Importantly, we suspected that mPFC disinhibition may affect reversal performance even under conditions when the mPFC is not required, because disinhibition causes aberrant neural activity within mPFC, which, in turn, may disrupt processing in prefrontal projection sites (Bast et al., 2017), including the OFC and striatum, which have been shown to be required for reversal learning (see Chpt. 1). Secondly, we aimed to complement currently available models of neural disinhibition via a novel chemogenetic alternative using an inhibitory DREADD to selectively silence GABAergic neurons.

In chapter 2 we set out to build on previous work by Mackintosh et al., (1968) and Rygula et al., (2010), highlighting substantial improvements in reversal performance across consecutive, serial, reversals (Experiment 1). More specifically, based on between-reversal changes in performance, we separated reversals into early and serial reversal 'phases', with the former being characterised by a high reversal cost at R1 and R2, which began to improve in subsequent stages, and the latter, serial, phase only commencing once reversal performance has reached relatively stable levels (at R5). Although there were still some more subtle between-stage performance changes, with some changes in Bayesian strategy implementation being noted between R5-10, performance measures, especially perseveration, had reached stable levels at this stage. These findings also supported the use of a within-subject design for future pharmacological experiments.

Subsequently, chapter 3 tested the effect of bi-directional GABAergic manipulation at both reversal stages in order to characterise the effect of neural

disinhibition within the mPFC of rodents on a task not typically associated with mPFC activity. Results revealed that prefrontal disinhibition by picrotoxin can disrupt reversal learning in several ways. Most prominently, mPFC disinhibition markedly disrupted serial reversal learning performance (Experiment 3), as reflected by increased RTCs, increased perseverative and regressive errors, as well as impaired reminder trial performance and reduced win-stay and lose-shift behaviour. On the other hand, whilst picrotoxin did not directly impair early learning performance (Experiment 2), disinhibition of the same dose as in the serial reversal paradigm induced substantial omissions to the point where rats in the picrotoxin group failed to reach the final reversal stage within 6 days of testing. We believe that this non-specific impairment was driven by an increased level of distractibility induced by mPFC disinhibition (Auger et al., 2017). Although this impairment did not result in impairments of typical reversal learning metrics (e.g., RTC), it is likely that this marked 'distractibility' interfered with aspects of the paradigm. Specifically, we believe that distractibility, leading to rats focussing on task-inappropriate aspects of the environment (such as the house or cue-lights), contributed to the marked omissions recorded during the start of each session in the picrotoxin group. In turn, these omissions would result in less reinforcement on the previous rule prior to rule change, compared to saline or muscimol groups, which ultimately may have aided during the rule reversal, as the old rule is less salient at the time of reversal, and therefore may not require as much effort to overcome.

In Chapter 3, alongside neural disinhibition, we also examined the effect of functional inhibition of the mPFC. We hypothesised that this may still impair reversal performance during task stages where increased attentional demands, or the ability to inhibit pre-existing response biases, necessitate medial prefrontal involvement (Marquis et al., 2007), such as during early reversal stages. Indeed, we observed a reversal learning deficit following infusions of muscimol during early, but not late, reversal stages. Specifically, this impairment, centred around R2, manifested as increased RTC in conjunction with increased perseveration, as well as impaired lose-shift behaviour. Interestingly this impairment was not

additive to the initial reversal cost observed at R1, and instead impaired processes required to overcome this early reversal cost, ultimately resulting in a slower improvement in performance between stages.

To address the second aim of the thesis, chapter 4 used histological and electrophysiological methods to examine the use of a GABA-neuron specific hM4Di DREADD in rats. The VGAT-Cre Long Evans rats in conjunction with the inhibitory hM4Di DREADD offers a novel approach to inhibiting prefrontal GABA neurons. The histological studies in this chapter suggested injections of 1.0 µl compared to 0.5 µl resulted in greater spread across the PFC, centred on the prelimbic cortex. Furthermore, the DREADD was primarily expressed on GABAergic, as opposed to cholinergic or glutamatergic, cells. Observed penetrance of the DREADD across the total population of GAD_{67}+ cells in the PFC was substantial, at around 30% of all GAD_{67}+ cells expressing DREADDs. Subsequent *in vivo* electrophysiology highlighted functionality of the DREADD construct, with several key electrophysiological characteristics of prefrontal disinhibition evident following hM4Di activation via 6 mg/ml/kg of CNO2HCl. More specifically, chemogenetic prefrontal disinhibition resulted in a marked, long lasting change in LFP pattern, characterized by marked LFP SWD and an overall increase in LFP power. Additionally, burst firing was markedly intensified, with an increase in within-burst firing rate, alongside a reduced burst duration.

Overall, this thesis showed that both mPFC disinhibition and functional inhibition have a role to play in reversal learning in rats. More specifically, we showed that although perhaps not directly required in reversal learning, disinhibition can impair reversal performance in several ways. Firstly, disinhibition may increase distractibility in unfamiliar environments which has the potential to disrupt aspects of behaviour. On the other hand, when familiarity increases, disinhibition was shown to explicitly disrupt reversal performance by disrupting exploratory and exploitative strategies in rats. In contrast, we showed that mPFC may still be important in task stages where attentional demands are high, necessitating controlled GABA activity in the mPFC in order to guide successful exploratory

strategies, such as lose-shift behaviour. However, when task proficiency is increased, our findings indicate that the mPFC is no longer required to guide these behaviours. Finally, our novel chemogenetic rat model of GABAergic disinhibition is the first GABA-specific rat model capable of complementing pharmacological alternatives. The outcomes of this encouraging for the implementation of this line in future research. In the following sections, I will discuss the current findings in light of the wider literature, consider limitations and clinical implications.

5.2 The effect of GABAergic prefrontal disinhibition on cognition

As outlined in chapter 1, the mPFC has been directly implicated in several forms of cognition via lesion experiments, including attention and working memory (for review see Bast et al., 2017). Studies of mPFC disinhibition in rats have largely replicated these findings, showing that neural disinhibition has the capacity to disrupt aspects of sustained attention, working memory or extra-dimensional set shifting (Enomoto et al., 2011; Pezze et al., 2014; Auger & Floresco, 2014). Current findings reported in chapter 3 highlight that serial reversal learning was also impaired by mPFC neural disinhibition, although our results of functional inhibition on the same task indicated that serial reversal learning does not require the rodent mPFC. One possibility, as we suggest, is that this impairment reflects disruption in mPFC projection sites that are more directly involved in reversal learning.

More specifically, controlled GABAergic activity has been shown to be critical for the maintenance of oscillatory coherence and pyramidal cell firing, which in turn is critical for local activity, but also inter-region communication (Penttonen et al., 1998; Gonzalez-Burgos & Lewis, 2008; Gregoriou et al., 2009). Furthermore, the rodent mPFC projects to several regions that have been directly implicated in deterministic reversal learning, namely the OFC and the striatum (Sesack et al., 1989; Mailly et al., 2013; Izquierdo et al., 2017). Interestingly, lesions of the OFC and striatum have been shown to cause distinct patterns of impairments in reversal performance. Lesions of the OFC, particularly the lateral OFC, caused

perseveration in both rats (Chudasama and Robbins, 2003; Floresco et al., 2008) and NHPs (Dias et al., 1996; Clarke et al., 2008; Rygula et al., 2010). Indeed, previous results of anticipatory neural firing within the OFC suggests some role in predicting expected outcome (Schoenbaum & Eichenbaum, 1995; Schoenbaum et al., 2009), which may be important to guide exploration if a response is expected to be unrewarded, and disruption of this process may, in turn, lead to impaired error correction. On the other hand, striatal lesions in NHPs, whilst also enhancing perseveration (Clarke et al., 2008), have been shown to impair a subject's ability to adhere to a newly rewarded rule, and as such have also been linked to driving exploitative (win-stay) behaviour (Ragozzino & Choi , 2004; Clarke et al., 2008).

Given these distinct patterns of reversal learning impairments caused by OFC and striatal lesions, our present finding that mPFC disinhibition impaired serial reversal learning by disrupting both exploration (lose-shift behaviour) and exploitation (win-stay behaviour) is in line with the possibility that mPFC disinhibition disrupts function of the OFC (which would mainly result in increased perseveration and impaired lose-shift behaviour) and striatum (which would be expected to increase perseveration and impair lose-shift behaviour and also impair win-stay behaviour). Future studies will have to examine the impact of mPFC disinhibition on mPFC projection sites.

On the other hand, during early reversal stages mPFC disinhibition did not impair reversal measures, but instead tended to reduce RTCs. Importantly, during early reversals, mPFC disinhibition markedly increased trial omissions. As discussed in chapter 3, due to increased omissions rats with mPFC disinhibition would have received substantially less reinforcement for the previous rule prior to rule change, compared to the other groups. I propose that it is this reduced reinforcement, instead of a real improvement in reversal learning, that explains why rats with mPFC disinhibition required less responses to switch from the previous to the new rule on the early reversal task. Therefore, one could also interpret these findings in such a way to suggest picrotoxin did in fact impair behaviour during the early reversal stages, but the current reversal task was not

designed to measure the type of impairment this induced. Consistent with our findings, previous studies have found that mPFC disinhibition increased omissions on other operant tasks (Pezze et al., 2014; Auger et al., 2017). As a result, it was suggested that these omissions reflected increased 'distractibility'. Moreover, Hervig et al. (2020), specifically linked omissions on reversal task to inactivation of the infralimbic cortex of the rodent mPFC. Therefore, increased omissions following mPFC disinhibition may reflect disruotion of infralimbic cortex function, driving a state of increased distractability. This could entail rats focussing on aspects of the task unrelated to the pertinent levers, such as the unrewarding cue-lights or the house-light at the back of the chamber, and when the 10 s response window is presented, they do not engage with the task.

Moreover, mPFC disinhibition in Experiment 2 and 3 resulted in substantially slower response latencies compared to saline and muscimol, and thus replicating previous observations of similar effects following $GABA_A$ antagonist bicuculline (Enomoto et al., 2011; Pezze et al., 2014; Auger et al., 2017). With regards to the response latencies, however, it remains unclear whether these represent deficits in processing speed as indicated by Auger et al., (2017), or if they reflect distraction and reduced focus on the task, which result in the rats being less close to the levers when they are extended, and extra time required to move across the box to make a response. Therefore, the increases in omissions and response latencies by mPFC neural disinhibition may both reflect increased distractibility.

Interestingly, current findings indicate that omissions and response latencies decrease as a result of increased task proficiency. Notably, the number of omissions decreased both within each experiment and across experiments, whereby the highest number of omissions were made early in Experiment 2, and omissions decreased gradually between R1 and R3. Omissions further decreased from infusion series 1 to 2 of Experiment 3. These findings suggest that, whilst prefrontal disinhibition increases distractibility, increasing task proficiency reduces requirement of GABA transmission to keep rats 'on task'. Overall, our findings suggest that mPFC disinhibition can indeed impair reversal learning, an

impairment that becomes most notable during later stages of the reversal task when increased task proficiency has reduced non-specific effects on the distractibility. Prior to this point, neural disinhibition resulted in substantial behavioural impairment which limits the interpretation of the effects of mPFC neural disinhibition on early operant reversal performance in the present studies.

5.3 Requirement of the mPFC for early, but not late, reversal learning

The rodent mPFC has been suggested to integrate information about reward outcome and error correction (Rushworth et al., 2011; Shenhav et al., 2013), as well as to guide exploratory behavior (Daw et al., 2006; Caracheo et al., 2013), and there is evidence that prelimbic inhibition and lesions impair lose-shift behavior and increase perseveration (Yang et al., 2014; Laskowski et al., 2016). Findings from Experiment 2 support this notion, with a clear disruption in lose-shift behavior, centered around R2, alongside marked reversal learning deficits, as reflected by increased RTCs, at that stage following prefrontal muscimol. The lack of impairment at R1 indicated that prefrontal inhibition does not additionally impair performance beyond the typically observed reversal cost (Floresco et al., 2008), but, rather, prefrontal functional inhibition impairs exploratory processes necessary to overcome this reversal cost.

This line of reasoning explains the improvement of reversal performance across early task stages as a consequence of better implementation of lose-shift behavior. Specifically, early poor performance was driven by a marked decline in of lose-shift behaviour during early reversals. This is corrected between subsequent stages, resulting in a gradual reduction in overall RTC. Interestingly, human research has shown that in situations with increased cognitive demand participants tend to decrease lose-shift behavior (Ivan et al., 2018). Therefore, the marked decline in lose-shift behaviour following rule reversal that we observed in rats, especially at early reversal stages, may reflect the increased cognitive demand during early reversal stages (i.e., the initial encounter with a rule change alongside uncertainty of cue-light relevance). It is possible that to overcome this

cognitive demand, and to hold the decline in lose-shift behaviour, requires mPFC engagement in rats. This notion would be in line with similar rodent studies outlined previously where it was suggested that the mPFC is required for attentionally demanding tasks (Bussey et al., 1997; Chudasama & Robbins, 2003; Kosaki & Watanabe, 2012).

These changes in response strategy also indirectly index something that is not explicitly measured in the current thesis, namely response inhibition (Miller & Cohen , 2001; Haddon & Killcross, 2006; Marquis et al., 2007). Reduced response inhibition may result in reduced lose-shift behaviour, such as in the event where rats make an inappropriate response on the previously correct lever due to the prepotent bias of that lever, compared to the newly correct lever. This behaviour would be classed as lose-stay, and as such bring about a reduction in the opposite, lose-shift, strategy. Additionally, improvements in response inhibition likely underly observable improvements in reversal performance, whereby subjects become better at inhibiting the inappropriate response in favour of the correct alternative ultimately enabling faster rule reversals (Cohen et al. 1990; Izquierdo & Jentsch , 2012). In light of this, impairments following mPFC functional inhibition during early task stages may be interpreted in terms of impaired response inhibition, which aligns with the vast number of perseverative errors at R2. Furthermore, this disruption of response inhibition may underline qualitative differences between mPFC lesions and functional inhibition, with similar lesion studies failing to find such impairments (e.g., Bussey et al., 1997). Additionally, as reversal learning improved as a function of task proficiency, these results may also reflect a reduced reliance on mPFC-mediated response inhibition, with the absence of a reversal impairment following muscimol on the serial reversal paradigm. This change may hint at a shift from active inhibition during early, unfamiliar reversal stages, to more passive, habitual responding which no longer required mPFC mediation (e.g., Hassett & Hampton, 2017).

5.4 A new chemogenetic model of mPFC disinhibition in rats

The final experimental chapter of this thesis reported several investigations validating a chemogenetic model of prefrontal disinhibition in rats to complement the pharmacological model that involves intra-cerebral infusions of the GABA-A receptor antagonist picrotoxin. The histological experiments showed good cell-type specificity and penetrance of the DREADD expression, with limited off-target expression. Subsequent *in vivo* electrophysiological recordings following activation by systemic injection of CNO2HCl (6 mg/ml/kg) assessed functionality of the DREADDs expressed within the mPFC of rats via. Recordings were compared to previous findings of intensified burst firing and marked LFP spike-wave discharges following pharmacologically induced prefrontal disinhibition (Pezze et al., 2014). Overall, we showed that inhibition of prefrontal GABAergic neurons via activation of the hM4Di DREADD resulted in comparable, long-lasting changes in burst firing parameters and LFP power, akin to those observed following pharmacological disinhibition.

Most importantly, whilst there are several chemogenetic mouse lines (Song et al. 2010; Weaver et al., 2018) available, the current work discussed in this thesis is the first to validate this GABA-specific model in rats. The new chemogenetic rat model opens many new avenues for behavioural testing, which were previously limited due to methodological constraints (such as repeated manipulations). However, there are several features of the new chemogenetic model that need to be considered. Firstly, there may be baseline differences in task proficiency or rate of learning between Lister hooded rats and the transgenic Long Evans rats expressing the inhibitory DREADD in GABAergic neurons. Therefore, it would be recommended to measure baseline performance on relevant tasks with this new strain, to ensure fair comparison between new chemogenetic data, and older findings in, for example, Lister hooded rats (similar to chapter 2).

Secondly, based on the electrophysiological effects of chemogenetic disinhibition of the mPFC, the duration of the manipulation is longer lasting than the effects of

pharmacological prefrontal disinhibition in previous work (Pezze et al., 2014). More specifically, the effect peaked 30 min post-injection, as opposed to 15 min post-infusion observed in Pezze et al. (2014), and values remained at this level until the end of recording 120 min after injection. This prolonged duration of disinhibition is largely beneficial for behavioural studies, with long testing session often limiting the effectiveness of pharmacological agents near the end of the session. Combining this finding with the notion that DREADDs can be activated repeatedly with little-to-no receptor desensitisation (Smith et al., 2016), the chemogenetic model enables the investigation long-lasting disinhibition across many different days and, if the ligand injections are appropriately timed, even of chronic silencing of GABAergic activity.

Thirdly, we noted convulsive seizures in several of the VGAT-Cre rats (see section 4.1). Whilst the exact cause of this remains unknown, it likely reflects strain-dependent differences compared to previous work with Lister hooded rats. Our electrophysiological recordings in chapter 4 revealed that baseline burst-firing was markedly higher in the VGAT-Cre Long Evans rats than in Lister hooded rats used previously (Pezze et al., 2014). Strain dependent differences in electrophysiological activity have been noted previously, including greater frequency of polyspiking activity alongside SWD in Long Evans rats compared to other strains (Kaplan, 1985). Moreover, this type of firing pattern, albeit more pronounced, has previously been associated with seizure onset (Neckelmann et al., 1998; Steriade et al., 1998). Therefore, the current parent strain may have a predisposition to developing seizures, which could be exacerbated by the insertion of Cre-recombinase into GABAergic cells.

5.5 General limitations

All examinations in this thesis were carried out in young adult male rats, in line with our previous studies involving prefrontal manipulations (Pezze et al., 2014) and most other related studies (e.g., Boulougouris et al., 2007; Floresco et al., 2008). However, the inclusion of female rats in rodent research is crucial for

advancing our understanding of biological and behavioural processes. Historically, much of the rodent work has been skewed toward male subjects, leading to a significant gap in our comprehension of sex-specific responses and outcomes (Karp & Reavey, 2019). Furthermore, this inclusivity is important for translational research, as it enhances the applicability of findings to both male and female populations, ultimately contributing to a more robust and nuanced understanding of health and disease (Leung et al., 2000; Becker et al., 2016; Karp & Reavey, 2019). Indeed, sex differences in cognitive flexibility have been reported in both NHPs and rats (Guillamon et al., 1986; Ha et al., 2011). Specifically, Guillamon et al. (1986) presented a connection between hormonal activity and reversal learning, whereby females initially made fewer errors and ths reached success cirteria before their male counterparts. Interestingly, this initial performance difference was reversed following castration or androgen administration in male and female rats, respectively. Most current NHP studies employ both males and females (e.g., Rygula et al., 2015), yet rodent equivalents still focus primarily on males (e.g., Hervig et al., 2020; Cernotova et al., 2021). Given the substantial and dissociable effects of GABAergic dysfunction observed here, it would be of interest to examine if these are robustly observed in females, as well. Such an investigation may provide insight into a potential hormonal modulation of neural disinhibition and the effects thereof, which, in turn, may play a critical role in further our understanding of sex differences in clinical populations, such as schizophrenia (Leung et al., 2000).

Another consideration of the pharmacological work discussed in this thesis is the housing and light cycles under which rats were tested. All handling and procedures with rats used for the studies in these thesis were conducted during the 12h light cycles (on at 0700), much like many other similar studies in the field (e.g., Chudasama & Robbins, 2003; McAlonan & Brown, 2003). However, it should be noted that rats are typically nocturnal, and therefore testing during light may impact several physiological properties, characteristic of stress responses, such as increased heart rate (Castelhano-Carlos & Baumans, 2009). This may impact reversal learning performance. For example, heightened stress has been shown

to reduce serotonin within the OFC, which, in turn, has been implicated in reversal learning (Lapiz-Bluhm et al., 2009; Roberts et al., 2011). Thus, other groups have tested rats on a reverse light cycle, or under infrared light, to reduce stressors (e.g., Boulougouris et al., 2007). Whilst the impact of light induced stress may be important, we believe this effect, if present at all, is controlled via several aspects. Firstly, it has been shown that rats adapt to changes in light-dark cycles within four to five days (van den Buuse et al., 1999). Given that there is always a one-week acclimation period included prior to any testing being conducted, this gives rats sufficient time to adapt prior to testing, likely reducing stress at the time of testing. Secondly, reversal testing was always conducted in dark chambers with light levels controlled and limited to low levels (40 lux). These levels are well within the preferred range of pigmented rats (<60 lux) (Blohm et al., 1995; Schlingmann et al., 1993), and thus should not induce any acute stress responses during testing. In sum, we believe the likely influence of light-induced chronic or acute stress is well controlled in the current examinations, but of course we do not explicitly measure signs of stress, and as such stress may yet influence results and as such should be considered. Thirdly, it should be noted that some key findings do not appear to be dependent on whether rats are tested during the light or dark phase. For example, work by Boulougouris et al. (2007) and Floresco et al., (2008) both lesioned the OFC, but used differing light-dark cycles. In both, OFC lesions were robustly observed, indicating that, at least in part, this observation was not due to a difference in stress levels of rats.

A final consideration relevant to the pharmacological work in chapter 3 is the exact location at which our manipulations took effect. As discussed in chapter 1, the rodent mPFC is functionally heterogenous, with prelimbic and infralimbic regions associated with different aspects of learning, as well as subtle differences in efferent projections. The coordinates used in our experiments targeted the prelimbic cortex, which has substantial projections to OFC regions (Sesack et al., 1989). However, diffusion to adjacent regions of the injection bolus is likely, even at the volume of 0.5 μl. Considering isotropic spread of the injection bolus, the minimal drug spread would be a radius of a 0.5 μl sphere, centred around the

injection site (around 0.5 mm in each direction). It remains difficult to exactly pinpoint the extent of this diffusion, but we believe a preferential route, if any, would be up the implanted cannula tract, covering a similar region as observed in the viral injections (0.5 μl) of chapter 4. A second factor determining the spread of the solution is the position of fibre bundles, which have been shown to effectively limit drug spread (Morris et al., 1989; McGarrity et al., 2017) Therefore, we do not claim to have solely affected prelimbic activity, and instead refer to the wider mPFC.

With regards to the chemogenetic findings discussed in chapter 4, there are several methodological limitations I encountered throughout the experimental process. Our investigations in rat cohort 1 of chapter 4 set out to measure Cre-recombinase expression and to provide a first indication of DREADD expression at two injection volumes. As there are no suitable immunological Cre probes to date, tissue was prepared for FISH. More specifically, this required tissue to be freshly frozen immediately after extraction, as opposed to perfusion fixed tissue for immunohistochemistry. Additionally, slicing of tissue was significantly thinner than for typical immunological staining (10 μm versus 50 μm). However, as discussed in chapter 4, several issues were encountered with FISH staining, with endogenous mCherry signal being lost. As a result, tissue that was previously prepared for FISH had to be used for immunological staining, yet the in-house protocol was not adapted for such fragile tissue. Ultimately, this led to substantial tissue damage observed in cohort 1, limiting the immunohistochemical data obtained from this. Nonetheless, the investigations in rat cohort 1 were still valuable in the validation of the VGAT-Cre rat line itself, confirming that Cre-expression was largely limited to GABAergic neurons, as well as measuring the extent of DREADD spread across the PFC, which did not require additional staining.

Likewise, histological findings in cohort 2 in chapter 4 indicated substantially lower levels of $GAD_{67}+$ immunoreactivity, compared to previous literature in the field (by about 30%) (Gabbott et al., 1997; Markram et al., 2004; Markham; 2007).

These findings suggest substantial limitations with the antibodies used in this protocol, which in turn would result in under-estimations of both specificity and penetrance of the DREADD. Notwithstanding this limitation, our histological results highlight substantial preference for GABAergic neurons, and essentially no expression by excitatory cells. Furthermore, the electrophysiological findings highlight functionality of the DREADD even if the low expression is accurate. As such, the reduced GAD_{67} signal does not undermine the validation of the chemogenetic model.

One final issue related to the chemogenetic studies is the use of CNO to activate the hM4Di receptors during electrophysiological recording of chapter 4. CNO can be back-metabolised into clozapine, with clozapine concentrations in the brain peaking as quickly as 15 min post-injection of CNO (Gomez et al., 2017; Jendryka et al., 2019). However, with respect to the current electrophysiological findings, we believe it is unlikely that clozapine would affect the electrophysiological recordings. This is because clozapine has been associated with increased GABA activity through indirect modulation of $GABA_A$ activity via allopregnanolone (Marx et al., 2003), or direct modulation of $GABA_B$ receptors (Kaster et al., 2015). Therefore, this receptor profile goes against the marked neural disinhibition observed in the electrophysiological recordings, and as such we suggest that it is unlikely that back-metabolism of CNO to clozapine confounded the current findings. However, for future work using this chemogenetic model for behavioural testing in rats, it is advised to include a CNO-only control (in rats not expressing a DREADD) to characterise any non-specific behavioural effects of the drug without modulation of the DREADD. This would build on previous work showing suitabile doses of up to 10 mg/ml/kg (Mahler & Aston-Jones, 2018).

5.6 Clinical implications

Current findings of reversal learning impairment following prefrontal GABA dysfunction are relevant for the understanding of cognitive impairments in clinical populations with reduced prefrontal GABA function, such as patients with

schizophrenia (Lewis et al., 2005; Bast et al., 2017). As outlined in chapter 3, *post-mortem* findings of schizophrenia have commonly associated the illness with reductions in prefrontal GABAergic markers, such as GAD_{67} activity, likely resulting in a state of tonic neural disinhibition, alongside elements of prefrontal hypo-activity (Ingvar & Franzen , 1974; Carter et al., 1998; Bennes & Berretta, 2001; Lewis et al., 2008; Minzenberg et al., 2009, Ortiz-Gil et al., 2011). Interestingly, although it may seem that the GABAergic deficits observed in *post-mortem* studies and the hypofrontality in patients with schizophrenia are separate phenotypes of the illness, a recent hypothesis by Krystal and Anticevic (2015) suggested a causal link between the two depending on the stage of the illness. In this framework early hyper-excitability is exacerbated by persistent GABAergic deficits (disinhibition) resulting in synaptic-downscaling later in the illness, a likely precursor to hypofrontality (Uhlhaas, 2013; Krystal & Anticevic, 2015). This notion was based on findings from exploratory analysis of clinical trials where novel pharmacotherapy via the metabotropic glutamate receptor agonist Pomaglumetad Methionyl showed better efficacy in early-in-illness subgroups of schizophrenia patients (Kinon et al., 2015). This difference indicated the presence of a disinhibited network in early-, but not late-in-illness patients, which was attenuated by administration of the glutamate agonist. Specifically, the agonist binds to presynaptic mGlu terminals of glutamatergic neurons and inhibits further glutamate release, ultimately reducing glutamatergic activity over time (O'Neill et al., 2010). Additionally, prodromal stages of the illness are often characterised by hyper-glutamatergic pathophysiology and greater changes in glutamate levels compared to healthy controls, which re-align with control levels after around 10-20 years in-illness (De la Fuente-Sandoval et al., 2011; Marsman et al., 2013). These findings from early stages of the illness were combined with results noting that hypofrontality correlated strongly with both age and chronicity of illness, suggesting a prevalence for hypofrontality in late-in-illness patients (Hill et al., 2004). Therefore, it was proposed that this shift from early disinhibition to late hypofrontality could be driven by homeostatic adaptations of neural firing, which, in presence of a hyper-excited network, downregulate excitatory pathways

alongside potential excitotoxic atrophy, ultimately resulting in a hypo-active network (Krystal & Anticevic, 2015; Fauth & Tetzlaf, 2016).

Given this hypothesis, prefrontal neural disinhibition, as examined in the present thesis, may contribute to cognitive deficits present early in the illness, such as in the case of first-episode patients who exhibited marked reversal learning deficits (Hutton et al., 1998; Murray et al., 2008; Leeson et al., 2009). Specifically, prefrontal disinhibition, present during prodromal and early stages of the illness, may disrupt performance on familiar reversal problems, or within familiar contexts, resembling the serial reversal impairment caused by prefrontal disinhibition in rats. On the other hand, we find that hypofrontality, as examined here via functional inhibition, may contribute to reversal learning impairments. This may be most relevant to later stages in scenarios where patients are faced for the first time (i.e., unfamiliar tasks). This interpretation aligns with the robust simple reversal learning deficits observed in early-stage schizophrenia patients, where task parameters were not entirely novel due to the nature of the CANTAB, with patients being exposed to similar stimuli both within sessions, and across the entire study (Leeson et al., 2009).

5.7 Future studies and conclusion

The finding that mPFC disinhibition disrupted serial reversal learning, which was unaffected by mPFC functional inhibition, i.e., did not require the mPFC, raises the question of how mPFC disinhibition may affect processing in prefrontal projection sites in a way that could contribute to the serial reversal learning impairment. Possible approaches to address this question include mapping of brain-wide activation changes caused by mPFC disinhibition, using whole-brain imaging approaches (e.g., SPECT metabolic imaging as used Williams, 2021) or electrophysiological recordings in projection sites in conjunction with mPFC disinhibition. As stated, we hypothesised that aberrant mPFC activity following disinhibition may result in aberrant neural activity in prefrontal projection sites, but the extent of this is not sufficiently characterised yet. Therefore, such

recordings would be beneficial to further our understanding of how local changes in neural firing translate to distal regions.

Another avenue to explore the role of specific mPFC projections is the use of targeted silencing of distinct projections by use of anterogradely transported DREADDs (Roth, 2016; Nelson et al., 2020), selective silencing/lesion of the pathway of interest could be used in conjunction with mPFC disinhibition to further probe the relevance of certain prefrontal efferent projections. Based on the current hypotheses, if the reversal disruptions observed here were indeed driven by aberrant projections, selective lesions may recover reversal performance, or aspects thereof (such as specifically perseveration), depending on the pathway targeted (such as potentially to the OFC).

With respect to the chemogenetic validation discussed in the current thesis, an immediate next step would be to examine the effect of chemogenetic mPFC disinhibition on reversal learning in rats, using similar paradigms as discussed here. Importantly, due to potential strain difference, baseline performance curves need to be re-evaluated for the transgenic Long Evans strain, to assess if the serial paradigm is applicable across strains, or if adjustments are required if performance does not reach asymptote by R5. Furthermore, it would be beneficial to characterise the extent of non-specific behavioural effects of hM4Di activation in awake rats (e.g., locomotor changes, or the 'distractibility' observed here following picrotoxin) in order to quantify potential side effects of this activation. In a similar vein, it could be beneficial to also examine how the activation of the current DREADD construct using CNO-based actuators compares to the more recent introduction of compound-21, which is regarded as a beneficial over CNO, as it does not involve any secondary effect of back-metabolised clozapine (Jendryka et al., 2019).

Next, it would be of interest to examine if chemogenetic mPFC disinhibition causes a similarly marked serial reversal learning deficit pharmacological disinhibition. The rationale for this is based on the fact that current pharmacological models of

neural disinhibition are transient and act post-synaptically, limiting translatability to clinically observed phenotypes which are primarily pre-synaptic in nature (Bennes & Berretta, 2001). On the other hand, the new chemogenetic model can modulate GABAergic activity pre-synaptic pre-synaptically, which may be more suitable to mimic the nature of GABA neuron dysfunction in schizophrenia. Additionally, the chemogenetic effect has a substantially longer effect than previous pharmacological models, and with the suggestion of little-to-no reduction in receptor sensitivity these aspects may be able to simulate the chronic nature of GABA dysfunction in schizophrenia (Smith et al., 2016).

In conclusion, this thesis has demonstrated the importance of the mPFC and local GABAergic inhibition in reversal learning of rats. Additionally, I have developed novel behavioural and chemogenetic models relevant to future investigations in this field, and implications for clinical populations characterised by prefrontal GABAergic dysfunction, such as schizophrenia, have been discussed.

6 References

Akbarian, S., Kim, J. J., Potkin, S. G., Hagman, J. O., Tafazzoli, A., Bunney, W. E., & Jones, E. G. (1995). Gene-Expression for Glutamic-Acid Decarboxylase Is Reduced without Loss of Neurons in Prefrontal Cortex of Schizophrenics. *Archives of general psychiatry, 52*(4), 258-266. https://doi.org/10.1001/archpsyc.1995.03950160008002

Akert, K. (1964). Comparative anatomy of frontal cortex and thalamofrontal connection. *The frontal granular cortex and behavior*, 372-396.

Alexander, G. M., Rogan, S. C., Abbas, A. I., Armbruster, B. N., Pei, Y., Allen, J. A., Nonneman, R. J., Hartmann, J., Moy, S. S., Nicolelis, M. A., McNamara, J. O., & Roth, B. L. (2009). Remote control of neuronal activity in transgenic mice expressing evolved G protein-coupled receptors. *Neuron, 63*(1), 27-39. https://doi.org/10.1016/j.neuron.2009.06.014

Alexander, W. H., & Brown, J. W. (2010). Computational models of performance monitoring and cognitive control. *Top Cogn Sci, 2*(4), 658-677. https://doi.org/10.1111/j.1756-8765.2010.01085.x

Allen, J. A., & Roth, B. L. (2011). Strategies to Discover Unexpected Targets for Drugs Active at G Protein-Coupled Receptors. *Annual Review of Pharmacology and Toxicology, Vol 51, 2011, 51*, 117-144. https://doi.org/10.1146/annurev-pharmtox-010510-100553

Andreasen, N. C., Rezai, K., Alliger, R., Swayze, V. W., 2nd, Flaum, M., Kirchner, P., Cohen, G., & O'Leary, D. S. (1992). Hypofrontality in neuroleptic-naive patients and in patients with chronic schizophrenia. Assessment with xenon 133 single-photon emission computed tomography and the Tower of London. *Arch Gen Psychiatry, 49*(12), 943-958. https://doi.org/10.1001/archpsyc.1992.01820120031006

Anticevic, A., Hu, X., Xiao, Y., Hu, J., Li, F., Bi, F., Cole, M. W., Savic, A., Yang, G. J., Repovs, G., Murray, J. D., Wang, X. J., Huang, X., Lui, S., Krystal, J. H., & Gong, Q. (2015). Early-course unmedicated schizophrenia patients exhibit elevated prefrontal connectivity associated with longitudinal change. *J Neurosci, 35*(1), 267-286. https://doi.org/10.1523/JNEUROSCI.2310-14.2015

Armbruster, B. N., & Roth, B. L. (2005). Mining the receptorome. *J Biol Chem, 280*(7), 5129-5132. https://doi.org/10.1074/jbc.R400030200

Atasoy, D., Aponte, Y., Su, H. H., & Sternson, S. M. (2008). A FLEX switch targets Channelrhodopsin-2 to multiple cell types for imaging and long-range circuit mapping. *J Neurosci, 28*(28), 7025-7030. https://doi.org/10.1523/JNEUROSCI.1954-08.2008

Auger, M. L., & Floresco, S. B. (2014). Prefrontal cortical GABA modulation of spatial reference and working memory. *Int J Neuropsychopharmacol, 18*(2), pyu013-pyu013. https://doi.org/10.1093/ijnp/pyu013

Auger, M. L., & Floresco, S. B. (2017). Prefrontal cortical GABAergic and NMDA glutamatergic regulation of delayed responding. *Neuropharmacology, 113*(Pt A), 10-20. https://doi.org/10.1016/j.neuropharm.2016.09.022

Auger, M. L., Meccia, J., & Floresco, S. B. (2017). Regulation of sustained attention, false alarm responding and implementation of conditional rules by prefrontal GABA(A) transmission: comparison with NMDA transmission. *Psychopharmacology (Berl), 234*(18), 2777-2792. https://doi.org/10.1007/s00213-017-4670-1

Bannerman, D., Grubb, M., Deacon, R., Yee, B., Feldon, J., & Rawlins, J. (2003). Ventral hippocampal lesions affect anxiety but not spatial learning. *Behavioural Brain Research, 139*(1-2), 197-213.

Barbas, H., Henion, T. H., & Dermon, C. R. (1991). Diverse thalamic projections to the prefrontal cortex in the rhesus monkey. *J Comp Neurol, 313*(1), 65-94. https://doi.org/10.1002/cne.903130106

Barbey, A. K., Koenigs, M., & Grafman, J. (2013). Dorsolateral prefrontal contributions to human working memory. *cortex, 49*(5), 1195-1205. https://doi.org/10.1016/j.cortex.2012.05.022

Bartolo, R., & Averbeck, B. B. (2020). Prefrontal Cortex Predicts State Switches during Reversal Learning. *Neuron, 106*(6), 1044-1054 e1044. https://doi.org/10.1016/j.neuron.2020.03.024

Bartos, M., & Elgueta, C. (2012). Functional characteristics of parvalbumin- and cholecystokinin-expressing basket cells. *J Physiol, 590*(4), 669-681. https://doi.org/10.1113/jphysiol.2011.226175

Bast, T., & Feldon, J. (2003). Hippocampal modulation of sensorimotor processes. *Prog Neurobiol, 70*(4), 319-345. https://doi.org/10.1016/s0301-0082(03)00112-6

Bast, T., Pezze, M., & McGarrity, S. (2017). Cognitive deficits caused by prefrontal cortical and hippocampal neural disinhibition. *Br J Pharmacol, 174*(19), 3211-3225. https://doi.org/10.1111/bph.13850

Bast, T., Zhang, W. N., & Feldon, J. (2001). Hyperactivity, decreased startle reactivity, and disrupted prepulse inhibition following disinhibition of the rat ventral hippocampus by the GABA(A) receptor antagonist picrotoxin. *Psychopharmacology (Berl), 156*(2-3), 225-233. https://doi.org/10.1007/s002130100775

Becker, J. B., Prendergast, B. J., & Liang, J. W. (2016). Female rats are not more variable than male rats: a meta-analysis of neuroscience studies. *Biology of sex differences, 7*(1), 1-7.

Behrens, M. M., Ali, S. S., Dao, D. N., Lucero, J., Shekhtman, G., Quick, K. L., & Dugan, L. L. (2007). Ketamine-induced loss of phenotype of fast-spiking interneurons is mediated by NADPH-oxidase. *Science, 318*(5856), 1645-1647. https://doi.org/10.1126/science.1148045

Benes, F. M., & Berretta, S. (2001). GABAergic interneurons: implications for understanding schizophrenia and bipolar disorder. *Neuropsychopharmacology, 25*(1), 1-27. https://doi.org/10.1016/S0893-133X(01)00225-1

Bennett, J. P., Jr., Enna, S. J., Bylund, D. B., Gillin, J. C., Wyatt, R. J., & Snyder, S. H. (1979). Neurotransmitter receptors in frontal cortex of schizophrenics. *Arch Gen Psychiatry, 36*(9), 927-934. https://doi.org/10.1001/archpsyc.1979.01780090013001

Berendse, H. W., Galis-de Graaf, Y., & Groenewegen, H. J. (1992). Topographical organization and relationship with ventral striatal compartments of prefrontal corticostriatal projections in the rat. *J Comp Neurol, 316*(3), 314-347. https://doi.org/10.1002/cne.903160305

Bird, J. M. (1985). Computed tomographic brain studies and treatment response in schizophrenia. *Can J Psychiatry, 30*(4), 251-254. https://doi.org/10.1177/070674378503000407

Birrell, J. M., & Brown, V. J. (2000). Medial frontal cortex mediates perceptual attentional set shifting in the rat. *J Neurosci, 20*(11), 4320-4324. https://doi.org/10.1523/JNEUROSCI.20-11-04320.2000

Bissonette, G. B., & Powell, E. M. (2012). Reversal learning and attentional set-shifting in mice. *Neuropharmacology, 62*(3), 1168-1174. https://doi.org/10.1016/j.neuropharm.2011.03.011

Blasi, G., Goldberg, T. E., Weickert, T., Das, S., Kohn, P., Zoltick, B., Bertolino, A., Callicott, J. H., Weinberger, D. R., & Mattay, V. S. (2006). Brain regions underlying response inhibition and interference monitoring and suppression. *European Journal of Neuroscience, 23*(6), 1658-1664. https://doi.org/10.1111/j.1460-9568.2006.04680.x

Blom, H., Van Tintelen, G., Baumans, V., Van Den Broek, J., & Beynen, A. (1995). Development and application of a preference test system to evaluate housing conditions for laboratory rats. *Applied Animal Behaviour Science, 43*(4), 279-290. https://doi.org/https://doi.org/10.1016/0168-1591(95)00561-6

Bloom, F., & Iversen, L. (1971). Localizing 3 H-GABA in nerve terminals of rat cerebral cortex by electron microscopic autoradiography. *Nature, 229*(5287), 628-630. https://doi.org/10.1038/229628a0

Bohn, I., Giertler, C., & Hauber, W. (2003). Orbital prefrontal cortex and guidance of instrumental behaviour in rats under reversal conditions. *Behavioural Brain Research, 143*(1), 49-56.

Bormann, J., & Feigenspan, A. (1995). GABAC receptors. *Trends Neurosci, 18*(12), 515-519. https://doi.org/10.1016/0166-2236(95)98370-e

Bortz, D. M., Feistritzer, C. M., Power, C. C., & Grace, A. A. (2022). *Medial septum activation improves strategy switching once strategies are well learned via bidirectional regulation of dopamine neuron population activity*. Cold Spring Harbor Laboratory. https://dx.doi.org/10.1101/2022.03.07.483306

Bortz, D. M., Gazo, K. L., & Grace, A. A. (2019). The medial septum enhances
    reversal learning via opposing actions on ventral tegmental area and
    substantia nigra dopamine neurons. *Neuropsychopharmacology, 44*(13),
    2186-2194. https://doi.org/10.1038/s41386-019-0453-1

Boulougouris, V., Dalley, J. W., & Robbins, T. W. (2007). Effects of orbitofrontal,
    infralimbic and prelimbic cortical lesions on serial spatial reversal learning
    in the rat. *Behav Brain Res, 179*(2), 219-228.
    https://doi.org/10.1016/j.bbr.2007.02.005

Boulougouris, V., & Robbins, T. W. (2010). Enhancement of spatial reversal
    learning by 5-HT2C receptor antagonism is neuroanatomically specific. *J
    Neurosci, 30*(3), 930-938. https://doi.org/10.1523/JNEUROSCI.4312-
    09.2010

Brady, A. M., & Floresco, S. B. (2015). Operant procedures for assessing
    behavioral flexibility in rats. *J Vis Exp*(96), e52387.
    https://doi.org/10.3791/52387

Brigman, J. L., Daut, R. A., Wright, T., Gunduz-Cinar, O., Graybeal, C., Davis, M. I.,
    Jiang, Z., Saksida, L. M., Jinde, S., Pease, M., Bussey, T. J., Lovinger, D. M.,
    Nakazawa, K., & Holmes, A. (2013). GluN2B in corticostriatal circuits
    governs choice learning and choice shifting. *Nat Neurosci, 16*(8), 1101-
    1110. https://doi.org/10.1038/nn.3457

Brosnan, M. B., & Wiegand, I. (2017). The Dorsolateral Prefrontal Cortex, a
    Dynamic Cortical Area to Enhance Top-Down Attentional Control. *J
    Neurosci, 37*(13), 3445-3446. https://doi.org/10.1523/JNEUROSCI.0136-
    17.2017

Brown, V. J., & Bowman, E. M. (2002). Rodent models of prefrontal cortical function. *Trends in Neurosciences, 25*(7), 340-343. https://doi.org/https://doi.org/10.1016/S0166-2236(02)02164-1

Burman, K. J., Palmer, S. M., Gamberini, M., & Rosa, M. G. (2006). Cytoarchitectonic subdivisions of the dorsolateral frontal cortex of the marmoset monkey (Callithrix jacchus), and their projections to dorsal visual areas. *J Comp Neurol, 495*(2), 149-172. https://doi.org/10.1002/cne.20837

Bussey, T. J., Muir, J. L., Everitt, B. J., & Robbins, T. W. (1997). Triple dissociation of anterior cingulate, posterior cingulate, and medial frontal cortices on visual discrimination tasks using a touchscreen testing procedure for the rat. *Behav Neurosci, 111*(5), 920-936. https://doi.org/10.1037//0735-7044.111.5.920

Cabrera, S. M., Chavez, C. M., Corley, S. R., Kitto, M. R., & Butt, A. E. (2006). Selective lesions of the nucleus basalis magnocellularis impair cognitive flexibility. *Behavioral neuroscience, 120*(2), 298.

Caracheo, B. F., Emberly, E., Hadizadeh, S., Hyman, J. M., & Seamans, J. K. (2013). Abrupt changes in the patterns and complexity of anterior cingulate cortex activity when food is introduced into an environment. *Frontiers in neuroscience, 7*, 74. https://doi.org/10.3389/fnins.2013.00074

Cardin, J. A., Carlen, M., Meletis, K., Knoblich, U., Zhang, F., Deisseroth, K., Tsai, L. H., & Moore, C. I. (2009). Driving fast-spiking cells induces gamma rhythm and controls sensory responses. *Nature, 459*(7247), 663-667. https://doi.org/10.1038/nature08002

Carmichael, S. T., & Price, J. L. (1995). Limbic connections of the orbital and medial prefrontal cortex in macaque monkeys. *J Comp Neurol, 363*(4), 615-641. https://doi.org/10.1002/cne.903630408

Carmichael, S. T., & Price, J. L. (1996). Connectional networks within the orbital and medial prefrontal cortex of macaque monkeys. *Journal of Comparative Neurology, 371*(2), 179-207. https://doi.org/Doi 10.1002/(Sici)1096-9861(19960722)371:2<179::Aid-Cne1>3.0.Co;2-#

Carter, C. S., Perlstein, W., Ganguli, R., Brar, J., Mintun, M., & Cohen, J. D. (1998). Functional hypofrontality and working memory dysfunction in schizophrenia. *Am J Psychiatry, 155*(9), 1285-1287. https://doi.org/10.1176/ajp.155.9.1285

Castelhano-Carlos, M. J., & Baumans, V. (2009). The impact of light, noise, cage cleaning and in-house transport on welfare and stress of laboratory rats. *Laboratory animals, 43*(4), 311-327. https://doi.org/https://doi.org/10.1258/la.2009.0080098

Cenci, M. A., Kalen, P., Mandel, R. J., & Bjorklund, A. (1992). Regional differences in the regulation of dopamine and noradrenaline release in medial frontal cortex, nucleus accumbens and caudate-putamen: a microdialysis study in the rat. *Brain Res, 581*(2), 217-228. https://doi.org/10.1016/0006-8993(92)90711-h

Cernotova, D., Stuchlik, A., & Svoboda, J. (2021). Roles of the ventral hippocampus and medial prefrontal cortex in spatial reversal learning and attentional set-shifting. *Neurobiol Learn Mem, 183*, 107477. https://doi.org/10.1016/j.nlm.2021.107477

Chaudhry, F. A., Reimer, R. J., Bellocchio, E. E., Danbolt, N. C., Osen, K. K., Edwards, R. H., & Storm-Mathisen, J. (1998). The vesicular GABA transporter, VGAT,

localizes to synaptic vesicles in sets of glycinergic as well as GABAergic neurons. *Journal of Neuroscience, 18*(23), 9733-9750. <Go to ISI>://WOS:000077169800017

Chen, C. M., Stanford, A. D., Mao, X., Abi-Dargham, A., Shungu, D. C., Lisanby, S. H., Schroeder, C. E., & Kegeles, L. S. (2014). GABA level, gamma oscillation, and working memory performance in schizophrenia. *Neuroimage Clin, 4*, 531-539. https://doi.org/10.1016/j.nicl.2014.03.007

Chen, S., Tan, Z., Xia, W., Gomes, C. A., Zhang, X., Zhou, W., Liang, S., Axmacher, N., & Wang, L. (2021). Theta oscillations synchronize human medial prefrontal cortex and amygdala during fear learning. *Sci Adv, 7*(34), eabf4198. https://doi.org/10.1126/sciadv.abf4198

Chudasama, Y., Daniels, T. E., Gorrin, D. P., Rhodes, S. E., Rudebeck, P. H., & Murray, E. A. (2013). The role of the anterior cingulate cortex in choices based on reward value and reward contingency. *Cereb Cortex, 23*(12), 2884-2898. https://doi.org/10.1093/cercor/bhs266

Chudasama, Y., & Robbins, T. W. (2003). Dissociable contributions of the orbitofrontal and infralimbic cortex to Pavlovian autoshaping and discrimination reversal learning: Further evidence for the functional heterogeneity of the rodent frontal cortex. *Journal of Neuroscience, 23*(25), 8771-8780. https://doi.org/10.1523/JNEUROSCI.23-25-08771.2003

Ciranna, L. (2006). Serotonin as a modulator of glutamate- and GABA-mediated neurotransmission: Implications in physiological functions and in pathology. *Current neuropharmacology, 4*(2), 101-114. https://doi.org/Doi 10.2174/157015906776359540

Clark, P. J., Brodnik, Z. D., & Espana, R. A. (2022). Chemogenetic Signaling in Space and Time: Considerations for Designing Neuroscience Experiments

Using DREADDs. *Neuroscientist*, 10738584221134587.
https://doi.org/10.1177/10738584221134587

Clarke, H. F., Robbins, T. W., & Roberts, A. C. (2008). Lesions of the Medial
Striatum in Monkeys Produce Perseverative Impairments during Reversal
Learning Similar to Those Produced by Lesions of the Orbitofrontal Cortex.
Journal of Neuroscience, 28(43), 10972-10982.
https://doi.org/10.1523/Jneurosci.1521-08.2008

Clarke, H. F., Walker, S. C., Crofts, H. S., Dalley, J. W., Robbins, T. W., & Roberts, A.
C. (2005). Prefrontal serotonin depletion affects reversal learning but not
attentional set shifting. *J Neurosci, 25*(2), 532-538.
https://doi.org/10.1523/JNEUROSCI.3690-04.2005

Cohen, J. D., Dunbar, K., & McClelland, J. L. (1990). On the control of automatic
processes: a parallel distributed processing account of the Stroop effect.
Psychol Rev, 97(3), 332-361. https://doi.org/10.1037/0033-295x.97.3.332

Cohen, J. D., McClure, S. M., & Yu, A. J. (2007). Should I stay or should I go? How
the human brain manages the trade-off between exploitation and
exploration. *Philosophical Transactions of the Royal Society B: Biological
Sciences, 362*(1481), 933-942.

Colgin, L. L. (2016). Rhythms of the hippocampal network. *Nat Rev Neurosci,
17*(4), 239-249. https://doi.org/10.1038/nrn.2016.21

Conde, F., Audinat, E., Maire-Lepoivre, E., & Crepel, F. (1990). Afferent
connections of the medial frontal cortex of the rat. A study using retrograde
transport of fluorescent dyes. I. Thalamic afferents. *Brain Res Bull, 24*(3),
341-354. https://doi.org/10.1016/0361-9230(90)90088-h

Conti, F., Minelli, A., & Melone, M. (2004). GABA transporters in the mammalian cerebral cortex: localization, development and pathological implications. *Brain Res Brain Res Rev, 45*(3), 196-212. https://doi.org/10.1016/j.brainresrev.2004.03.003

Cope, Z. A., Vazey, E. M., Floresco, S. B., & Aston Jones, G. S. (2019). DREADD-mediated modulation of locus coeruleus inputs to mPFC improves strategy set-shifting. *Neurobiol Learn Mem, 161*, 1-11. https://doi.org/10.1016/j.nlm.2019.02.009

Costa, V. D., Tran, V. L., Turchi, J., & Averbeck, B. B. (2015). Reversal Learning and Dopamine: A Bayesian Perspective. *Journal of Neuroscience, 35*(6), 2407-2416. https://doi.org/10.1523/Jneurosci.1989-14.2015

Cunningham, M. G., Ames, H. M., Donalds, R. A., & Benes, F. M. (2008). Construction and implantation of a microinfusion system for sustained delivery of neuroactive agents. *Journal of Neuroscience Methods, 167*(2), 213-220. https://doi.org/10.1016/j.jneumeth.2007.08.016

Curtis, C. E., & D'Esposito, M. (2003). Persistent activity in the prefrontal cortex during working memory. *Trends Cogn Sci, 7*(9), 415-423. https://doi.org/10.1016/s1364-6613(03)00197-9

Dalley, J. W., Cardinal, R. N., & Robbins, T. W. (2004). Prefrontal executive and cognitive functions in rodents: neural and neurochemical substrates. *Neurosci Biobehav Rev, 28*(7), 771-784. https://doi.org/10.1016/j.neubiorev.2004.09.006

Dalton, G. L., Ma, L. M., Phillips, A. G., & Floresco, S. B. (2011). Blockade of NMDA GluN2B receptors selectively impairs behavioral flexibility but not initial discrimination learning. *Psychopharmacology, 216*, 525-535.

Dalton, G. L., Wang, N. Y., Phillips, A. G., & Floresco, S. B. (2016). Multifaceted Contributions by Different Regions of the Orbitofrontal and Medial Prefrontal Cortex to Probabilistic Reversal Learning. *J Neurosci, 36*(6), 1996-2006. https://doi.org/10.1523/JNEUROSCI.3366-15.2016

Daw, N. D., O'Doherty, J. P., Dayan, P., Seymour, B., & Dolan, R. J. (2006). Cortical substrates for exploratory decisions in humans. *Nature, 441*(7095), 876-879. https://doi.org/10.1038/nature04766

Dawson, L. A., Nguyen, H. Q., & Li, P. (2001). The 5-HT receptor antagonist SB-271046 selectively enhances excitatory neurotransmission in the rat frontal cortex and hippocampus. *Neuropsychopharmacology, 25*(5), 662-668. https://doi.org/Doi 10.1016/S0893-133x(01)00265-2

de la Fuente-Sandoval, C., Leon-Ortiz, P., Favila, R., Stephano, S., Mamo, D., Ramirez-Bermudez, J., & Graff-Guerrero, A. (2011). Higher levels of glutamate in the associative-striatum of subjects with prodromal symptoms of schizophrenia and patients with first-episode psychosis. *Neuropsychopharmacology, 36*(9), 1781-1791. https://doi.org/10.1038/npp.2011.65

Dermon, C. R., & Barbas, H. (1994). Contralateral thalamic projections predominantly reach transitional cortices in the rhesus monkey. *J Comp Neurol, 344*(4), 508-531. https://doi.org/10.1002/cne.903440403

Dhawan, S. S., Tait, D. S., & Brown, V. J. (2019). More rapid reversal learning following overtraining in the rat is evidence that behavioural and cognitive flexibility are dissociable. *Behavioural Brain Research, 363*, 45-52. https://doi.org/10.1016/j.bbr.2019.01.055

Dias, R., Robbins, T. W., & Roberts, A. C. (1996). Primate analogue of the
Wisconsin Card Sorting Test: effects of excitotoxic lesions of the prefrontal
cortex in the marmoset. *Behav Neurosci, 110*(5), 872-886.
https://doi.org/10.1037//0735-7044.110.5.872

Dias, R., Robbins, T. W., & Roberts, A. C. (1997). Dissociable forms of inhibitory
control within prefrontal cortex with an analog of the Wisconsin Card Sort
Test: restriction to novel situations and independence from "on-line"
processing. *J Neurosci, 17*(23), 9285-9297.
https://doi.org/10.1523/JNEUROSCI.17-23-09285.1997

Duncan, J., & Owen, A. M. (2000). Common regions of the human frontal lobe
recruited by diverse cognitive demands. *Trends Neurosci, 23*(10), 475-483.
https://doi.org/10.1016/s0166-2236(00)01633-7

Eckenstein, F., & Thoenen, H. (1983). Cholinergic neurons in the rat cerebral
cortex demonstrated by immunohistochemical localization of choline
acetyltransferase. *Neurosci Lett, 36*(3), 211-215.
https://doi.org/10.1016/0304-3940(83)90002-2

Enomoto, T., Tse, M. T., & Floresco, S. B. (2011). Reducing prefrontal gamma-
aminobutyric acid activity induces cognitive, behavioral, and dopaminergic
abnormalities that resemble schizophrenia. *Biol Psychiatry, 69*(5), 432-441.
https://doi.org/10.1016/j.biopsych.2010.09.038

Erlander, M. G., Tillakaratne, N. J., Feldblum, S., Patel, N., & Tobin, A. J. (1991).
Two genes encode distinct glutamate decarboxylases. *Neuron, 7*(1), 91-100.
https://doi.org/10.1016/0896-6273(91)90077-d

Euston, D. R., Gruber, A. J., & McNaughton, B. L. (2012). The role of medial
prefrontal cortex in memory and decision making. *Neuron, 76*(6), 1057-
1070. https://doi.org/10.1016/j.neuron.2012.12.002

Fang, P. C., Stepniewska, I., & Kaas, J. H. (2006). The thalamic connections of motor, premotor, and prefrontal areas of cortex in a prosimian primate (Otolemur garnetti). *Neuroscience, 143*(4), 987-1020. https://doi.org/10.1016/j.neuroscience.2006.08.053

Faul, F., Erdfelder, E., Lang, A. G., & Buchner, A. (2007). G*Power 3: a flexible statistical power analysis program for the social, behavioral, and biomedical sciences. *Behav Res Methods, 39*(2), 175-191. https://doi.org/10.3758/bf03193146

Fauth, M., & Tetzlaff, C. (2016). Opposing Effects of Neuronal Activity on Structural Plasticity. *Front Neuroanat, 10*, 75. https://doi.org/10.3389/fnana.2016.00075

Feng, J., Cai, X., Zhao, J. H., & Yan, Z. (2001). Serotonin receptors modulate GABA receptor channels through activation of anchored protein kinase C in prefrontal cortical neurons. *Journal of Neuroscience, 21*(17), 6502-6511. https://doi.org/Doi 10.1523/Jneurosci.21-17-06502.2001

Floresco, S. B., Block, A. E., & Tse, M. T. (2008). Inactivation of the medial prefrontal cortex of the rat impairs strategy set-shifting, but not reversal learning, using a novel, automated procedure. *Behav Brain Res, 190*(1), 85-96. https://doi.org/10.1016/j.bbr.2008.02.008

Floresco, S. B., Zhang, Y., & Enomoto, T. (2009). Neural circuits subserving behavioral flexibility and their relevance to schizophrenia. *Behavioural Brain Research, 204*(2), 396-409. https://doi.org/10.1016/j.bbr.2008.12.001

Ford, L. M., Norman, A. B., & Sanberg, P. R. (1989). The topography of MK-801-induced locomotor patterns in rats. *Physiology & behavior, 46*(4), 755-758.

Fray, P. J., Robbins, T. W., & Sahakian, B. J. (1996). Neuorpsychiatyric applications of CANTAB. *International journal of geriatric psychiatry*.

Fries, P., Reynolds, J. H., Rorie, A. E., & Desimone, R. (2001). Modulation of oscillatory neuronal synchronization by selective visual attention. *Science, 291*(5508), 1560-1563. https://doi.org/10.1126/science.1055465

Fujita, A., Bonnavion, P., Wilson, M. H., Mickelsen, L. E., Bloit, J., de Lecea, L., & Jackson, A. C. (2017). Hypothalamic Tuberomammillary Nucleus Neurons: Electrophysiological Diversity and Essential Role in Arousal Stability. *J Neurosci, 37*(39), 9574-9592. https://doi.org/10.1523/JNEUROSCI.0580-17.2017

Fukuda, T., Aika, Y., Heizmann, C. W., & Kosaka, T. (1998). GABAergic axon terminals at perisomatic and dendritic inhibitory sites show different immunoreactivities against two GAD isoforms, GAD67 and GAD65, in the mouse hippocampus: a digitized quantitative analysis. *Journal of Comparative Neurology, 395*(2), 177-194. https://doi.org/10.1002/(SICI)1096-9861(19980928)399:3<424::AID-CNE10>3.0.CO;2-8

Fung, S. J., Webster, M. J., Sivagnanasundaram, S., Duncan, C., Elashoff, M., & Weickert, C. S. (2010). Expression of interneuron markers in the dorsolateral prefrontal cortex of the developing human and in schizophrenia. *Am J Psychiatry, 167*(12), 1479-1488. https://doi.org/10.1176/appi.ajp.2010.09060784

Fuster, J. M. (1997). Network memory. *Trends Neurosci, 20*(10), 451-459. https://doi.org/10.1016/s0166-2236(97)01128-4

Gabbott, P. L., Dickie, B. G., Vaid, R. R., Headlam, A. J., & Bacon, S. J. (1997). Local-circuit neurones in the medial prefrontal cortex (areas 25, 32 and 24b) in the rat: morphology and quantitative distribution. *J Comp Neurol, 377*(4), 465-499. https://doi.org/10.1002/(sici)1096-9861(19970127)377:4<465::aid-cne1>3.0.co;2-0

Garey, L. J. (1999). *Brodmann's' localisation in the cerebral cortex'*. World Scientific.

Giustino, T. F., & Maren, S. (2015). The Role of the Medial Prefrontal Cortex in the Conditioning and Extinction of Fear. *Front Behav Neurosci, 9*, 298. https://doi.org/10.3389/fnbeh.2015.00298

Glahn, D. C., Ragland, J. D., Abramoff, A., Barrett, J., Laird, A. R., Bearden, C. E., & Velligan, D. I. (2005). Beyond hypofrontality: a quantitative meta-analysis of functional neuroimaging studies of working memory in schizophrenia. *Hum Brain Mapp, 25*(1), 60-69. https://doi.org/10.1002/hbm.20138

Goldman-Rakic, P. S. (1994). Working memory dysfunction in schizophrenia. *J Neuropsychiatry Clin Neurosci, 6*(4), 348-357. https://doi.org/10.1176/jnp.6.4.348

Gomez, J. L., Bonaventura, J., Lesniak, W., Mathews, W. B., Sysa-Shah, P., Rodriguez, L. A., Ellis, R. J., Richie, C. T., Harvey, B. K., & Dannals, R. F. (2017). Chemogenetics revealed: DREADD occupancy and activation via converted clozapine. *Science, 357*(6350), 503-507.

Gonçalves, S., Hathway, G. J., Woodhams, S. G., Chapman, V., & Bast, T. (2023). No evidence for cognitive impairment in an experimental rat model of knee osteoarthritis and associated chronic pain. *The Journal of Pain, 24*(8), 1478-1492. https://doi.org/10.1016/j.jpain.2023.04.002

Gonzalez-Burgos, G., & Lewis, D. A. (2008). GABA neurons and the mechanisms of network oscillations: implications for understanding cortical dysfunction in schizophrenia. *Schizophr Bull, 34*(5), 944-961. https://doi.org/10.1093/schbul/sbn070

Granger, A. J., Mulder, N., Saunders, A., & Sabatini, B. L. (2016). Cotransmission of acetylcholine and GABA. *Neuropharmacology, 100*, 40-46. https://doi.org/10.1016/j.neuropharm.2015.07.031

Granger, A. J., Wang, W., Robertson, K., El-Rifai, M., Zanello, A. F., Bistrong, K., Saunders, A., Chow, B. W., Nunez, V., Turrero Garcia, M., Harwell, C. C., Gu, C., & Sabatini, B. L. (2020). Cortical ChAT(+) neurons co-transmit acetylcholine and GABA in a target- and brain-region-specific manner. *Elife, 9*, e57749. https://doi.org/10.7554/eLife.57749

Gregoriou, G. G., Gotts, S. J., Zhou, H. H., & Desimone, R. (2009). Long-range neural coupling through synchronization with attention. *Attention, 176*, 35-45. https://doi.org/10.1016/S0079-6123(09)17603-3

Gremel, C. M., & Costa, R. M. (2013). Orbitofrontal and striatal circuits dynamically encode the shift between goal-directed and habitual actions. *Nature communications, 4*(1), 1-12. https://doi.org/10.1038/ncomms3264

Groenewegen, H. J. (1988). Organization of the afferent connections of the mediodorsal thalamic nucleus in the rat, related to the mediodorsal-prefrontal topography. *Neuroscience, 24*(2), 379-431. https://doi.org/10.1016/0306-4522(88)90339-9

Groenewegen, H. J., & Witter, M. P. (2004). Thalamus. *The rat nervous system*, 407-453. https://doi.org/https://doi.org/10.1016/B978-012547638-6/50018-3

Guidotti, A., Auta, J., Davis, J. M., Di-Giorgi-Gerevini, V., Dwivedi, Y., Grayson, D. R., Impagnatiello, F., Pandey, G., Pesold, C., Sharma, R., Uzunov, D., & Costa, E. (2000). Decrease in reelin and glutamic acid decarboxylase67 (GAD67) expression in schizophrenia and bipolar disorder: a postmortem brain study. *Arch Gen Psychiatry, 57*(11), 1061-1069. https://doi.org/10.1001/archpsyc.57.11.1061

Haddon, J. E., & Killcross, S. (2006). Prefrontal cortex lesions disrupt the contextual control of response conflict. *J Neurosci, 26*(11), 2933-2940. https://doi.org/10.1523/JNEUROSCI.3243-05.2006

Hampshire, A., Chaudhry, A. M., Owen, A. M., & Roberts, A. C. (2012). Dissociable roles for lateral orbitofrontal cortex and lateral prefrontal cortex during preference driven reversal learning. *Neuroimage, 59*(4), 4102-4112. https://doi.org/10.1016/j.neuroimage.2011.10.072

Hampshire, A., & Owen, A. M. (2006). Fractionating attentional control using event-related fMRI. *Cerebral Cortex, 16*(12), 1679-1689.

Hanada, S., Mita, T., Nishino, N., & Tanaka, C. (1987). [3H]muscimol binding sites increased in autopsied brains of chronic schizophrenics. *Life Sci, 40*(3), 259-266. https://doi.org/10.1016/0024-3205(87)90341-9

Harris, C., Aguirre, C., Kolli, S., Das, K., Izquierdo, A., & Soltani, A. (2021). Unique features of stimulus-based probabilistic reversal learning. *Behav Neurosci, 135*(4), 550-570. https://doi.org/10.1037/bne0000474

Hashimoto, T., Volk, D. W., Eggan, S. M., Mirnics, K., Pierri, J. N., Sun, Z., Sampson, A. R., & Lewis, D. A. (2003). Gene expression deficits in a subclass of GABA neurons in the prefrontal cortex of subjects with schizophrenia. *J Neurosci, 23*(15), 6315-6326. https://doi.org/10.1523/JNEUROSCI.23-15-06315.2003

Hasselmo, M. E. (2006). The role of acetylcholine in learning and memory. *Curr Opin Neurobiol, 16*(6), 710-715. https://doi.org/10.1016/j.conb.2006.09.002

Hassett, T. C., & Hampton, R. R. (2017). Change in the relative contributions of habit and working memory facilitates serial reversal learning expertise in rhesus monkeys. *Animal cognition, 20*(3), 485-497. https://doi.org/https://doi.org/10.1007/s10071-017-1076-8

Heffner, C. S., Herbert Pratt, C., Babiuk, R. P., Sharma, Y., Rockwood, S. F., Donahue, L. R., Eppig, J. T., & Murray, S. A. (2012). Supporting conditional mouse mutagenesis with a comprehensive cre characterization resource. *Nat Commun, 3*(1), 1218. https://doi.org/10.1038/ncomms2186

Hendry, S. H., Schwark, H. D., Jones, E. G., & Yan, J. (1987). Numbers and proportions of GABA-immunoreactive neurons in different areas of monkey cerebral cortex. *J Neurosci, 7*(5), 1503-1519. https://doi.org/10.1523/JNEUROSCI.07-05-01503.1987

Hervig, M. E., Fiddian, L., Piilgaard, L., Bozic, T., Blanco-Pozo, M., Knudsen, C., Olesen, S. F., Alsio, J., & Robbins, T. W. (2020). Dissociable and Paradoxical Roles of Rat Medial and Lateral Orbitofrontal Cortex in Visual Serial Reversal Learning. *Cereb Cortex, 30*(3), 1016-1029. https://doi.org/10.1093/cercor/bhz144

Hill, K., Mann, L., Laws, K. R., Stephenson, C. M., Nimmo-Smith, I., & McKenna, P. J. (2004). Hypofrontality in schizophrenia: a meta-analysis of functional imaging studies. *Acta Psychiatr Scand, 110*(4), 243-256. https://doi.org/10.1111/j.1600-0447.2004.00376.x

Hock, R. M. (2020). *Too little and too much: investigating the role of balanced prefrontal neural activity in behavioural flexibility* (Doctoral dissertation, University of Nottingham)].

https://eprints.nottingham.ac.uk/id/eprint/60573

Homayoun, H., & Moghaddam, B. (2007a). NMDA receptor hypofunction produces opposite effects on prefrontal cortex Interneurons and pyramidal neurons. *Journal of Neuroscience, 27*(43), 11496-11500.

https://doi.org/10.1523/Jneurosci.2213-07.2007

Homayoun, H., & Moghaddam, B. (2007b). NMDA receptor hypofunction produces opposite effects on prefrontal cortex interneurons and pyramidal neurons. *J Neurosci, 27*(43), 11496-11500.

https://doi.org/10.1523/JNEUROSCI.2213-07.2007

Hornak, J., O'Doherty, J., Bramham, J., Rolls, E. T., Morris, R. G., Bullock, P. R., & Polkey, C. E. (2004). Reward-related reversal learning after surgical excisions in orbito-frontal or dorsolateral prefrontal cortex in humans. *J Cogn Neurosci, 16*(3), 463-478.

https://doi.org/10.1162/089892904322926791

Horst, N. K., & Laubach, M. (2009). The role of rat dorsomedial prefrontal cortex in spatial working memory. *Neuroscience, 164*(2), 444-456.

https://doi.org/10.1016/j.neuroscience.2009.08.004

Hu, H., Cavendish, J. Z., & Agmon, A. (2013). Not all that glitters is gold: off-target recombination in the somatostatin–IRES-Cre mouse line labels a subset of fast-spiking interneurons. *Frontiers in Neural Circuits, 7*, 195.

https://doi.org/10.3389/fncir.2013.00195

Hutton, S. B., Puri, B. K., Duncan, L. J., Robbins, T. W., Barnes, T. R., & Joyce, E. M. (1998). Executive function in first-episode schizophrenia. *Psychol Med, 28*(2), 463-473. https://doi.org/10.1017/s0033291797006041

Ingvar, D. H., & Franzén, G. (1974). Abnormalities of cerebral blood flow distribution in patients with chronic schizophrenia. *Acta Psychiatrica Scandinavica*. https://doi.org/10.1111/j.1600-0447.1974.tb09707.x

Ivan, V. E., Banks, P. J., Goodfellow, K., & Gruber, A. J. (2018). Lose-Shift Responding in Humans Is Promoted by Increased Cognitive Load. *Frontiers in integrative neuroscience, 12*, 9. https://doi.org/10.3389/fnint.2018.00009

Iversen, S. D., & Mishkin, M. (1970). Perseverative interference in monkeys following selective lesions of the inferior prefrontal convexity. *Experimental brain research, 11*, 376-386.

Izquierdo, A., Brigman, J. L., Radke, A. K., Rudebeck, P. H., & Holmes, A. (2017). The neural basis of reversal learning: An updated perspective. *Neuroscience, 345*, 12-26. https://doi.org/10.1016/j.neuroscience.2016.03.021

Izquierdo, A., Darling, C., Manos, N., Pozos, H., Kim, C., Ostrander, S., Cazares, V., Stepp, H., & Rudebeck, P. H. (2013). Basolateral amygdala lesions facilitate reward choices after negative feedback in rats. *J Neurosci, 33*(9), 4105-4109. https://doi.org/10.1523/JNEUROSCI.4942-12.2013

Izquierdo, A., & Jentsch, J. D. (2012). Reversal learning as a measure of impulsive and compulsive behavior in addictions. *Psychopharmacology (Berl), 219*(2), 607-620. https://doi.org/10.1007/s00213-011-2579-7

Izquierdo, A., Suda, R. K., & Murray, E. A. (2004). Bilateral orbital prefrontal cortex lesions in rhesus monkeys disrupt choices guided by both reward value and reward contingency. *Journal of Neuroscience, 24*(34), 7540-7548. https://doi.org/10.1523/Jneurosci.1921-04.2004

Izquierdo, A., Wiedholz, L. M., Millstein, R. A., Yang, R. J., Bussey, T. J., Saksida, L. M., & Holmes, A. (2006). Genetic and dopaminergic modulation of reversal learning in a touchscreen-based operant procedure for mice. *Behav Brain Res, 171*(2), 181-188. https://doi.org/10.1016/j.bbr.2006.03.029

Jang, A. I., Costa, V. D., Rudebeck, P. H., Chudasama, Y., Murray, E. A., & Averbeck, B. B. (2015). The Role of Frontal Cortical and Medial-Temporal Lobe Brain Areas in Learning a Bayesian Prior Belief on Reversals. *J Neurosci, 35*(33), 11751-11760. https://doi.org/10.1523/JNEUROSCI.1594-15.2015

Jendryka, M., Palchaudhuri, M., Ursu, D., van der Veen, B., Liss, B., Katzel, D., Nissen, W., & Pekcec, A. (2019). Pharmacokinetic and pharmacodynamic actions of clozapine-N-oxide, clozapine, and compound 21 in DREADD-based chemogenetics in mice. *Sci Rep, 9*(1), 4522. https://doi.org/10.1038/s41598-019-41088-2

Jones, B., & Mishkin, M. (1972). Limbic lesions and the problem of stimulus—reinforcement associations. *Experimental neurology, 36*(2), 362-377. https://doi.org/10.1016/0014-4886(72)90030-1

Jones, E. G. (1993). Gabaergic Neurons and Their Role in Cortical Plasticity in Primates. *Cerebral Cortex, 3*(5), 361-372. https://doi.org/10.1093/cercor/3.5.361-a

Kakava-Georgiadou, N., Zwartkruis, M. M., Bullich-Vilarrubias, C., Luijendijk, M. C. M., Garner, K. M., van der Plasse, G., & Adan, R. A. H. (2019). An Intersectional Approach to Target Neural Circuits With Cell- and

Projection-Type Specificity: Validation in the Mesolimbic Dopamine System. *Front Mol Neurosci, 12*, 49. https://doi.org/10.3389/fnmol.2019.00049

Kaplan, B. J. (1985). The Epileptic Nature of Rodent Electrocortical Polyspiking Is Still Unproven. *Experimental neurology, 88*(2), 425-436. https://doi.org/10.1016/0014-4886(85)90204-3

Karp, N. A., & Reavey, N. (2019). Sex bias in preclinical research and an exploration of how to change the status quo. *British journal of pharmacology, 176*(21), 4107-4118.

Katsuki, F., & Constantinidis, C. (2014). Bottom-up and top-down attention: different processes and overlapping neural systems. *Neuroscientist, 20*(5), 509-521. https://doi.org/10.1177/1073858413514136

Kaufman, D. L., Houser, C. R., & Tobin, A. J. (1991). Two forms of the γ-aminobutyric acid synthetic enzyme glutamate decarboxylase have distinct intraneuronal distributions and cofactor interactions. *Journal of neurochemistry, 56*(2), 720-723. https://doi.org/10.1111/j.1471-4159.1991.tb08211.x

Keefe, R. S., & Harvey, P. D. (2012). Cognitive impairment in schizophrenia. *Handb Exp Pharmacol*(213), 11-37. https://doi.org/10.1007/978-3-642-25758-2_2

Keilhoff, G., Bernstein, H. G., Becker, A., Grecksch, G., & Wolf, G. (2004). Increased neurogenesis in a rat ketamine model of schizophrenia. *Biol Psychiatry, 56*(5), 317-322. https://doi.org/10.1016/j.biopsych.2004.06.010

Kinon, B. J., Millen, B. A., Zhang, L., & McKinzie, D. L. (2015). Exploratory analysis for a targeted patient population responsive to the metabotropic glutamate

2/3 receptor agonist pomaglumetad methionil in schizophrenia. *Biol Psychiatry, 78*(11), 754-762. https://doi.org/10.1016/j.biopsych.2015.03.016

Koolschijn, R. S., Shpektor, A., Clarke, W. T., Ip, I. B., Dupret, D., Emir, U. E., & Barron, H. C. (2021). Memory recall involves a transient break in excitatory-inhibitory balance. *Elife, 10*, e70071.

Kosaki, Y., & Watanabe, S. (2012). Dissociable roles of the medial prefrontal cortex, the anterior cingulate cortex, and the hippocampus in behavioural flexibility revealed by serial reversal of three-choice discrimination in rats. *Behav Brain Res, 227*(1), 81-90. https://doi.org/10.1016/j.bbr.2011.10.039

Krettek, J. E., & Price, J. L. (1977). The cortical projections of the mediodorsal nucleus and adjacent thalamic nuclei in the rat. *J Comp Neurol, 171*(2), 157-191. https://doi.org/10.1002/cne.901710204

Krystal, J. H., & Anticevic, A. (2015). Toward illness phase-specific pharmacotherapy for schizophrenia. *Biol Psychiatry, 78*(11), 738-740. https://doi.org/10.1016/j.biopsych.2015.08.017

Lakatos, P., Karmos, G., Mehta, A. D., Ulbert, I., & Schroeder, C. E. (2008). Entrainment of neuronal oscillations as a mechanism of attentional selection. *Science, 320*(5872), 110-113. https://doi.org/10.1126/science.1154735

Lapiz-Bluhm, M. D., Soto-Pina, A. E., Hensler, J. G., & Morilak, D. A. (2009). Chronic intermittent cold stress and serotonin depletion induce deficits of reversal learning in an attentional set-shifting test in rats. *Psychopharmacology (Berl), 202*(1-3), 329-341. https://doi.org/10.1007/s00213-008-1224-6

Laskowski, C. S., Williams, R. J., Martens, K. M., Gruber, A. J., Fisher, K. G., & Euston, D. R. (2016). The role of the medial prefrontal cortex in updating reward value and avoiding perseveration. *Behav Brain Res, 306*, 52-63. https://doi.org/10.1016/j.bbr.2016.03.007

Laubach, M., Amarante, L. M., Swanson, K., & White, S. R. (2018). What, if anything, is rodent prefrontal cortex? *eneuro, 5*(5).

Lee, J., & Park, S. (2005). Working memory impairments in schizophrenia: a meta-analysis. *J Abnorm Psychol, 114*(4), 599-611. https://doi.org/10.1037/0021-843X.114.4.599

Leeson, V. C., Robbins, T. W., Matheson, E., Hutton, S. B., Ron, M. A., Barnes, T. R., & Joyce, E. M. (2009). Discrimination learning, reversal, and set-shifting in first-episode schizophrenia: stability over six years and specific associations with medication type and disorganization syndrome. *Biol Psychiatry, 66*(6), 586-593. https://doi.org/10.1016/j.biopsych.2009.05.016

Leonard, C. M. (1969). The prefrontal cortex of the rat. I. Cortical projection of the mediodorsal nucleus. II. Efferent connections. *Brain Res, 12*(2), 321-343. https://doi.org/10.1016/0006-8993(69)90003-1

Letzkus, J. J., Wolff, S. B., & Luthi, A. (2015). Disinhibition, a Circuit Mechanism for Associative Learning and Memory. *Neuron, 88*(2), 264-276. https://doi.org/10.1016/j.neuron.2015.09.024

Leung MD, D. A., & Chue MRC Psych, D. P. (2000). Sex differences in schizophrenia, a review of the literature. *Acta Psychiatrica Scandinavica, 101*(401), 3-38.

Levsky, J. M., & Singer, R. H. (2003). Fluorescence in situ hybridization: past, present and future. *J Cell Sci, 116*(Pt 14), 2833-2838. https://doi.org/10.1242/jcs.00633

Lewis, D. A., Hashimoto, T., & Morris, H. M. (2008). Cell and receptor type-specific alterations in markers of GABA neurotransmission in the prefrontal cortex of subjects with schizophrenia. *Neurotox Res, 14*(2-3), 237-248. https://doi.org/10.1007/BF03033813

Lewis, D. A., Hashimoto, T., & Volk, D. W. (2005). Cortical inhibitory neurons and schizophrenia. *Nat Rev Neurosci, 6*(4), 312-324. https://doi.org/10.1038/nrn1648

Lin, H., Hsu, F. C., Baumann, B. H., Coulter, D. A., Anderson, S. A., & Lynch, D. R. (2014). Cortical parvalbumin GABAergic deficits with alpha7 nicotinic acetylcholine receptor deletion: implications for schizophrenia. *Mol Cell Neurosci, 61*, 163-175. https://doi.org/10.1016/j.mcn.2014.06.007

Lisman, J. E. (1997). Bursts as a unit of neural information: Making unreliable synapses reliable. *Trends in Neurosciences, 20*(1), 38-43. https://doi.org/10.1016/S0166-2236(96)10070-9

Liston, C., McEwen, B. S., & Casey, B. J. (2009). Psychosocial stress reversibly disrupts prefrontal processing and attentional control. *Proc Natl Acad Sci U S A, 106*(3), 912-917. https://doi.org/10.1073/pnas.0807041106

Lupinsky, D., Moquin, L., & Gratton, A. (2010). Interhemispheric regulation of the medial prefrontal cortical glutamate stress response in rats. *J Neurosci, 30*(22), 7624-7633. https://doi.org/10.1523/JNEUROSCI.1187-10.2010

Mackintosh, N. (1962). The effects of overtraining on a reversal and a
    nonreversal shift. *Journal of Comparative and Physiological Psychology,
    55*(4), 555.

Mackintosh, N., & Little, L. (1969). Selective attention and response strategies as
    factors in serial reversal learning. *Canadian Journal of Psychology/Revue
    canadienne de psychologie, 23*(5), 335.

Mackintosh, N. J. (1969). Further analysis of the overtraining reversal effect.
    Journal of Comparative and Physiological Psychology, 67(2p2), 1.

Mackintosh, N. J., McGonigle, B., Holgate, V., & Vanderver, V. (1968). Factors
    underlying improvement in serial reversal learning. *Can J Psychol, 22*(2),
    85-95. https://doi.org/10.1037/h0082753

Maggi, S., Hock, R. M., O'Neill, M., Buckley, M. J., Moran, P. M., Bast, T., Sami, M., &
    Humphries, M. D. (2023). Tracking subject's strategies in behavioural
    choice experiments at trial resolution. *bioRxiv*.
    https://doi.org/10.1101/2022.08.30.505807

Mahler, S. V., & Aston-Jones, G. (2018). CNO Evil? Considerations for the Use of
    DREADDs in Behavioral Neuroscience. *Neuropsychopharmacology, 43*(5),
    934-936. https://doi.org/10.1038/npp.2017.299

Mahler, S. V., Vazey, E. M., Beckley, J. T., Keistler, C. R., McGlinchey, E. M., Kaufling,
    J., Wilson, S. P., Deisseroth, K., Woodward, J. J., & Aston-Jones, G. (2014).
    Designer receptors show role for ventral pallidum input to ventral
    tegmental area in cocaine seeking. *Nature neuroscience, 17*(4), 577-U136.
    https://doi.org/10.1038/nn.3664

Mailly, P., Aliane, V., Groenewegen, H. J., Haber, S. N., & Deniau, J. M. (2013). The
    rat prefrontostriatal system analyzed in 3D: evidence for multiple

interacting functional units. *J Neurosci, 33*(13), 5718-5727. https://doi.org/10.1523/JNEUROSCI.5248-12.2013

Mandler, G., & Watson, D. L. (1966). Anxiety and the interruption of behavior. *Anxiety and behavior, 1*.

Markham, J. A., Morris, J., & Juraska, J. M. (2007). Neuron number decreases in the rat ventral, but not dorsal, medial prefrontal cortex between adolescence and adulthood. *Neuroscience, 144*(3), 961-968. https://doi.org/10.1016/j.neuroscience.2006.10.015

Markram, H., Toledo-Rodriguez, M., Wang, Y., Gupta, A., Silberberg, G., & Wu, C. (2004). Interneurons of the neocortical inhibitory system. *Nat Rev Neurosci, 5*(10), 793-807. https://doi.org/10.1038/nrn1519

Marquis, J. P., Killcross, S., & Haddon, J. E. (2007). Inactivation of the prelimbic, but not infralimbic, prefrontal cortex impairs the contextual control of response conflict in rats. *Eur J Neurosci, 25*(2), 559-566. https://doi.org/10.1111/j.1460-9568.2006.05295.x

Marsman, A., van den Heuvel, M. P., Klomp, D. W., Kahn, R. S., Luijten, P. R., & Hulshoff Pol, H. E. (2013). Glutamate in schizophrenia: a focused review and meta-analysis of (1)H-MRS studies. *Schizophr Bull, 39*(1), 120-129. https://doi.org/10.1093/schbul/sbr069

McAlonan, K., & Brown, V. J. (2003). Orbital prefrontal cortex mediates reversal learning and not attentional set shifting in the rat. *Behav Brain Res, 146*(1-2), 97-103. https://doi.org/10.1016/j.bbr.2003.09.019

Millan, M. J., Agid, Y., Brune, M., Bullmore, E. T., Carter, C. S., Clayton, N. S., Connor, R., Davis, S., Deakin, B., DeRubeis, R. J., Dubois, B., Geyer, M. A., Goodwin, G. M., Gorwood, P., Jay, T. M., Joels, M., Mansuy, I. M., Meyer-Lindenberg, A.,

Murphy, D., Rolls, E., Saletu, B., Spedding, M., Sweeney, J., Whittington, M., & Young, L. J. (2012). Cognitive dysfunction in psychiatric disorders: characteristics, causes and the quest for improved therapy. *Nat Rev Drug Discov, 11*(2), 141-168. https://doi.org/10.1038/nrd3628

Miller, E. K., & Cohen, J. D. (2001). An integrative theory of prefrontal cortex function. *Annu Rev Neurosci, 24*(1), 167-202. https://doi.org/10.1146/annurev.neuro.24.1.167

Minzenberg, M. J., Laird, A. R., Thelen, S., Carter, C. S., & Glahn, D. C. (2009). Meta-analysis of 41 functional neuroimaging studies of executive function in schizophrenia. *Arch Gen Psychiatry, 66*(8), 811-822. https://doi.org/10.1001/archgenpsychiatry.2009.91

Moghaddam, B., Adams, B., Verma, A., & Daly, D. (1997). Activation of glutamatergic neurotransmission by ketamine: a novel step in the pathway from NMDA receptor blockade to dopaminergic and cognitive disruptions associated with the prefrontal cortex. *J Neurosci, 17*(8), 2921-2927. https://doi.org/10.1523/JNEUROSCI.17-08-02921.1997

Morris, J. S., & Dolan, R. J. (2004). Dissociable amygdala and orbitofrontal responses during reversal fear conditioning. *Neuroimage, 22*(1), 372-380. https://doi.org/10.1016/j.neuroimage.2004.01.012

Morris, R. G., Halliwell, R. F., & Bowery, N. (1989). Synaptic plasticity and learning II: do different kinds of plasticity underlie different kinds of learning? *Neuropsychologia, 27*(1), 41-59.

Mostofsky, S. H., & Simmonds, D. J. (2008). Response inhibition and response selection: two sides of the same coin. *J Cogn Neurosci, 20*(5), 751-761. https://doi.org/10.1162/jocn.2008.20500

Mufson, E. J., & Mesulam, M. M. (1984). Thalamic connections of the insula in the rhesus monkey and comments on the paralimbic connectivity of the medial pulvinar nucleus. *J Comp Neurol, 227*(1), 109-120. https://doi.org/10.1002/cne.902270112

Munsch, T., Freichel, M., Flockerzi, V., & Pape, H. C. (2003). Contribution of transient receptor potential channels to the control of GABA release from dendrites. *Proc Natl Acad Sci U S A, 100*(26), 16065-16070. https://doi.org/10.1073/pnas.2535311100

Murray, G. K., Cheng, F., Clark, L., Barnett, J. H., Blackwell, A. D., Fletcher, P. C., Robbins, T. W., Bullmore, E. T., & Jones, P. B. (2008). Reinforcement and reversal learning in first-episode psychosis. *Schizophr Bull, 34*(5), 848-855. https://doi.org/10.1093/schbul/sbn078

Nagahama, Y., Okada, T., Katsumi, Y., Hayashi, T., Yamauchi, H., Oyanagi, C., Konishi, J., Fukuyama, H., & Shibasaki, H. (2001). Dissociable mechanisms of attentional control within the human prefrontal cortex. *Cerebral Cortex, 11*(1), 85-92. https://doi.org/10.1093/cercor/11.1.85

Nagy, A. (2000). Cre recombinase: the universal reagent for genome tailoring. *genesis, 26*(2), 99-109. https://doi.org/10.1002/(SICI)1526-968X(200002)26:2<99::AID-GENE1>3.0.CO;2-B

Nahar, L., Delacroix, B. M., & Nam, H. W. (2021). The Role of Parvalbumin Interneurons in Neurotransmitter Balance and Neurological Disease. *Front Psychiatry, 12*, 679960. https://doi.org/10.3389/fpsyt.2021.679960

Neafsey, E. J., Bold, E. L., Haas, G., Hurley-Gius, K. M., Quirk, G., Sievert, C. F., & Terreberry, R. R. (1986). The organization of the rat motor cortex: a microstimulation mapping study. *Brain Res, 396*(1), 77-96. https://doi.org/10.1016/s0006-8993(86)80191-3

Neckelmann, D., Amzica, F., & Steriade, M. (1998). Spike-wave complexes and fast components of cortically generated seizures. III. Synchronizing mechanisms. *J Neurophysiol, 80*(3), 1480-1494. https://doi.org/10.1152/jn.1998.80.3.1480

Nelson, A. J. D., Kinnavane, L., Amin, E., O'Mara, S. M., & Aggleton, J. P. (2020). Deconstructing the Direct Reciprocal Hippocampal-Anterior Thalamic Pathways for Spatial Learning. *J Neurosci, 40*(36), 6978-6990. https://doi.org/10.1523/JNEUROSCI.0874-20.2020

Neumann, K., Grittner, U., Piper, S. K., Rex, A., Florez-Vargas, O., Karystianis, G., Schneider, A., Wellwood, I., Siegerink, B., Ioannidis, J. P., Kimmelman, J., & Dirnagl, U. (2017). Increasing efficiency of preclinical research by group sequential designs. *PLoS Biol, 15*(3), e2001307. https://doi.org/10.1371/journal.pbio.2001307

Nguyen, R., Morrissey, M. D., Mahadevan, V., Cajanding, J. D., Woodin, M. A., Yeomans, J. S., Takehara-Nishiuchi, K., & Kim, J. C. (2014). Parvalbumin and GAD65 interneuron inhibition in the ventral hippocampus induces distinct behavioral deficits relevant to schizophrenia. *J Neurosci, 34*(45), 14948-14960. https://doi.org/10.1523/JNEUROSCI.2204-14.2014

Nicoll, R. A., Malenka, R. C., & Kauer, J. A. (1990). Functional comparison of neurotransmitter receptor subtypes in mammalian central nervous system. *Physiol Rev, 70*(2), 513-565. https://doi.org/10.1152/physrev.1990.70.2.513

Nogueira, L., & Lavin, A. (2010). Strong somatic stimulation differentially regulates the firing properties of prefrontal cortex neurons. *Brain Res, 1351*, 57-63. https://doi.org/10.1016/j.brainres.2010.07.002

O'Doherty, J., Kringelbach, M. L., Rolls, E. T., Hornak, J., & Andrews, C. (2001). Abstract reward and punishment representations in the human orbitofrontal cortex. *Nat Neurosci, 4*(1), 95-102. https://doi.org/10.1038/82959

O'Neill, M. J., Fell, M. J., Svensson, K. A., Witkin, J. M., & Mitchell, S. N. (2010). Recent Developments in Metabotropic Glutamate Receptors as Novel Drug Targets. *Drugs of the Future, 35*(4), 307-324. https://doi.org/10.1358/dof.2010.35.4.1487693

Ongur, D. (2000). The Organization of Networks within the Orbital and Medial Prefrontal Cortex of Rats, Monkeys and Humans. *Cerebral Cortex, 10*(3), 206-219. https://doi.org/10.1093/cercor/10.3.206

Ortiz-Gil, J., Pomarol-Clotet, E., Salvador, R., Canales-Rodriguez, E. J., Sarro, S., Gomar, J. J., Guerrero, A., Sans-Sansa, B., Capdevila, A., Junque, C., & McKenna, P. J. (2011). Neural correlates of cognitive impairment in schizophrenia. *Br J Psychiatry, 199*(3), 202-210. https://doi.org/10.1192/bjp.bp.110.083600

Owen, A. M., Roberts, A. C., Hodges, J. R., & Robbins, T. W. (1993). Contrasting mechanisms of impaired attentional set-shifting in patients with frontal lobe damage or Parkinson's disease. *Brain, 116*(5), 1159-1175.

Owen, A. M., Roberts, A. C., Polkey, C. E., Sahakian, B. J., & Robbins, T. W. (1991). Extra-dimensional versus intra-dimensional set shifting performance following frontal lobe excisions, temporal lobe excisions or amygdalo-hippocampectomy in man. *Neuropsychologia, 29*(10), 993-1006.

Parnaudeau, S., Taylor, K., Bolkan, S. S., Ward, R. D., Balsam, P. D., & Kellendonk, C. (2015). Mediodorsal thalamus hypofunction impairs flexible goal-

directed behavior. *Biol Psychiatry, 77*(5), 445-453.
https://doi.org/10.1016/j.biopsych.2014.03.020

Passetti, F., Chudasama, Y., & Robbins, T. W. (2002). The frontal cortex of the rat
and visual attentional performance: dissociable functions of distinct medial
prefrontal subregions. *Cereb Cortex, 12*(12), 1254-1268.
https://doi.org/10.1093/cercor/12.12.1254

Paxinos, G., & Watson, C. (1998). *The rat brain in stereotaxic coordinates*. New
York: Academic.

Pehrson, A. L., Bondi, C. O., Totah, N. K., & Moghaddam, B. (2013). The influence
of NMDA and GABA(A) receptors and glutamic acid decarboxylase (GAD)
activity on attention. *Psychopharmacology (Berl), 225*(1), 31-39.
https://doi.org/10.1007/s00213-012-2792-z

Penttonen, M., Kamondi, A., Acsady, L., & Buzsaki, G. (1998). Gamma frequency
oscillation in the hippocampus of the rat: intracellular analysis in vivo. *Eur J
Neurosci, 10*(2), 718-728. https://doi.org/10.1046/j.1460-
9568.1998.00096.x

Petersen, S. E., & Posner, M. I. (2012). The attention system of the human brain:
20 years after. *Annu Rev Neurosci, 35*, 73-89.
https://doi.org/10.1146/annurev-neuro-062111-150525

Pezze, M., McGarrity, S., Mason, R., Fone, K. C., & Bast, T. (2014). Too little and too
much: hypoactivation and disinhibition of medial prefrontal cortex cause
attentional deficits. *J Neurosci, 34*(23), 7931-7946.
https://doi.org/10.1523/JNEUROSCI.3450-13.2014

Posner, M. I., & Petersen, S. E. (1990). The attention system of the human brain. *Annu Rev Neurosci, 13*(1), 25-42. https://doi.org/10.1146/annurev.ne.13.030190.000325

Preuss, T. M. (1995). Do rats have prefrontal cortex? The rose-woolsey-akert program reconsidered. *J Cogn Neurosci, 7*(1), 1-24. https://doi.org/10.1162/jocn.1995.7.1.1

Preuss, T. M., & Wise, S. P. (2022). Evolution of prefrontal cortex. *Neuropsychopharmacology, 47*(1), 3-19. https://doi.org/10.1038/s41386-021-01076-5

Price, J. L. (2007). Definition of the orbital cortex in relation to specific connections with limbic and visceral structures and other cortical regions. *Ann N Y Acad Sci, 1121*(1), 54-71. https://doi.org/10.1196/annals.1401.008

Prior, M. J. W., Bast, T., McGarrity, S., Goldschmidt, J., Vincenz, D., Seaton, A., Hall, G., & Pitiot, A. (2021). Ratlas-LH: An MRI template of the Lister hooded rat brain with stereotaxic coordinates for neurosurgical implantations. *Brain Neurosci Adv, 5*, 23982128211036332. https://doi.org/10.1177/23982128211036332

Ragozzino, M. E., & Choi, D. (2004). Dynamic changes in acetylcholine output in the medial striatum during place reversal learning. *Learn Mem, 11*(1), 70-77. https://doi.org/10.1101/lm.65404

Reid, L. S. (1953). The Development of Noncontinuity Behavior through Continuity Learning. *Journal of experimental psychology, 46*(2), 107-112. https://doi.org/DOI 10.1037/h0062488

Remijnse, P. L., Nielen, M. M., Uylings, H. B., & Veltman, D. J. (2005). Neural correlates of a reversal learning task with an affectively neutral baseline: an event-related fMRI study. *Neuroimage, 26*(2), 609-618. https://doi.org/10.1016/j.neuroimage.2005.02.009

Remijnse, P. L., Nielen, M. M., van Balkom, A. J., Cath, D. C., van Oppen, P., Uylings, H. B., & Veltman, D. J. (2006). Reduced orbitofrontal-striatal activity on a reversal learning task in obsessive-compulsive disorder. *Arch Gen Psychiatry, 63*(11), 1225-1236. https://doi.org/10.1001/archpsyc.63.11.1225

Robbins, T. W., James, M., Owen, A. M., Sahakian, B. J., McInnes, L., & Rabbitt, P. (1994). Cambridge Neuropsychological Test Automated Battery (CANTAB): a factor analytic study of a large sample of normal elderly volunteers. *Dementia, 5*(5), 266-281. https://doi.org/10.1159/000106735

Robbins, T. W., & Roberts, A. C. (2007). Differential regulation of Fronto-Executive function by the Monoamines and acetylcholine. *Cerebral Cortex, 17*(suppl_1), I151-I160. https://doi.org/10.1093/cercor/bhm066

Roberts, A. C. (2011). The importance of serotonin for orbitofrontal function. *Biological psychiatry, 69*(12), 1185-1191.

Roberts, A. C. (2020). Prefrontal Regulation of Threat-Elicited Behaviors: A Pathway to Translation. *Annu Rev Psychol, 71*, 357-387. https://doi.org/10.1146/annurev-psych-010419-050905

Roberts, A. C., & Clarke, H. F. (2019). Why we need nonhuman primates to study the role of ventromedial prefrontal cortex in the regulation of threat- and reward-elicited responses. *Proc Natl Acad Sci U S A, 116*(52), 26297-26304. https://doi.org/10.1073/pnas.1902288116

Roberts, A. C., Desalvia, M. A., Wilkinson, L. S., Collins, P., Muir, J. L., Everitt, B. J., & Robbins, T. W. (1994). 6-Hydroxydopamine Lesions of the Prefrontal Cortex in Monkeys Enhance Performance on an Analog of the Wisconsin Card Sort Test - Possible Interactions with Subcortical Dopamine. *Journal of Neuroscience, 14*(5), 2531-2544. <Go to ISI>://WOS:A1994NK23600007

Roberts, A. C., Robbins, T. W., Everitt, B. J., Jones, G. H., Sirkia, T. E., Wilkinson, J., & Page, K. (1990). The effects of excitotoxic lesions of the basal forebrain on the acquisition, retention and serial reversal of visual discriminations in marmosets. *Neuroscience, 34*(2), 311-329. https://doi.org/10.1016/0306-4522(90)90142-q

Roberts, A. C., Robbins, T. W., Everitt, B. J., & Muir, J. L. (1992). A specific form of cognitive rigidity following excitotoxic lesions of the basal forebrain in marmosets. *Neuroscience, 47*(2), 251-264. https://doi.org/10.1016/0306-4522(92)90241-s

Roberts, A. C., Tomic, D. L., Parkinson, C. H., Roeling, T. A., Cutter, D. J., Robbins, T. W., & Everitt, B. J. (2007). Forebrain connectivity of the prefrontal cortex in the marmoset monkey (Callithrix jacchus): an anterograde and retrograde tract-tracing study. *J Comp Neurol, 502*(1), 86-112. https://doi.org/10.1002/cne.21300

Robinson, S., Todd, T. P., Pasternak, A. R., Luikart, B. W., Skelton, P. D., Urban, D. J., & Bucci, D. J. (2014). Chemogenetic silencing of neurons in retrosplenial cortex disrupts sensory preconditioning. *J Neurosci, 34*(33), 10982-10988. https://doi.org/10.1523/JNEUROSCI.1349-14.2014

Rogan, S. C., & Roth, B. L. (2011). Remote control of neuronal signaling. *Pharmacol Rev, 63*(2), 291-315. https://doi.org/10.1124/pr.110.003020

Rogers, R. D., Andrews, T. C., Grasby, P. M., Brooks, D. J., & Robbins, T. W. (2000). Contrasting cortical and subcortical activations produced by attentional-set shifting and reversal learning in humans. *J Cogn Neurosci, 12*(1), 142-162. https://doi.org/10.1162/089892900561931

Rose, J. E., & Woolsey, C. N. (1948). Structure and relations of limbic cortex and anterior thalamic nuclei in rabbit and cat. *J Comp Neurol, 89*(3), 279-347. https://doi.org/10.1002/cne.900890307

Rossi, A. F., Bichot, N. P., Desimone, R., & Ungerleider, L. G. (2007). Top down attentional deficits in macaques with lesions of lateral prefrontal cortex. *J Neurosci, 27*(42), 11306-11314. https://doi.org/10.1523/JNEUROSCI.2939-07.2007

Rossi, A. F., Pessoa, L., Desimone, R., & Ungerleider, L. G. (2009). The prefrontal cortex and the executive control of attention. *Exp Brain Res, 192*(3), 489-497. https://doi.org/10.1007/s00221-008-1642-z

Roth, B. L. (2016). DREADDs for Neuroscientists. *Neuron, 89*(4), 683-694. https://doi.org/10.1016/j.neuron.2016.01.040

Rushworth, M. F., Noonan, M. P., Boorman, E. D., Walton, M. E., & Behrens, T. E. (2011). Frontal cortex and reward-guided learning and decision-making. *Neuron, 70*(6), 1054-1069. https://doi.org/10.1016/j.neuron.2011.05.014

Rygula, R., Clarke, H. F., Cardinal, R. N., Cockcroft, G. J., Xia, J., Dalley, J. W., Robbins, T. W., & Roberts, A. C. (2015). Role of Central Serotonin in Anticipation of Rewarding and Punishing Outcomes: Effects of Selective Amygdala or Orbitofrontal 5-HT Depletion. *Cereb Cortex, 25*(9), 3064-3076. https://doi.org/10.1093/cercor/bhu102

Rygula, R., Papciak, J., & Popik, P. (2014). The effects of acute pharmacological stimulation of the 5-HT, NA and DA systems on the cognitive judgement bias of rats in the ambiguous-cue interpretation paradigm. *Eur Neuropsychopharmacol, 24*(7), 1103-1111. https://doi.org/10.1016/j.euroneuro.2014.01.012

Rygula, R., Walker, S. C., Clarke, H. F., Robbins, T. W., & Roberts, A. C. (2010). Differential contributions of the primate ventrolateral prefrontal and orbitofrontal cortex to serial reversal learning. *J Neurosci, 30*(43), 14552-14559. https://doi.org/10.1523/JNEUROSCI.2631-10.2010

Saalmann, Y. B., Pigarev, I. N., & Vidyasagar, T. R. (2007). Neural mechanisms of visual attention: How top-down feedback highlights relevant locations. *Science, 316*(5831), 1612-1615. https://doi.org/10.1126/science.1139140

Saunders, A., Granger, A. J., & Sabatini, B. L. (2015). Corelease of acetylcholine and GABA from cholinergic forebrain neurons. *Elife, 4*. https://doi.org/10.7554/eLife.06412

Schlingmann, F., De Rijk, S., Pereboom, W., & Remie, R. (1993). Avoidance'as a behavioural parameter in the determination of distress amongst albino and pigmented rats at various light intensities. *Animal Technology, 44*, 87-87.

Schoenbaum, G., & Eichenbaum, H. (1995). Information coding in the rodent prefrontal cortex. I. Single-neuron activity in orbitofrontal cortex compared with that in pyriform cortex. *Journal of neurophysiology, 74*(2), 733-750. https://doi.org/10.1152/jn.1995.74.2.733

Schoenbaum, G., Roesch, M. R., Stalnaker, T. A., & Takahashi, Y. K. (2009). A new perspective on the role of the orbitofrontal cortex in adaptive behaviour. *Nat Rev Neurosci, 10*(12), 885-892. https://doi.org/10.1038/nrn2753

Schoenbaum, G., Setlow, B., Nugent, S. L., Saddoris, M. P., & Gallagher, M. (2003). Lesions of orbitofrontal cortex and basolateral amygdala complex disrupt acquisition of odor-guided discriminations and reversals. *Learn Mem, 10*(2), 129-140. https://doi.org/10.1101/lm.55203

Sciolino, N. R., Plummer, N. W., Chen, Y. W., Alexander, G. M., Robertson, S. D., Dudek, S. M., McElligott, Z. A., & Jensen, P. (2016). Recombinase-Dependent Mouse Lines for Chemogenetic Activation of Genetically Defined Cell Types. *Cell Rep, 15*(11), 2563-2573. https://doi.org/10.1016/j.celrep.2016.05.034

Sesack, S. R., Deutch, A. Y., Roth, R. H., & Bunney, B. S. (1989). Topographical organization of the efferent projections of the medial prefrontal cortex in the rat: an anterograde tract-tracing study with Phaseolus vulgaris leucoagglutinin. *J Comp Neurol, 290*(2), 213-242. https://doi.org/10.1002/cne.902900205

Shenhav, A., Botvinick, M. M., & Cohen, J. D. (2013). The expected value of control: an integrative theory of anterior cingulate cortex function. *Neuron, 79*(2), 217-240. https://doi.org/10.1016/j.neuron.2013.07.007

Simmonite, M., Steeby, C. J., & Taylor, S. F. (2023). Medial Frontal Cortex GABA Concentrations in Psychosis Spectrum and Mood Disorders: A Meta-analysis of Proton Magnetic Resonance Spectroscopy Studies. *Biol Psychiatry, 93*(2), 125-136. https://doi.org/10.1016/j.biopsych.2022.08.004

Smith, K. S., Bucci, D. J., Luikart, B. W., & Mahler, S. V. (2016). DREADDS: Use and application in behavioral neuroscience. *Behav Neurosci, 130*(2), 137-155. https://doi.org/10.1037/bne0000135

Soghomonian, J. J., & Martin, D. L. (1998). Two isoforms of glutamate decarboxylase: why? *Trends Pharmacol Sci, 19*(12), 500-505. https://doi.org/10.1016/s0165-6147(98)01270-x

Sohal, V. S., Zhang, F., Yizhar, O., & Deisseroth, K. (2009). Parvalbumin neurons and gamma rhythms enhance cortical circuit performance. *Nature, 459*(7247), 698-702. https://doi.org/10.1038/nature07991

Song, J., Xu, Y., Hu, X., Choi, B., & Tong, Q. (2010). Brain expression of Cre recombinase driven by pancreas-specific promoters. *genesis, 48*(11), 628-634.

Steele, J. D., & Lawrie, S. M. (2004). Segregation of cognitive and emotional function in the prefrontal cortex: a stereotactic meta-analysis. *Neuroimage, 21*(3), 868-875.

Steriade, M., Amzica, F., Neckelmann, D., & Timofeev, I. (1998). Spike-wave complexes and fast components of cortically generated seizures. II. Extra- and intracellular patterns. *J Neurophysiol, 80*(3), 1456-1479. https://doi.org/10.1152/jn.1998.80.3.1456

Sternson, S. M., & Roth, B. L. (2014). Chemogenetic tools to interrogate brain functions. *Annu Rev Neurosci, 37*, 387-407. https://doi.org/10.1146/annurev-neuro-071013-014048

Sutton, R. S., & Barto, A. G. (2018). *Reinforcement learning: An introduction*. MIT press.

Suzuki, M., & Gottlieb, J. (2013). Distinct neural mechanisms of distractor suppression in the frontal and parietal lobe. *Nat Neurosci, 16*(1), 98-104. https://doi.org/10.1038/nn.3282

Tait, D. S., & Brown, V. J. (2008). Lesions of the basal forebrain impair reversal learning but not shifting of attentional set in rats. *Behav Brain Res, 187*(1), 100-108. https://doi.org/10.1016/j.bbr.2007.08.035

Takahashi, Y. K., Roesch, M. R., Stalnaker, T. A., Haney, R. Z., Calu, D. J., Taylor, A. R., Burke, K. A., & Schoenbaum, G. (2009). The orbitofrontal cortex and ventral tegmental area are necessary for learning from unexpected outcomes. *Neuron, 62*(2), 269-280. https://doi.org/10.1016/j.neuron.2009.03.005

Tighe, T. J., Brown, P. L., & Youngs, E. A. (1965). The Effect of Overtraining on the Shift-Behavior of Albino-Rats. *Psychonomic Science, 2*(5), 141-142. https://doi.org/Doi 10.3758/Bf03343372

Tremblay, R., Lee, S., & Rudy, B. (2016). GABAergic Interneurons in the Neocortex: From Cellular Properties to Circuits. *Neuron, 91*(2), 260-292. https://doi.org/10.1016/j.neuron.2016.06.033

Tse, M. T., Piantadosi, P. T., & Floresco, S. B. (2015). Prefrontal cortical gamma-aminobutyric acid transmission and cognitive function: drawing links to schizophrenia from preclinical research. *Biol Psychiatry, 77*(11), 929-939. https://doi.org/10.1016/j.biopsych.2014.09.007

Uhlhaas, P. J. (2013). Dysconnectivity, large-scale networks and neuronal dynamics in schizophrenia. *Curr Opin Neurobiol, 23*(2), 283-290. https://doi.org/10.1016/j.conb.2012.11.004

Urban, D. J., & Roth, B. L. (2015). DREADDs (designer receptors exclusively activated by designer drugs): chemogenetic tools with therapeutic utility. *Annu Rev Pharmacol Toxicol, 55*, 399-417. https://doi.org/10.1146/annurev-pharmtox-010814-124803

Uylings, H. B., Groenewegen, H. J., & Kolb, B. (2003). Do rats have a prefrontal cortex? *Behavioural Brain Research, 146*(1-2), 3-17.

van den Buuse, M. (1999). Circadian rhythms of blood pressure and heart rate in conscious rats: effects of light cycle shift and timed feeding. *Physiology & behavior, 68*(1-2), 9-15. https://doi.org/https://doi.org/10.1016/S0031-9384(99)00148-1

van der Staay, F. J., Rutten, K., Erb, C., & Blokland, A. (2011). Effects of the cognition impairer MK-801 on learning and memory in mice and rats. *Behavioural Brain Research, 220*(1), 215-229.

Volk, D., Austin, M., Pierri, J., Sampson, A., & Lewis, D. (2001). GABA transporter-1 mRNA in the prefrontal cortex in schizophrenia: decreased expression in a subset of neurons. *Am J Psychiatry, 158*(2), 256-265. https://doi.org/10.1176/appi.ajp.158.2.256

Wallis, C. U., Cardinal, R. N., Alexander, L., Roberts, A. C., & Clarke, H. F. (2017). Opposing roles of primate areas 25 and 32 and their putative rodent homologs in the regulation of negative emotion. *Proceedings of the National Academy of Sciences of the United States of America, 114*(20), E4075-E4084. https://doi.org/10.1073/pnas.1620115114

Wassef, A., Baker, J., & Kochan, L. D. (2003). GABA and schizophrenia: a review of basic science and clinical studies. *J Clin Psychopharmacol, 23*(6), 601-640. https://doi.org/10.1097/01.jcp.0000095349.32154.a5

Watakabe, A., Ohtsuka, M., Kinoshita, M., Takaji, M., Isa, K., Mizukami, H., Ozawa, K., Isa, T., & Yamamori, T. (2015). Comparative analyses of adeno-associated viral vector serotypes 1, 2, 5, 8 and 9 in marmoset, mouse and macaque cerebral cortex. *Neurosci Res, 93*, 144-157. https://doi.org/10.1016/j.neures.2014.09.002

Weaver, D. R., van der Vinne, V., Giannaris, E. L., Vajtay, T. J., Holloway, K. L., & Anaclet, C. (2018). Functionally complete excision of conditional alleles in the mouse suprachiasmatic nucleus by Vgat-ires-Cre. *Journal of biological rhythms, 33*(2), 179-191.

Weinberger, D. R., Berman, K. F., & Zec, R. F. (1986). Physiologic dysfunction of dorsolateral prefrontal cortex in schizophrenia. I. Regional cerebral blood flow evidence. *Arch Gen Psychiatry, 43*(2), 114-124. https://doi.org/10.1001/archpsyc.1986.01800020020004

Williams, S. (2021). *Neuro-behavioural impact of changes in hippocampal neural activity* University of Nottingham].

Yang, S. T., Shi, Y., Wang, Q., Peng, J. Y., & Li, B. M. (2014). Neuronal representation of working memory in the medial prefrontal cortex of rats. *Mol Brain, 7*(1), 61. https://doi.org/10.1186/s13041-014-0061-2

Yau, J. O., & McNally, G. P. (2015). Pharmacogenetic excitation of dorsomedial prefrontal cortex restores fear prediction error. *J Neurosci, 35*(1), 74-83. https://doi.org/10.1523/JNEUROSCI.3777-14.2015

Young, J. J., & Shapiro, M. L. (2009). Double dissociation and hierarchical organization of strategy switches and reversals in the rat PFC. *Behav Neurosci, 123*(5), 1028-1035. https://doi.org/10.1037/a0016822

Zhang, W., Vazquez, L., Apperson, M., & Kennedy, M. B. (1999). Citron binds to PSD-95 at glutamatergic synapses on inhibitory neurons in the hippocampus. *J Neurosci, 19*(1), 96-108. https://doi.org/10.1523/JNEUROSCI.19-01-00096.1999

Zhou, F. M., & Hablitz, J. J. (1999). Activation of serotonin receptors modulates synaptic transmission in rat cerebral cortex. *J Neurophysiol, 82*(6), 2989-2999. https://doi.org/10.1152/jn.1999.82.6.2989

Zhu, H., & Roth, B. L. (2014). Silencing synapses with DREADDs. *Neuron, 82*(4), 723-725. https://doi.org/10.1016/j.neuron.2014.05.002